

THE
DYNAMIC BEHAVIOUR
OF
PACKED DISTILLATION COLUMNS

A thesis presented for the degree of
Doctor of Philosophy in Chemical Engineering
at the
University of Canterbury,
Christchurch, New Zealand.

By

P.J. JORDAN

1977

~~THESIS~~

TP

159

P3

J82

1977

Copy 2

ACKNOWLEDGEMENTS

I would like to thank Dr. W.B.Earl for his supervision of this project and for the practical advise which he was able to offer. Thanks are also due to the technical staff of the Chemical Engineering Department for their help with modifications to the experimental column.

This project would probably never have reached completion without the support of Professor A.H.Kennedy, with his sympathetic understanding of the problems of members of staff doing Ph.D work, and the unfailing encouragement of my wife Erica during the long days of her "Ph.D widowhood".

Financial help from I.C.I. (N.Z.)Ltd. is gratefully acknowledged.

This thesis was formatted using a computer program written by G.F.Deecker of the Computer Science Department. For his help, and that of the Computer Centre Staff, especially G.Gregg of Lincoln College, I am much obliged.

ERRATA.

1. Page 20, first line after equation (2.14):
Change "where X_B is the equilibrium composition" to
"where X_B is the liquid composition"
2. Page 32, equation (4.1):
Change " $z(z,o)$ " to " $x(z,o)$ "
3. Page 34, second line after equation (2.4):
Change " $(L/Z)(\partial x/\partial t)$ " to " $(L/Z)(\partial x/\partial z)$ "
4. Page 64, para 2, line 4:
Change "This is about 5%" to "This is about 2.5%"
5. Page 77, second to last line:
Change "0.025 mV" to "0.0025 mV"
6. Page 87, para 1, line 1:
Insert "I" in the list: "At thermocouples D, E, H, J and L."
7. Page 106, equation (8.3):
Change " $\frac{L\partial x}{\partial z}$ " to " $\frac{L\partial x}{Z\partial z}$ "

ADDENDA.

It should be noted that equation (5.9), page 46, is only valid provided that the feed stream and the liquid stream leaving the enriching section are at the same temperature.

CONTENTS

SUMMARY.	1
CHAPTER 1: Introduction.	2
CHAPTER 2: Dynamic Model of a Packed Distillation Column.	14
CHAPTER 3: Numerical Solution of the Model.	22
CHAPTER 4: Results of the Computer Solution of the Model.	31
CHAPTER 5: Modifications to the Model for Other Column Arrangements.	42
CHAPTER 6: The Experimental Column and Mixture.	52
CHAPTER 7: Experimental Composition Profiles at Steady State.	82
CHAPTER 8: Experimental Composition Profiles at Unsteady State.	94
CHAPTER 9: Conclusions and Suggestions for Further Work.	110
SYMBOLS.	116
REFERENCES.	120
APPENDIX 1: Enthalpy Balance in the Packing.	122
APPENDIX 2: Computer Subroutines.	123
APPENDIX 3: Computer Mainline Program.	134
APPENDIX 4: Operating Variables.	141
APPENDIX 5: Transient Response Plots.	143

SUMMARY

The dynamic behaviour of packed distillation columns separating binary mixtures has been studied, both by means of a computer simulation, and by experimental testing of a column.

The numerical solution of the partial differential equations of the mathematical model, obtained using a digital computer, was found to be fast, accurate and stable. The advantages obtained by using this approach, compared with previous analytical solutions, included: no restriction on the equilibrium relationship which could be used, variable coefficients could be used in the partial differential equations, and the method allowed any desired boundary conditions to be used. The model was first solved for an enriching column section, and was later extended to the cases of batch and continuous columns.

A 150 mm diameter column packed with 10 mm Raschig rings was used to measure the transient response following step-change upsets in the liquid reflux rate. The shapes of the measured transient responses of the distillate composition agreed well with those predicted by the model. However, the predicted time scale of the response was from 0.6 to 2.2 times faster than the measured time scale. Factors which hindered the ability of the model to predict the experimental transient responses included poor correlation of the mass transfer coefficients with flow rates and composition, and lack of knowledge of the rate of change of the liquid holdup with time.

CHAPTER 1 INTRODUCTION

- 1.1 The Scope Of This Work.
- 1.2 Applications.
- 1.3 Previous Work On Packed Distillation Column Dynamics.
 - 1.3.1 Previous Models.
 - 1.3.2 Assumptions Made.
 - 1.3.3 Solution Of The Equations.
 - 1.3.4 Previous Experimental Results.
 - 1.3.5 Drawbacks To Previous Models.

1.1 THE SCOPE OF THIS WORK

The aim of this study was to use numerical solution techniques to solve the dynamic model of a packed distillation column, and to obtain experimental measurements to test the effectiveness of the model in predicting the dynamic behaviour of a real column. It was restricted to the study of columns separating binary mixtures.

The work falls into two parts. In chapters 1 to 5, the work of previous investigators on packed distillation column dynamics is first considered. Then the dynamic column model is presented in a form suitable for solution on a digital computer. Typical results are presented and it is shown that when a numerical solution is used, the model may be easily adapted for different column configurations by changing the boundary conditions.

The experimental column is described in chapter 6. Experimental results are presented for the column at steady state (chapter 7) and unsteady state (chapter 8). Chapter 9 summarises the effectiveness of the model in predicting the dynamic response of the experimental column to upsets in reflux ratio, and attempts to pinpoint those aspects which require better understanding before the performance of the model can be improved.

1.2 APPLICATIONS

A distillation column can be considered to be in a dynamic condition if any variable in the column (e.g. composition, holdup or flowrate) is changing with time. Otherwise the column is at steady state. There are three main situations in which knowledge of the dynamic behaviour of packed distillation columns may be important.

(i). Batch distillation . Compositions throughout a column continually change with time, making batch distillation a dynamic process. Most descriptions of batch distillation, e.g. Boqart(1937) and Rose and Welshans(1940), ignore the effect of column holdup. They therefore treat the column composition profile as being at steady state at any time, but with a time varying boundary condition (the reboiler composition). For a review of batch distillation models see Kropholler et. al.(1968).

(ii). Automatic control. Most industrial columns have some form of automatic product control, often achieved by manipulating the reflux ratio. In the design of such control loops by classical methods, the column must be represented by transfer functions; either empirical or derived from a dynamic model of the column. A review of the use of plate distillation column models in control is given by Posenbrock(1962).

(iii). Column startup. Columns are often started at total reflux and then switched to the operating reflux rate. The time taken to achieve steady state at total reflux in some situations may be so long that it cannot be ignored, especially in batch operations. Cohen(1940) has reported startup times of many days for columns separating isotopes by distillation .

1.3 PREVIOUS WORK ON PACKED DISTILLATION COLUMN DYNAMICS.

Investigation of the dynamic response of binary packed distillation columns has been reported by: Cohen(1940), Bowman and Briant(1947), Marshall and Pigford(1948), Jawson and Smith(1954), Heinke et. al. (1966), Heinke and Wagner(1965), Kropholler et. al.(1968), Tomassi and Rice(1970), Borchardt and Wagner (1971), and Kuznik and Krzyzanowski(1975). Of these, Heinke et. al. , Kropholler et. al. , Tomassi and Rice, and Borchardt and Wagner have reported experimental results. By comparison, there has been much more work published on the dynamics of plate distillation columns. This has been ably reviewed by

several authors including Archer and Rothfus(1961), Rosenbrock(1962) and Williams(1963). The dynamics of other types of packed columns such as packed absorption columns has been considered by Jawson and Smith(1954).

1.3.1 Previous Models.

In the works on packed distillation column dynamics cited above, the mathematical model has been derived by considering mass balances for the more volatile component in the liquid and vapour phases over a small element of packing height. These yield equations of the form:

$$\frac{H \cdot \partial x}{\partial t} = \frac{L \cdot \partial x}{\partial \gamma} + N \quad \dots\dots(1.1)$$

$$\frac{h \cdot \partial y}{\partial t} = -\frac{V \cdot \partial y}{\partial \gamma} + N \quad \dots\dots(1.2)$$

where:

H	=liquid holdup	mol/m
h	=vapour holdup	mol/m
L	=liquid flow rate	mol/s
V	=vapour flow rate	mol/s
x	=mole fraction of more volatile component in the liquid phase	
y	=mole fraction of more volatile component in the vapour phase	
t	=time	s
γ	=height from bottom of packing	m
Z	=total packing height	m
N	=mass transfer rate	mol/m/s

The mass transfer rate term N is usually expressed as:

$$N = K a \cdot S (y^* - y) \quad \dots\dots(1.3)$$

or:

6

$$N = K a_G S (x^* - x_L) \quad \dots (1.4)$$

where:

x^* = equilibrium mole fraction of the more volatile component in the liquid

y^* = equilibrium mole fraction of the more volatile component in the vapour

$K a_G$ = overall mass transfer coefficient times interfacial area mol/s/m^3

$K a_L$ = overall mass transfer coefficient times interfacial area mol/s/m^3

S = cross sectional area of column m^2

equations 1.1 and 1.2 are hyperbolic partial differential equations and are, in general, non-linear.

Similar equations have been presented by all the authors cited with some differences due to the differing assumptions made. The boundary conditions used will be discussed in more detail later. The equations require two initial conditions and two boundary conditions for solution. The latter have been written to handle the case of the stripping or enriching section of a column. Heinke et. al. have pointed out that the model could be extended to a continuously operating column by using one pair of equations 1.1 and 1.2 for each packed section, and two boundary conditions to tie them together at the feed point. However none of these authors have reported doing this.

1.3.2 Assumptions Made.

The following assumptions were made by all authors cited above in writing and solving the mathematical model:

- (i) constant molal liquid and vapour flow rates throughout any packing section,
- (ii) constant liquid and vapour holdups throughout any packing section,
- (iii) no radial variation in liquid or vapour composition,
- (iv) no axial dispersion in either phase. Kropholler et. al.(1968) investigated the effects of axial dispersion in both liquid and vapour phases, but found that their steady state experimental results were best fitted when axial dispersion was ignored.
- (v) the mass transfer rate is described by either equation (1.3) or equation (1.4). Bowman and Briant(1947) discuss various mass transfer mechanisms but use those just mentioned in solving the dynamic case.
- (vi) the mass transfer coefficient is constant throughout the column.

Most workers also assumed that:

- (vii) there is a linear equilibrium relationship.

$$\text{I.e.} \quad y^* = m.x + c$$

$$\text{or} \quad x^* = m.y + c$$

where m and c are constants.

Exceptions to this were Cohen(1940), Borchardt and Wagner (1971), and Heinke and Wagner(1965), who used a Raoult's Law relationship (i.e. constant relative volatility), although the latter authors then linearised this in the operating region.

Torassi and Rice(1970) and Heinke and Wagner(1965) made the further assumptions that:

- (viii) there is no vapour holdup. Although they do not state this, Tomassi and Pice must have assumed zero liquid holdup in arriving at equations (6) and (7) in their paper; otherwise there would be a $\partial x / \partial \theta$ term in equation (6).
- (ix) the compositions at the final steady state are known in advance. Heinke and Wagner use knowledge of the final steady state to linearise their equilibrium relationship. Tomassi and Rice use the initial and final compositions at the top and bottom of the column to fit their equilibrium curve before the initial composition profile or the transient response can be computed.

The following assumptions have usually been made concerning boundary conditions:

- (x) there is zero condenser holdup. This means that the liquid and vapour compositions at the top of the packing are equal.

$$\text{I.e., } y(Z,t) = x(Z,t)$$

Kropholler et. al.(1968) allow for the introduction of condenser time constants. Bowman and Briant(1947) discuss various possible boundary conditions while Marshall and Pigford(1948) do not insert any into their Laplace Transformed equations.

- (xi) there is infinite reboiler holdup. Alternative expressions of the same condition are that the reboiler composition is constant, or that the vapour composition entering the bottom of the packing is constant.

Jawson and Smith(1954) postulate that a discontinuity in an operating parameter (such as liquid reflux rate) will cause a number of succeeding discontinuities in liquid composition proceeding down the column, and in vapour composition proceeding up the column. This has not been reported by those authors quoted in section(1.3) as having done experimental work, and has not been observed in the experimental part of this present study.

1.3.3 Solution Of The Equations.

Those authors who have obtained solutions for the transient response of a packed distillation column from the mathematical model have done so using analytical methods. The majority have made use of the Laplace Transform method. Kropholler et. al.(1968) say that they have solved the equations numerically, but that their numerical solution took several hours to evaluate compared with seconds for the analytical solution. The analytical solution is usually presented as the sum of a series of exponential terms; the experimental results of Heinke et. al. (1966), Tomassi and Rice(1970) and Kropholler et. al. show that the first two terms are usually sufficient to characterise a transient response. Kropholler et. al. point out that the 'time constants' are the same for differing dynamic conditions, e.g. the response to upsets in liquid reflux or entering vapour rate or composition, and for the approach to equilibrium at total reflux after initial warming up. Borchardt and Wagner (1971) used a semi-empirical method to compute the 'time constants' from the steady state composition profiles. The term 'time constant' is not strictly applicable to a distributed parameter system such as a packed distillation column.

To obtain analytical solutions of the model, it has been necessary to have constant coefficients in equations (1.1) and (1.2). This has required the assumption of constant flow rates, holdups and mass transfer coefficient in the column as mentioned in the previous section. It has also been necessary to use a linear equilibrium relationship over the whole composition range in the column, or, as Kuznik and Krzyzanowski(1975) have done, to use linear approximations to the equilibrium curve over a number of segments. As Kropholler et. al. have remarked, some of the analytical solutions, notably those of Dawson and Smith(1954) and Bowman and Briant(1947), are extremely unwieldy.

1.3.4 Previous Experimental Results.

Heinke et. al. , Kropholler et. al. , Tomassi and Rice, and Boyle and Palmer(1973) have published experimental dynamic response measurements made on packed distillation columns.

Heinke et. al. (1966) measured the dynamic response of a packed distillation column to step changes in the liquid reflux rate large enough to cause large changes in composition, thus making the assumption of a linear equilibrium relationship poor. Their column was 75 mm in diameter, 3.9 m high and packed with 4 mm glass Raschig rings. The column wall was heated to maintain adiabatic operation. The test mixture used was benzene and trichloroethylene. The distillate was returned to the still to maintain an almost constant reboiler composition. The composition was measured at the top of the packing and at three intermediate levels by withdrawing a liquid stream and using a dielectric constant analyser.

The composition transient responses were presented mainly as graphs of $\log(\text{deviation from final steady state})$ versus time. On these plots, all lines for a given transient run became parallel straight lines after some time. The authors concerned themselves mainly with the approach to the final steady state and the 'time constants' obtained from these plots. They found that the dominant 'time constant' was the same at each level for a given final steady state and did not depend on the initial steady state. This was in agreement with the solutions of the model obtained by other workers using a linear equilibrium relationship. The response was found to be faster for decreasing reflux ratio between a given pair of steady states than for increasing reflux ratio between the same steady states. No quantitative comparison was made between the experimental results and the predictions of a mathematical model.

Kropholler et. al.(1968) used a column 4 inches in diameter with a total of 80 inches of stainless steel knitted mesh packing in four sections. As was done by Heinke et. al. , the response to step changes in reflux

ratio was studied and again the distillate was returned directly to the still. The liquid composition was measured only at the column head and base and in the still using an on-line gas liquid chromatograph. The system used was methylcyclohexane-toluene which has a nearly linear equilibrium relationship over a wide composition range. The fractional responses of the top composition for three changes in liquid reflux rate are presented in the paper, and the agreement between experimental and predicted compositions is excellent. However, no indication is given of the actual composition changes or how the holdups were estimated. In predicting the response, the value of K_a for the final liquid rate was L used throughout the transient response and any dependence on composition was ignored.

Tomassi and Rice(1970) used ethanol-water in a 60 mm diameter column with 4 sections 300 mm high packed with 4mm ceramic Berl saddles. They also measured the response to step changes in the liquid reflux rate with the top product returned to the still. The composition was measured at the end of each packing section by withdrawing samples and measuring refractive index or density. Tomassi and Rice found that their major 'time constants' were independent of height except for the one run done with decreasing reflux ratio. They forced the predicted final compositions at the top and bottom of the packing to match their experimental values by using these to compute the coefficients in their linear equilibrium relationship. The predicted and experimental final compositions at the intermediate levels then agreed well. For most of the six runs there was good agreement between the predicted and experimental unsteady state compositions, especially at the top of the packing. However for the run with decreasing liquid reflux rate, the predictions were very poor for the initial part of the run, and at the two top levels moved initially in the wrong direction by a significant amount. Tomassi and Rice say that in all cases 'the periods predicted for the change in concentration to reach 95% of its equilibrium values are accurate'. Although the 95% response time may be a good criterion for the study of the approach of a column to steady state on startup, for batch distillation and automatic control purposes the time to reach an

earlier percentage of the total change would be a better measure of the quality of a prediction. A model which may sometimes predict that the initial change in composition is in the opposite direction to the real situation could cause serious problems in the on-line control of a column.

All these workers have been concerned mainly with establishing the size of the major 'time constants' which control the approach to the new steady state conditions. However, in automatic control situations especially, the prediction of the early part of the response to an upset may be of more importance. None of them have proposed a suitable criterion for assessing how well a mathematical model performs in predicting the behaviour of a real column.

Measurements of the dynamic behaviour of a packed distillation column have also been reported by Boyle and Palmer(1973) who used a column 34 feet high and 6 inches in diameter to test the method of using pseudo-random binary signals for obtaining the frequency response of a process. The frequency response of the top composition of their continuously operating column was found for disturbances in the liquid reflux rate, and the results were compared with frequency responses obtained by step testing and sine wave testing. The liquid compositions were found by measuring the temperature of the binary system. The authors were interested in the use of system identification methods rather than in the dynamics of packed distillation columns, and made no attempt to model the column other than by comparing the response with that of a lumped-parameter first order system.

1.3.5 Drawbacks To Previous Models.

.....

The main drawbacks in the previous dynamic mathematical models of packed distillation columns have been the restrictions that have had to be imposed in order to obtain an analytical solution. Of these, the assumption of a linear equilibrium relationship is likely to be far from the truth except for systems with components which are very difficult to

separate. The requirement of constant coefficients may be satisfied by carefully choosing the binary system to have equal molal latent heats and molecular weights, and by operating the column adiabatically. While this may be possible under laboratory conditions, it is obviously impossible that these conditions will all be met in applying the model to many industrial columns.

It should be possible to eliminate these disadvantages by using a numerical solution of the model. It can then be written with limitations imposed only by the extent of our knowledge of such factors as the mass transfer and the hydrodynamics, and not by difficulties involved in solving the equations. A numerical solution should also allow flexibility in modelling the boundary conditions to handle various column configurations including batch columns and continuous columns, and allow modelling of the reboiler and condenser dynamics.

CHAPTER 2 DYNAMIC MODEL OF A PACKED DISTILLATION COLUMN.

2.1 Introduction

2.2 The Dynamic Mass Balance Equations

2.3 Boundary Conditions

2.3.1 Condenser Boundary Condition

2.3.2 Reboiler Boundary Condition

2.4 Initial Conditions

2.4.1 Steady State Composition Equations

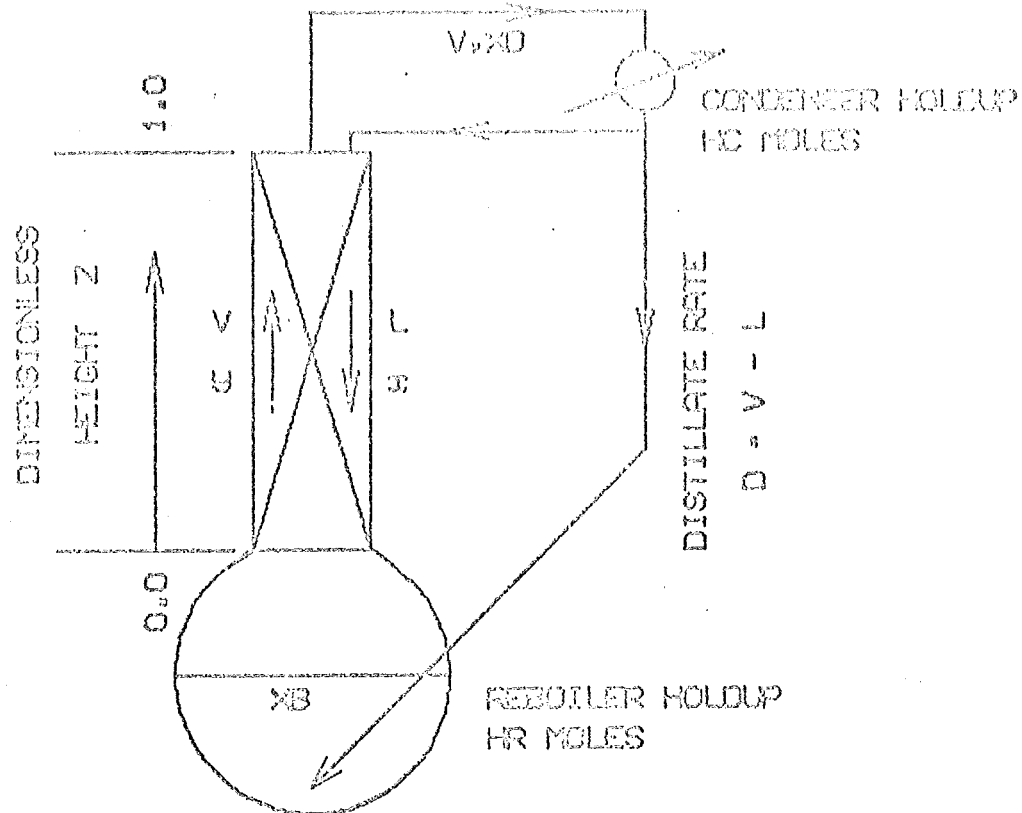


FIG 2.1 THE BASIC COLUMN

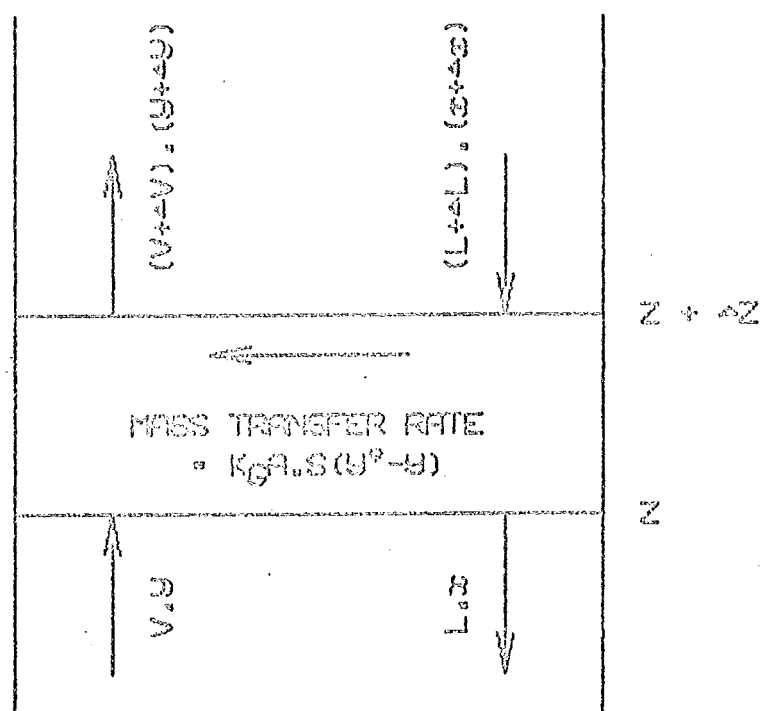


FIG 2.2 MASS BALANCE OVER A SMALL PACKING HEIGHT

Some of the drawbacks of the previous analytical solutions of the dynamic equations may be avoided by the use of a numerical solution. These have become much more practical with the increased speed of digital computers. The advantages of a numerical solution are that the equilibrium relationship may be taken as any desired non-linear curve, and that any boundary conditions may be used. The solution is also easily adapted to handle different situations.

In this chapter, the model will be developed for the most simple situation and it will later be extended to handle other cases. The column described by the basic model is shown in fig. 2.1. This is essentially a batch column with the product returned immediately to the still to provide almost constant reboiler holdup and reboiler composition. It is the same arrangement as that used by Heinke et. al. (1966), Kropholler et. al. (1968) and Tomassi and Rice (1970).

2.2 THE DYNAMIC MASS BALANCE EQUATIONS.

Mass balances for the accumulation of the more volatile component within the liquid and vapour phases over a small increment of column height Δz (see fig. 2.2) are given by:

$$\frac{\partial(H,x)}{\partial t} = \frac{\partial(L,x)}{Z \cdot \partial z} - \frac{K a \cdot S(y^* - y)}{G} \quad \dots\dots(2.1)$$

$$\frac{\partial(h,y)}{\partial t} = - \frac{\partial(V,y)}{Z \cdot \partial z} + \frac{K a \cdot S(y^* - y)}{G} \quad \dots\dots(2.2)$$

where z is the dimensionless height measured from the bottom of the

packing, ($z=0.0$ at the bottom of the packing and 1.0 at the top of the packing), and the other variables are as defined in section 1.3.1,

The assumptions made in writing equations 2.1 and 2.2 are that :

- (i) the mass transfer rate is given by $K_a \cdot S(y - y_g)$. This is the most widely used mass transfer rate expression for packed column mass transfer.
- (ii) axial dispersion has been ignored.
- (iii) the dead time following an upset has been ignored. The longest time delay would be for upsets in the liquid reflux rate to the top of the packing, as the liquid residence time is much greater than that of the vapour. If the dead time is significant, then the transformation of the time variable to:

$$t' = t - Z(1-Z)H/L \quad \dots (2.3)$$

could be made. The variable t would then be the total time elapsed since the upset and t' would be the time since the upset reached height z assuming plug flow. Since $dt'/dt = 1.0$, the dynamic mass balance equations would be unchanged by this transformation.

It will now be assumed that:

- (iv) there is no radial variation of the composition in either phase. This assumption is not required for equations 2.1 and 2.2 to be valid, provided that x and y are taken to be the mean compositions at height z .

The variation of liquid and vapour rate with height may be computed from an enthalpy balance, taking account of : (a) heat losses from the column, (b) the difference in the molal latent heats of the binary components, and (c) the heat of mixing if this is known. Such an enthalpy balance is presented in appendix 1.

In setting up the equations for the model, it will now be assumed that:

- (v) the liquid and vapour rates are constant throughout the column.
- (vi) the mass transfer coefficient is independent of column position, flow rate and composition. The likely variation in practice will be discussed further in chapter 6, and experimental values will be given in chapters 6 and 7.
- (vii) the liquid holdup and vapour holdup are constants. In chapter 6, it will be shown that the liquid holdup can be expected to vary strongly with liquid composition for the experimental column in this work, because the two components used have widely differing molecular weights. The liquid holdup is also expected to depend on liquid rate to the power of 0.6, so that for a change in liquid rate, there will be a change in H. The difficulty in predicting the rate of change of liquid holdup with time, is shown in chapter 8 to be a possible source of major problems in situations where the liquid holdup changes significantly. The molal vapour holdup will be independent of composition for ideal gases and will change very little with changes in flowrates.

With these assumptions included, the mass balance equations

$$\frac{H \partial x}{\partial t} = \frac{L \partial x}{Z \partial z} - \frac{K a S (y^* - y)}{G} \quad \text{.....(2.4)}$$

$$\frac{h \partial y}{\partial t} = \frac{-V \partial y}{Z \partial z} + \frac{K a S (y^* - y)}{G} \quad \text{.....(2.5)}$$

The assumptions made so far are those which have been used by previous workers (see chapter 1). No restricting assumptions have been required concerning the equilibrium relationship $y^*(x)$. This may be an

analytical function, or an empirical curve fitted to experimental data.

For convenience, $y^*(x)$ will be replaced by the symbol f where it is understood that f is a function of x .

Because the vapour holdup is usually small compared with the liquid holdup, the equations for the case of negligible vapour holdup will be developed together with the case for finite vapour holdup. For $h=0$, equation (2.5) becomes:

$$0 = \frac{-V_1 \partial y}{Z \partial z} + \frac{K_1 a_1 S (f-y)}{G} \quad \text{.....(2.5a)}$$

The equations are now written as:

$$-b_1 \frac{\partial y}{\partial z} - c_1 (y-f) = \frac{\partial y}{\partial t} \quad \text{.....(2.6)}$$

$$b_2 \frac{\partial x}{\partial z} + c_2 (y-f) = \frac{\partial x}{\partial t} \quad \text{.....(2.7)}$$

where: $b_1 = V_1 / (h, Z) \quad \text{.....(2.8)}$

$$c_1 = \frac{K_1 a_1 S}{h} = \frac{V_1 N_{OG}}{(Z, h)} \quad \text{.....(2.9)}$$

$$b_2 = L / (H, Z) \quad \text{.....(2.10)}$$

$$c_2 = \frac{K_2 a_2 S}{H} = \frac{V_2 N_{OG}}{(Z, H)} \quad \text{.....(2.11)}$$

and $N_{OG} = \frac{Z}{H} = \frac{Z}{(V/K_1 a_1 S)} \quad \text{.....(2.12)}$

N_{OG} is the number of overall gas-phase transfer units and

H is the height of an overall gas-phase transfer unit.

If $h = 0$ then (2.6) becomes:

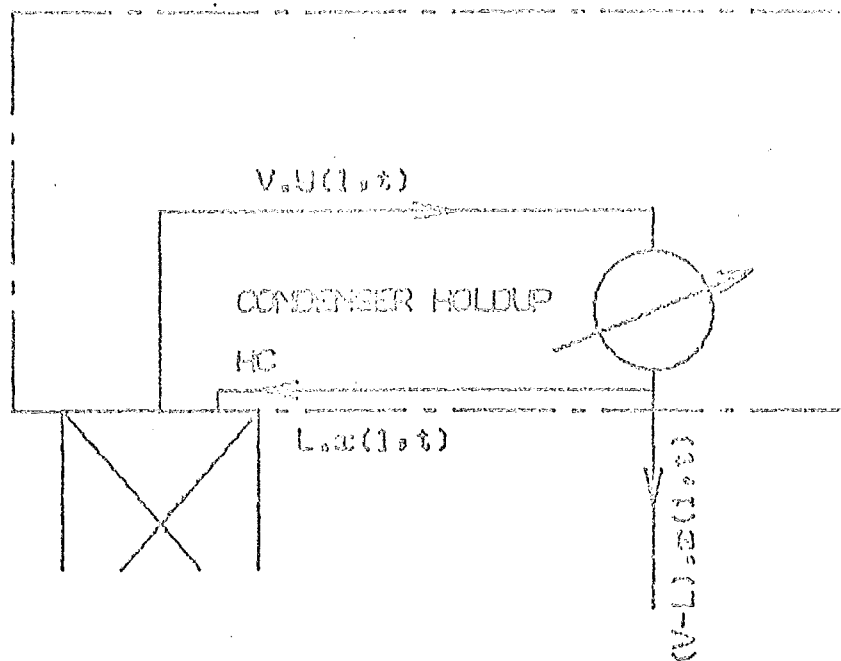


FIG 2.3

CONDENSER MASS BALANCE

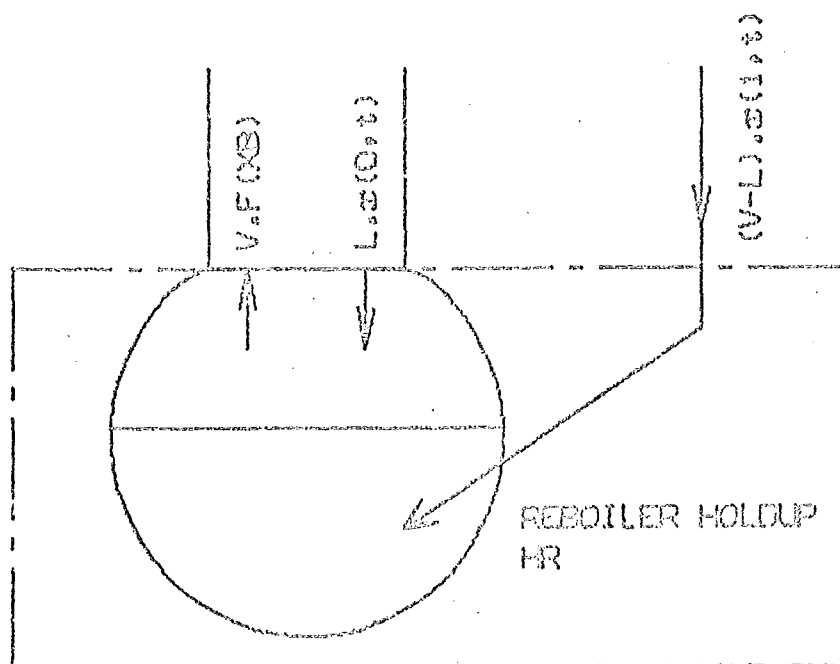


FIG 2.4

REBOILER MASS BALANCE

$$-b \frac{\partial y}{\partial z} - c (y-f) = 0 \quad \text{.....(2.6a)}$$

$$\text{with } b = \frac{V}{Z} \quad \text{.....(2.8a)}$$

$$\text{and } c = \frac{K a_1 S}{G} = \frac{V_1 N}{OG} \quad \text{.....(2.9a)}$$

Equations (2.6) and (2.7) are non-linear, implicit, hyperbolic, partial differential equations. The numerical solution of such equations is well described by von Rosenberg(1969). Two boundary conditions and two initial conditions are needed before the solution can be computed.

2.3 BOUNDARY CONDITIONS.

2.3.1 Condenser Boundary Condition.

The composition of the liquid returning from the condenser to the top of the column is provided by a mass balance around the condenser (fig. 2.3).

$$\frac{HC \cdot dx(1,t)}{dt} = V \cdot y(1,t) - V \cdot x(1,t) \quad \text{.....(2.13)}$$

where HC is the condenser holdup in moles. The notation $y(1,t)$ means y at height $z=1.0$ and time t . The condenser is thus represented by a first order stage with constant holdup. If the condenser holdup is not constant, this can easily be accounted for by including a term for $x(1,t) \cdot dHC/dt$ in equation (2.13). If desired, a deadtime could also be included by writing the equation as

$$\frac{HC \cdot dx(1,t)}{dt} = V \cdot y(1,t-DTC) - V \cdot x(1,t) \quad \text{.....(2.13a)}$$

where DTC is the condenser dead time.

When the condenser holdup is negligible, equation (2.13) reduces to:

$$y(1,t) = x(1,t) \quad \text{.....(2.13b)}$$

2.3.2 Reboiler Boundary Condition.

The composition of the vapour entering the bottom of the column is taken to be in equilibrium with the liquid in the reboiler.

$$\text{Thus } y(0,t) = f(XB) \quad \text{.....(2.14)}$$

where XB is the equilibrium composition in the reboiler. If XB does not change, then $y(0,t) = \text{const.}$ If XB changes with time, then $XB(t)$ is found from a mass balance around the reboiler (fig. 2.4).

$$\frac{HR \cdot dXB}{dt} = (V-L) \cdot x(1,t) + L \cdot x(0,t) - V \cdot f(XB) \quad \text{.....(2.15)}$$

where HR is the reboiler holdup in moles.

2.4 INITIAL CONDITIONS.

The initial conditions are the liquid and vapour composition profiles at time zero, i.e. $x(z,0)$ and $y(z,0)$. The initial condition may be a steady state, or a dynamic condition due to some previous upset. The equations for computing the steady state composition profiles are presented in the next section.

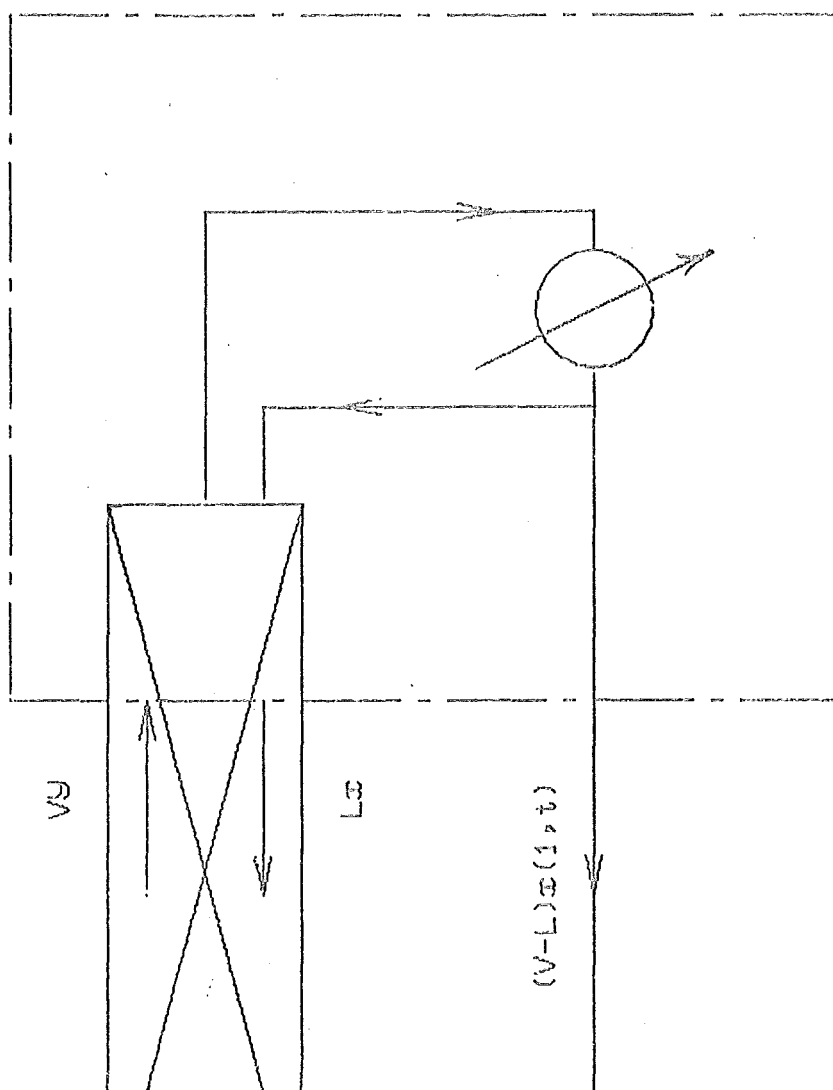


FIG 2.5 STEADY
STATE MASS BALANCE

2.4.1 Steady State Composition Equations.

The steady state is given by equations (2.8) and 2.9) with the time derivatives set to zero.

$$\text{I.e.:} \quad -b_1 \frac{dy}{dz} - c_1 (y-f) = 0 \quad \dots\dots(2.16)$$

$$\text{and} \quad b_2 \frac{dx}{dz} + c_2 (y-f) = 0 \quad \dots\dots(2.17)$$

Substituting for b_1 etc. leads to:

$$\frac{dy}{dz} = N_{OG} (f-y) \quad \dots\dots(2.18)$$

$$\text{and} \quad R \frac{dx}{dz} = N_{OG} (f-y) \quad \dots\dots(2.19)$$

where $R = L/V$. Note that these equations are independent of holdup.

An explicit relationship between x and y is also given by a mass balance around the envelope shown in fig. 2.5. The mass balance gives:

$$V.y = L.x + (V-L).x(1,0) \quad \dots\dots(2.20)$$

Any two of the three equations (2.18) to (2.20) will give the solution for $x(z)$ and $y(z)$ at steady state. The choice of equations will depend on whether it is necessary to determine any of the parameters (e.g. L, V, K_a) to match the boundary conditions. This choice will be discussed in section 3.2.

CHAPTER 3 NUMERICAL SOLUTION OF THE MODEL.

- 3.1 The Model In Finite Difference Form.
 - 3.1.1 The Dynamic Mass Balances.
 - 3.1.2 Boundary Conditions.
 - 3.1.3 Initial Conditions.
- 3.2 Solution Of The Steady State Equations.
 - 3.2.1 Reboiler Composition Unknown. Subroutine FINDXB.
 - 3.2.2 Reflux Ratio Unknown. Subroutine FINDR.
 - 3.2.3 Number Of Transfer Units Unknown. Subroutine
 FINDTU.
 - 3.2.4 Top Composition XD Unknown. Subroutine FINDXD.
- 3.3 Solution Of The Unsteady State.
- 3.4 Truncation Error In The Unsteady State Solution.

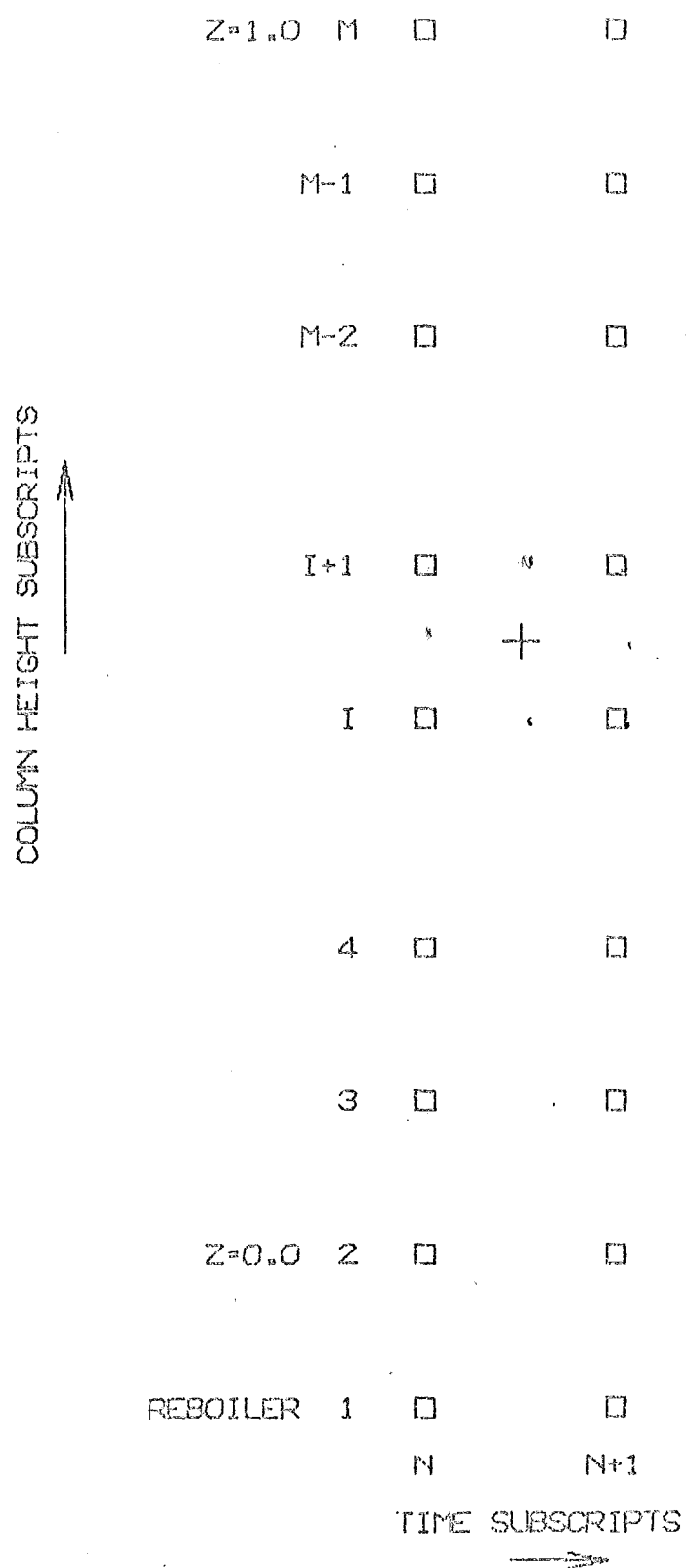


FIG 3.1

SUBSCRIPTS FOR X, Y AND F

3.1 THE MODEL IN FINITE DIFFERENCE FORM.

So that the equations can be expressed in finite difference form, the composition variables x , y and f are given subscripts as shown in fig. 3.1. The first subscript indicates height with 1 representing the reboiler, 2 the bottom of the packing, and m the top of the packing. The second subscript shows the number of time intervals since an upset was introduced into the column. Note that x_1 is identical to x_B , x_m to x_D , and that $f_1 = y_1 = y_2$.

The values which are calculated from the boundary conditions are x_1 (and hence y_2) and x_m . The problem is thus a split boundary value problem, since the boundary conditions give the value of one variable at one end of the packing and the other variable at the other end.

3.1.1 The Dynamic Mass Balances.

Equations (2.6) and (2.7) are converted to finite difference form by taking central differences at the point marked by + on fig 3.1. That is, the point $i+1/2, n+1/2$. At this point:

$$\left(\frac{\partial y}{\partial z}\right)_{i+1/2, n+1/2} = \frac{1}{2} \left(\frac{y_{i+1, n+1} - y_{i, n+1}}{\Delta z} + \frac{y_{i+1, n} - y_{i, n}}{\Delta z} \right) \quad \dots\dots(3.1)$$

$$\left(\frac{\partial y}{\partial t}\right)_{i+1/2, n+1/2} = \frac{1}{2} \left(\frac{y_{i+1, n+1} - y_{i+1, n}}{\Delta t} + \frac{y_{i, n+1} - y_{i, n}}{\Delta t} \right) \quad \dots\dots(3.2)$$

$$\left(\frac{\partial x}{\partial z}\right)_{i+1/2, n+1/2} = \frac{1}{2} \left(\frac{x_{i+1, n+1} - x_{i, n+1}}{\Delta z} + \frac{x_{i+1, n} - x_{i, n}}{\Delta z} \right) \quad \dots\dots(3.3)$$

$$\left(\frac{\partial x}{\partial t}\right)_{i+1/2, n+1/2} = \frac{1}{2} \left(\frac{x_{i+1, n+1} - x_{i+1, n}}{\Delta t} + \frac{x_{i, n+1} - x_{i, n}}{\Delta t} \right) \quad \dots\dots(3.4)$$

These centred difference approximations are second order correct.

The values of $y_{i+1/2,n+1/2}$ and $f_{i+1/2,n+1/2}$ are taken as:

$$y_{i+1/2,n+1/2} = 0.25(y_{i+1,n+1} + y_{i+1,n} + y_{i,n+1} + y_{i,n}) \quad \dots\dots(3.5)$$

$$f_{i+1/2,n+1/2} = 0.25(f_{i+1,n+1} + f_{i+1,n} + f_{i,n+1} + f_{i,n}) \quad \dots\dots(3.6)$$

These approximations are substituted into (2.6) and (2.7) to give:

$$\begin{aligned} AB.y_{i+1,n+1} = & -AA.y_{i,n+1} + AE(f_{i+1,n+1} + f_{i,n+1} + f_{i+1,n} + f_{i,n}) \\ & + AC.y_{i,n} + AD.y_{i+1,n} \quad \dots\dots(3.7) \end{aligned}$$

$$\begin{aligned} BB.x_{i+1,n+1} = & +BB.x_{i,n+1} - BA(y_{i+1,n+1} + y_{i,n+1} + y_{i+1,n} + y_{i,n} \\ & - f_{i+1,n+1} - f_{i+1,n} - f_{i,n+1} - f_{i,n}) \\ & + BC(x_{i,n} - x_{i+1,n+1}) \quad \dots\dots(3.8) \end{aligned}$$

where: $AA = -b + c + 1$
 $\frac{1}{\Delta z} \quad \frac{1}{2} \quad \frac{1}{\Delta t}$

$$AB = +b + c + 1$$

$$\frac{1}{\Delta z} \quad \frac{1}{2} \quad \frac{1}{\Delta t}$$

$$AC = +b - c + 1$$

$$\frac{1}{\Delta z} \quad \frac{1}{2} \quad \frac{1}{\Delta t}$$

$$AD = -b - c + 1$$

$$\frac{1}{\Delta z} \quad \frac{1}{2} \quad \frac{1}{\Delta t}$$

$$AE = c/2$$

$$1$$

$$BA = c/2$$

$$2$$

$$BB = -b - 1$$

$$\frac{2}{\Delta z} \quad \frac{1}{\Delta t}$$

$$BC = +b - 1$$

$$\frac{2}{\Delta z} \quad \frac{1}{\Delta t}$$

When $h=0$, the term $(1/\Delta t)$ is removed from the definitions for AA, AB, AC and AD. Also b_1 and c_1 are then defined by equations (2.8a) and (2.9a).

3.1.2 Boundary Conditions.

Taking central differences at time $n+1/2$ for the condenser equation (2.13) gives:

$$\frac{HC(x_{m,n+1} - x_{m,n})}{\Delta t} = 0.5V(y_{m,n+1} + y_{m,n}) - 0.5V(x_{m,n+1} + x_{m,n})$$

which is rearranged to:

$$x_{m,n+1} = \frac{(1-C)x_{m,n}}{(1+C)} + \frac{C(y_{m,n+1} + y_{m,n})}{(1+C)} \quad \dots (3.9)$$

where $C = 0.5(V \cdot \Delta t / HC)$.

Similarly for the reboiler at time $n+1/2$, equation (2.15) is expressed as:

$$(HP/\Delta t)(x_{1,n+1} - x_{1,n}) = 0.5(V-L)(x_{m,n+1} + x_{m,n})$$

$$+ 0.5L(x_{2,n+1} + x_{2,n}) - 0.5V(f_{1,n+1} + f_{1,n})$$

which yields:

$$x_{1,n+1} = x_{1,n} + (0.5\Delta t/HR) \left((V-L)(x_{m,n+1} + x_{m,n}) \right.$$

$$\left. + L(x_{2,n+1} + x_{2,n}) - V(f_{1,n} + f_{1,n+1}) \right) \dots (3.10)$$

3.1.3 Initial Conditions.

The initial condition equations must also be expressed in finite difference form, so that they can be used as the starting point for a dynamic solution. The value of x and y is needed at each grid point up the column. I.e. we need:

$$x_{i,0} \quad i=2,3,4,\dots,m$$

$$y_{i,0} \quad i=2,3,4,\dots,m$$

as well as the initial reboiler composition x_1 . As the initial condition will usually be a steady state condition, the steady state equations will now be written in terms of finite differences. The time subscript is dropped since x and y are time-independent at steady state.

Equation (2.20) in the new notation becomes:

$$y_{i+1} = R \cdot x_i + (1-R)x_m \quad \dots\dots(3.11)$$

Taking central differences we get:

$$\left(\frac{\partial y}{\partial z}\right)_{i+1/2} = \frac{y_{i+1} - y_i}{\Delta z}$$

$$\left(\frac{\partial x}{\partial z}\right)_{i+1/2} = \frac{x_{i+1} - x_i}{\Delta z}$$

$$y_{i+1/2} = 0.5(y_i + y_{i+1})$$

$$f_{i+1/2} = 0.5(f_i + f_{i+1})$$

Substitution in (2.18) and (2.19) gives:

$$y_{i+1} \left(\frac{1}{\Delta z} + 0.5N_{OG} \right) = y_i \left(\frac{1}{\Delta z} - N_{OG} \right) + 0.5N_{OG} (f_{i+1} + f_i) \quad \dots\dots(3.12)$$

$$x_{i+1} = x_i + (0.5M_{OG} \cdot \Delta Z/R) (f_{i+1} + f_i - y_{i+1} - y_i) \quad \dots (3.13)$$

The steady state boundary conditions in this notation are:

$$x_m = y_m \quad \dots (3.14)$$

$$\text{and } y_2 = f_1 \quad \dots (3.15)$$

3.2 SOLUTION OF THE STEADY STATE EQUATIONS.

As stated in section 2.4.1, any two of equations (2.18), (2.19) and (2.20) may be used to compute the values of x and y throughout the column at steady state. The choice of the equations depends on whether any of the variables X_B , X_D , R or N_{OG} are unknown. Provided any three of these four variables are specified, the fourth may be computed along with the x and y composition profiles in the packing. Fortran subroutines were written to obtain the solutions in all four cases. The method is briefly outlined below and the subroutines are listed in appendix 2.

When the steady state composition profiles are required, subroutine SSTATE is called. This subroutine will call another depending on which of the four variables is unknown.

3.2.1 Reboiler Composition Unknown. Subroutine FINDXB.

This subroutine is used when R, N_{OG} and X_D are known. Starting from the known top composition, it evaluates x and y moving down the column using equations (3.11) and (3.12). The equilibrium relationship subroutine, YSTAR, is then used iteratively to find the value of X_B which has an equilibrium value f_1 equal to the computed value of y_2 .

3.2.2 Reflux Ratio Unknown. Subroutine FINDR.

This subroutine is used when X_B , X_D and N_{OG} are specified. The

value of R is set first to 1.0 and adjusted until the value of X_B calculated by FINDXB is equal to the specified value of X_B . The initial step in R is $(1-R_{min})/2$ and the step size is halved at each step. R_{min} is the minimum reflux ratio which will give the required separation.

3.2.3 Number Of Transfer Units Unknown. Subroutine FINDTU.

With X_B , X_D and R specified, the number of transfer units is computed numerically using the equation :

$$N_{OG} = \int_{Y_1}^{Y_2} \frac{dy}{(f-y)} \quad \dots\dots(3.15)$$

subroutine FINDXB is then used to find the composition profiles in the column.

3.2.4 Top Composition X_D Unknown. Subroutine FINDXD.

Because equation (3.11) requires prior knowledge of the value of X_D (i.e. x_m), it is better to use equations (3.12) and (3.13). These still need an initial guess of the value of f at each point in the column. Subroutine FINDXD does this by assuming at first that f varies linearly with z , and then updates the f values at each succeeding iteration until convergence is obtained.

The first attempt at writing FINDXD made use of equations (3.11) and (3.12). A value of X_D was assumed for use in equation (3.11) and was then compared with the value of x_m found by integrating up the column using (3.11) and (3.12). The value of X_D was updated after each

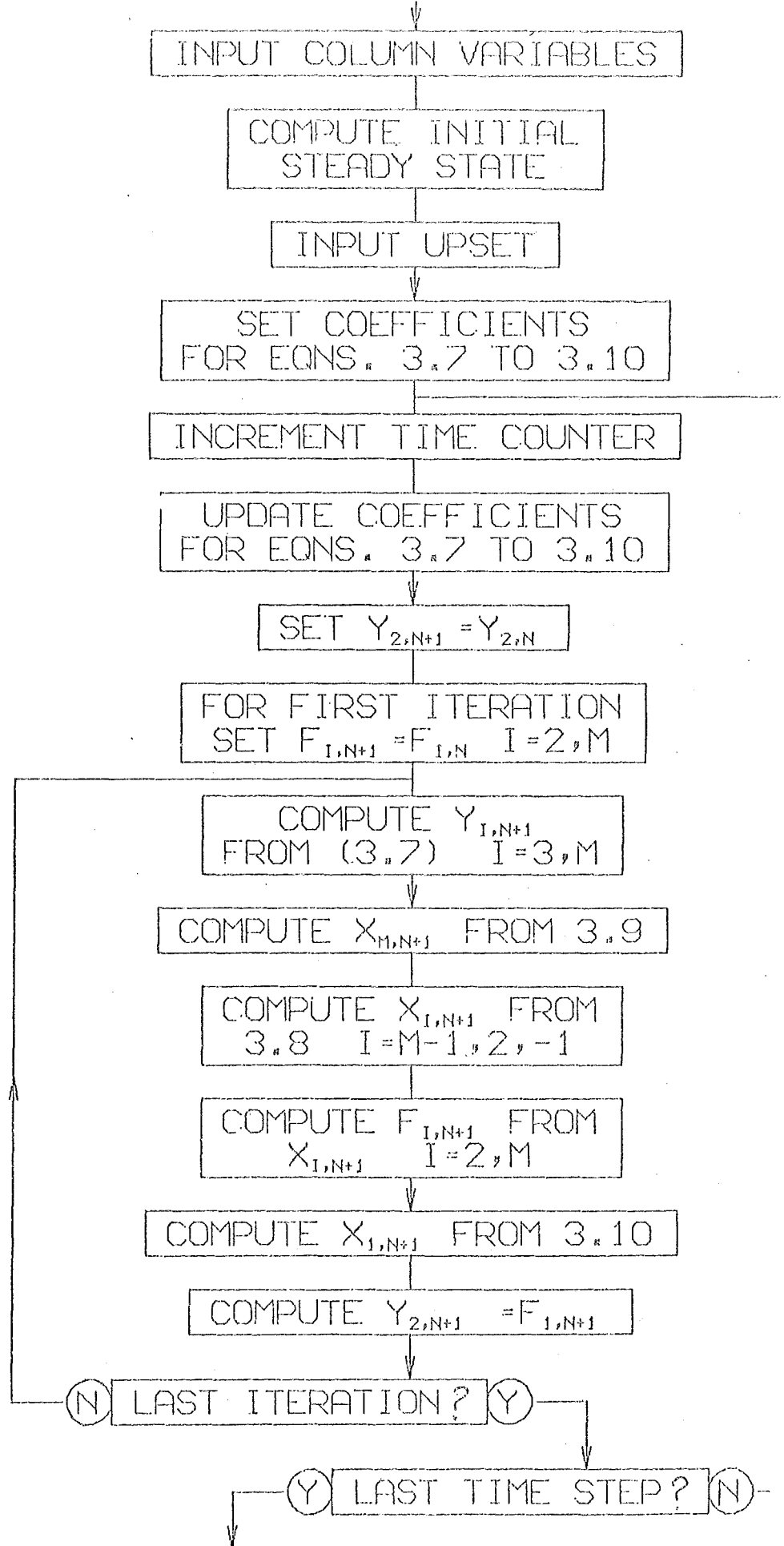


FIG 3.2

SOLUTION OF THE UNSTEADY-STATE EQUATIONS

iteration until agreement was found between X_D and x . This worked well for high reflux ratios, but for low reflux ratios (say $R < 0.8$), convergence became very difficult. This was because the bottom of the column was then in a very tight pinch zone, and a small error in the assumed value of X_D caused a very large error in the value of X_D obtained by integrating up the column.

3.3 SOLUTION OF THE UNSTEADY STATE.

It is required to compute x, y and f at time $n+1$ when all values at time n are known. (When $n=0$, then x and y are given by the initial steady state).

Since $y_{2,n+1}$ is given from the reboiler boundary condition, equation (3.7) would enable $y_{1,n+1}$ to be found explicitly for $i = 3, 4, \dots, m$ if all the $f_{1,n+1}$ were known. As they are not, an iterative solution is required. For the first iteration at time $n+1$, it is assumed that $f_{1,n+1} = f_{1,n}$. For subsequent iterations, the values of $f_{1,n+1}$ are updated after the $x_{1,n+1}$ have been found. After all the y values at time $n+1$ have been estimated from (3.7), the condenser boundary condition is used to give $x_{m,n+1}$. Equation (3.8) is then used to compute the x values working down the column. From the values of x thus obtained, the values of f at time $n+1$ are then updated. After the reboiler boundary condition has been used to update the value of $y_{2,n+1}$, a further iteration can be made at the same time. It was found that two iterations at each time step usually gave a convergence in all the compositions to within 0.0001 mole fraction. The decision to proceed to the next time step may be based on some convergence criteria, or a fixed number of iterations at each time step may be used. A flow diagram for the calculation is given

In fig. 3.2.

If L , V , H or K_a are expected to vary with composition, time, or position in the column, the coefficients in equations (3.7) and (3.8) can be updated at each time step. They would then be vectors, rather than constants, with a value for each height interval in the column.

A Fortran program to calculate the transient solution is listed in appendix 3. It is called MAINLINE1.

3.4 TRUNCATION ERROR IN THE UNSTEADY STATE SOLUTION.

von Rosenberg(1969) shows that for a single dependent-variable, hyperbolic, partial differential equation, there is zero truncation error in the finite difference approximation provided that $\Delta z/\Delta t = b_1$. With two dependent variables, a choice must be made between using b_1 and b_2 to set the time interval. It was decided that $\Delta z/\Delta t = b_2$ should be used. It seems reasonable to try to minimise the truncation error in the liquid composition, because the liquid holdup has a much greater bearing on the column dynamics than does the vapour holdup. On comparing the results of solutions with different sized increments, it was found that there was no truncation error for $\Delta z/\Delta t = b_2$ provided that Δz was not greater than 0.1. If Δt was given some value other than $\Delta z/b_2$ then the truncation error was proportional to $\left| \Delta t - \Delta z/b_2 \right|$.

TABLE 4.1 OPERATING CONDITIONS FOR RUNS DISCUSSED IN CHAPTER 4.

Variable	Run 1	2	3	4	5	6	7	8	9	10
Initial XB	0.2000	0.2000	0.1052	0.1052	0.1052	0.1052	0.1052	0.0500	0.0500	0.2000
Initial XD	0.6787	0.6825	0.8560	0.8000	0.7648	0.6337	0.5408	0.9811	0.4566	0.6825
Final XD	0.6525	0.5432	0.7247	0.7247	0.7247	0.7247	0.7247	0.4566	0.9811	0.6315
Initial R	0.82	0.80	1.00	0.90	0.85	0.70	0.60	1.00	0.92	0.80
Final R	0.80	0.70	0.80	0.80	0.80	0.80	0.80	0.92	1.00	0.70
NTU	4.0	5.0	8.0	8.0	8.0	8.0	8.0	10.0	10.0	5.0
Time interval	1.25	1.43	1.25	1.25	1.25	1.25	1.25	1.09	1.00	1.43

The following variables were the same for most or all runs:

vapour holdup = 0.0 liquid holdup = 10.0 condenser holdup = 0.0
 reboiler holdup = infinity (= 50.0 for run 10) packing height = 10.0
 height interval = 0.1
 equilibrium system: as for isopropanol-methanol (runs 1,2,8-10);
 linear relationship (runs 3-7).

CHAPTER 4 RESULTS OF THE COMPUTER SOLUTION OF THE MODEL.

- 4.1 Typical Results.
 - 4.1.1 Examples Of Near-Linear First Order Response Curves.
 - 4.1.2 Examples Of Non-Linear Response Curves.
 - 4.1.3 Comparison With Results Of Tomassi And Rice.
- 4.2 Fitting Of 'Time Constants' To The Transient Responses.
- 4.3 Effect Of Column Holdups.

The model was used to compute the response of the basic column to step changes in reflux ratio for a wide range of operating conditions. The responses were all computed assuming that the height of a transfer unit, holdups and vapour rate did not vary with position or time. Some results are illustrated and discussed in this chapter. The operating conditions for the runs considered are listed in table 4.1. A sample computer printout is included in appendix 3.

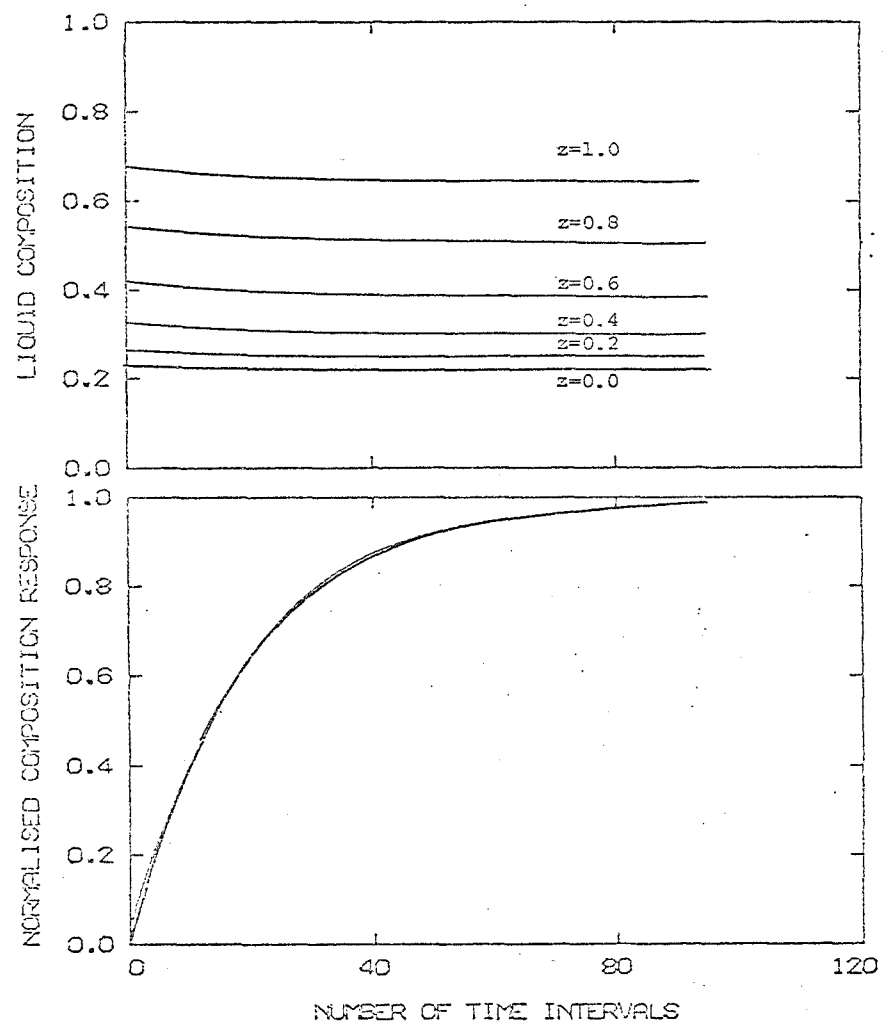


FIG 4.1 RUN 1

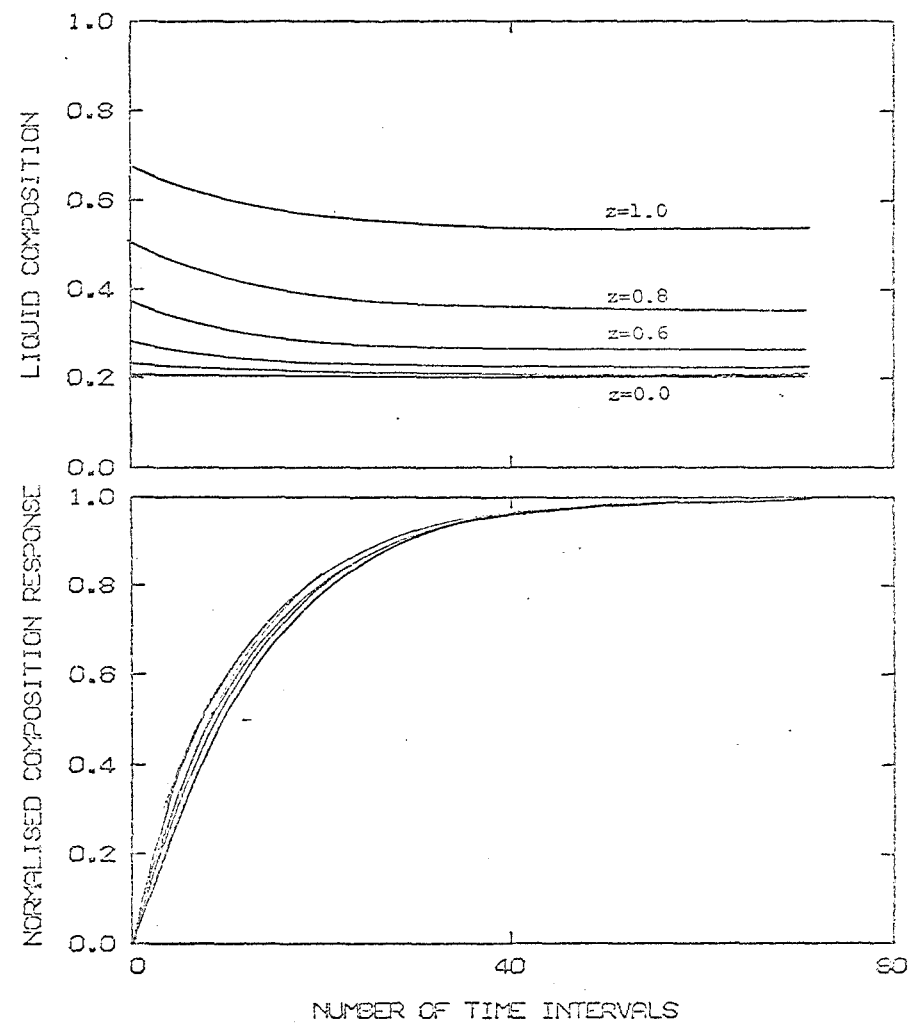


FIG 4.2 RUN 2

4.1 TYPICAL RESULTS.

The way in which the computed responses are presented is shown in fig. 4.1 for run 1. The upper graph is the composition response $x(z,t)$ for $z = 0.0, 0.2, 0.4, 0.6, 0.8$ and 1.0 . The lower graph contains the normalised response curves at these levels. The normalised response x_N is defined by:

$$x_N(z,t) = (x(z,t) - x(z,0)) / (x(z,\infty) - x(z,0)) \quad \dots (4.1)$$

4.1.1 Examples Of Near-Linear First Order Response Curves.

Runs 1 and 2 are examples of upsets which cause transients of the type produced by linear first-order systems.

$$\text{I.e.} \quad x_N(z,t) = 1 - \exp(-t/\tau) \quad \dots (4.2)$$

$$\text{or:} \quad x(z,t) = x(z,0) + (x(z,\infty) - x(z,0)) \cdot (1 - \exp(-t/\tau))$$

For run 1 (fig. 4.1), the composition changes were very small and the composition driving force $f-y$ did not change very much for any point in the column during the transient. Under these conditions, a response approximating to the form of equation 4.2 can be expected. Fig. 4.1 shows that the normalised response curves were almost coincident, so that the 'time constant' of 20 time intervals was virtually independent of height. For run 2 (fig. 4.2), the composition changed more than for run 1, but the normalised response curves again had a similar shape. The 'time constants' ranged from 11 time intervals at the bottom of the packing to 14 at the top.

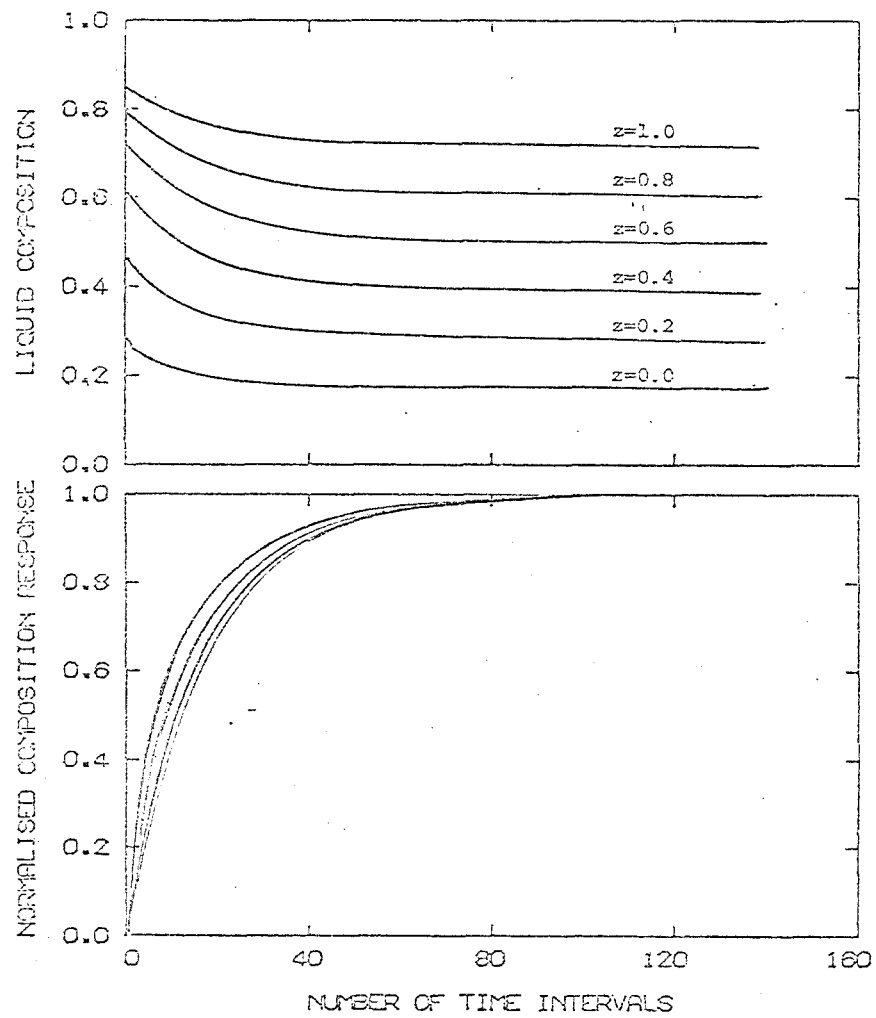


FIG 4.3 RUN 3

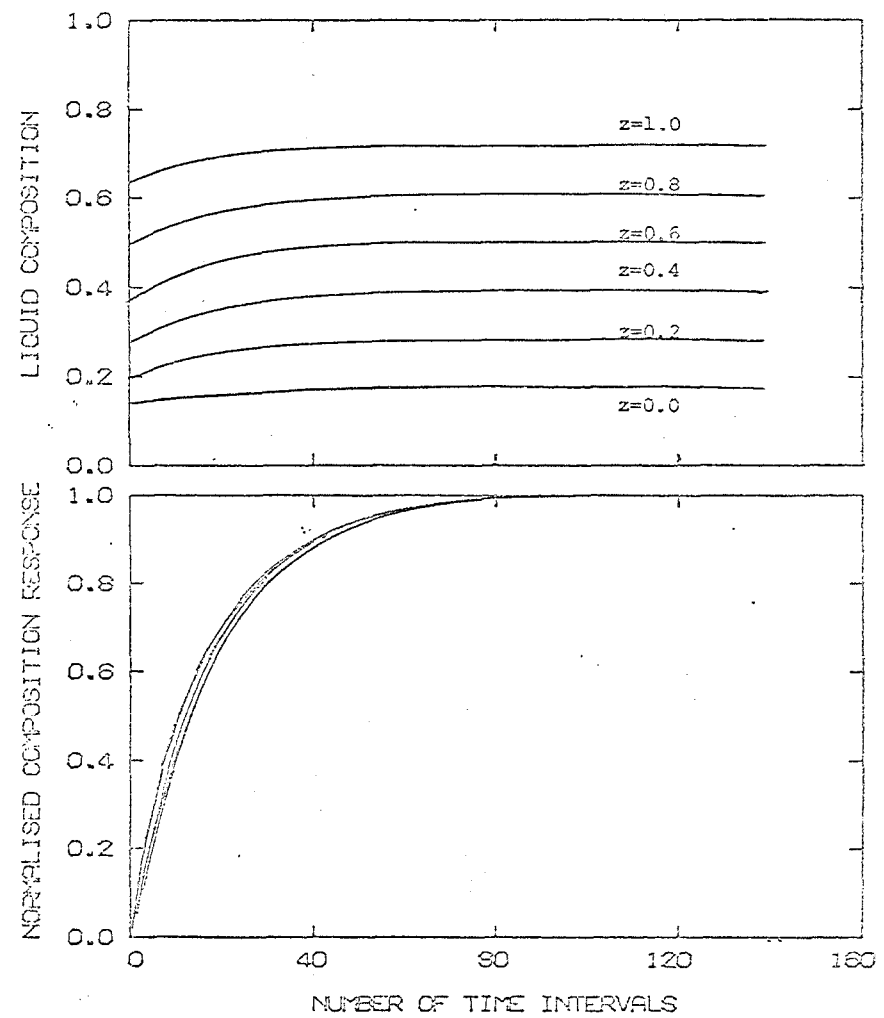


FIG 4.4 RUN 6

The equilibrium curve for runs 1 and 2 was based on the data of Ballard and van Winkle (1952) for isopropanol and methanol. For runs 3 to 7 a linear equilibrium relationship:

$$f = 0.2 + 0.8 x$$

was used. For these runs, responses fitting equation 4.2 were obtained, even for large changes in reflux ratio. However for large upsets, the 'time constants' tended to depend on the position in the column. For runs 3 to 7, the transients were computed for varying initial reflux ratios with the same final reflux ratio of 0.8 in each case. Fig. 4.3 shows the response for run 3 and fig. 4.4 shows that for run 6. The dependence of the 'time constant' on column position was obviously greater for the larger change (run 3) than for the smaller one (run 6). The response at $z=1.0$ for runs 3 to 7 is plotted in fig. 4.5. It shows the 'time constant' to be almost independent of the initial steady state, varying from 18 time intervals for run 3 to 15 time intervals for run 7. However at $z=0.0$, the 'time constant' varied from 11 to 23 time intervals for the same runs.

4.1.2 Examples Of Non-Linear Response Curves.

In this section, some results are shown where equation 4.2 would have to be extended to:

$$x_N(z,t) = 1 + \sum_{i=1}^n \frac{c_i}{1} \exp(-t/\tau_i) \quad \dots\dots(4.3)$$

to adequately describe the composition response curves. In equation 4.3 $\sum_{i=1}^n c_i = 1.0$ and the number of exponential terms, n , would usually range from 1 to 3.

Runs 8 and 9 (figs. 4.6 and 4.7) had response curves which equation 4.2 cannot model. In run 8, the response was fastest at $z=0.0$ and slowest at $z=1.0$. The curve for $z=1.0$ did not have its maximum slope

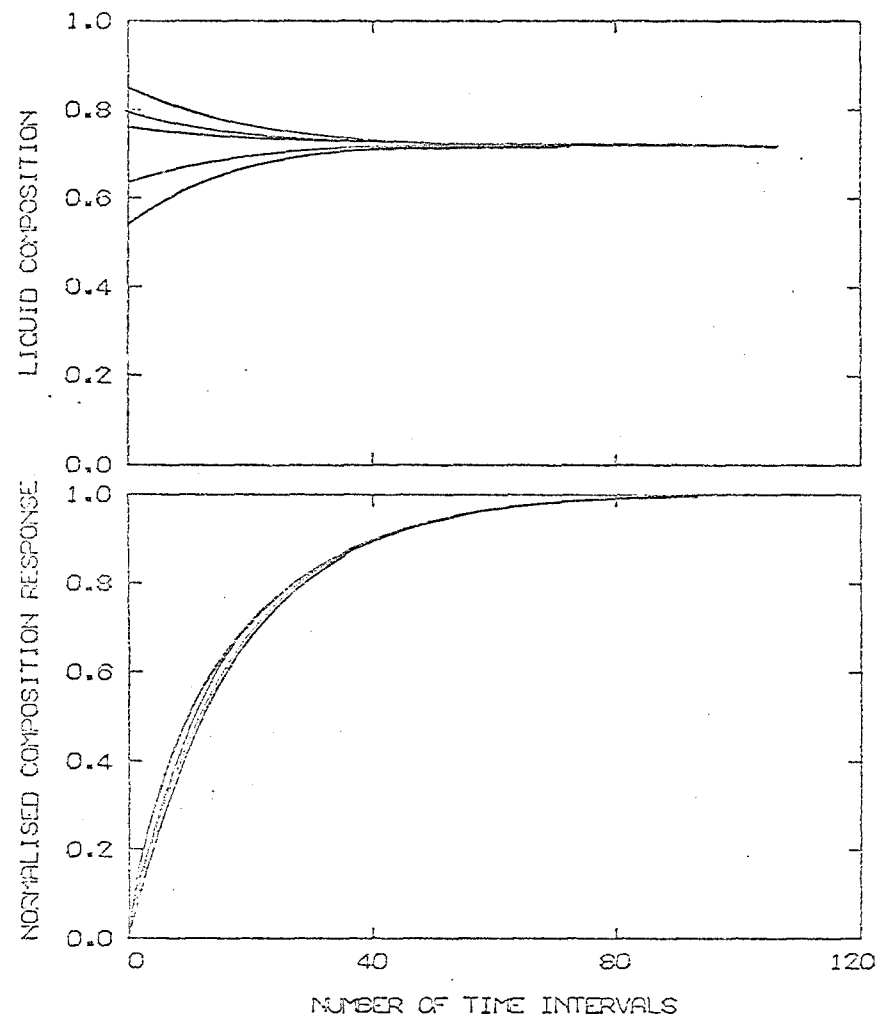


FIG 4.5 $Z=1.0$ RUNS 3-7

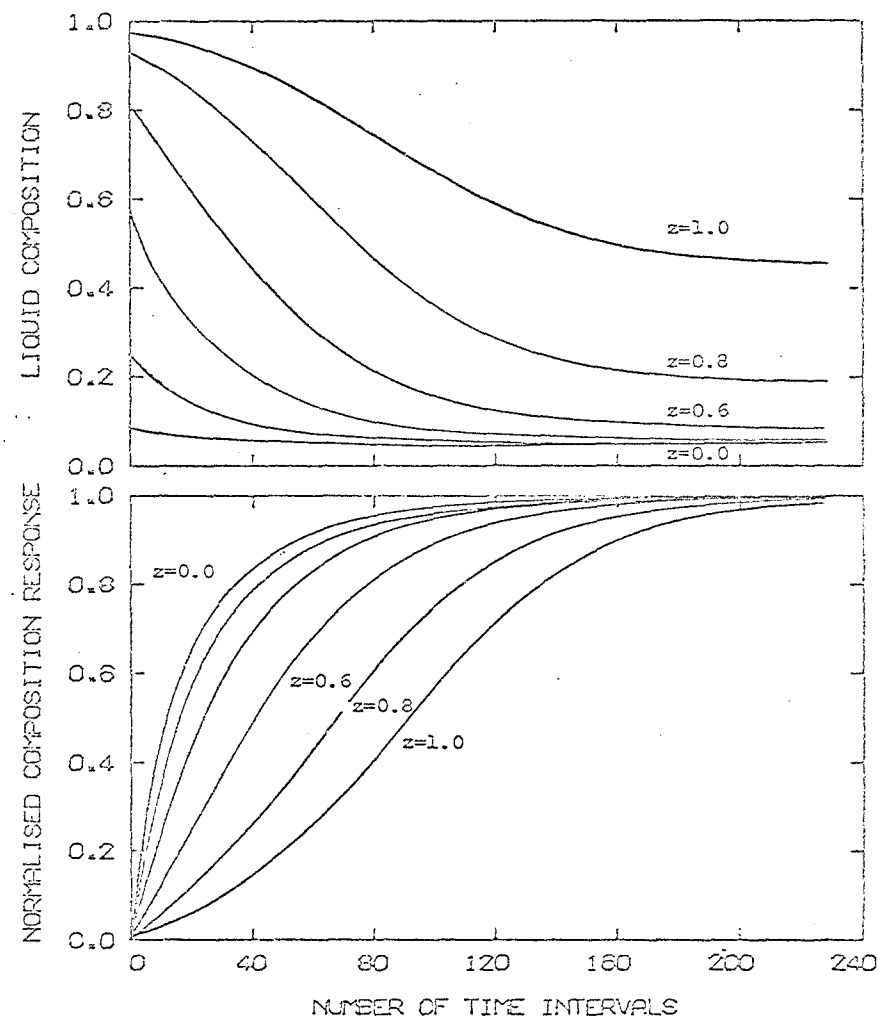


FIG 4.6 RUN 8

at the beginning but after some time had elapsed, showing that a linear first-order response did not describe it. In run 9, the reflux ratio was the reverse of that in run 8. The response was now most rapid at $z=1.0$ and slowest at $z=0.0$. The reasons for this change in response time with position in the column and direction of reflux ratio change can be explained in terms of the composition driving force $f-y$. Recalling equation 2.4:

$$\frac{H\partial x}{\partial t} = \frac{L\partial x}{Z\partial z} - K \frac{a}{G} S(f-y) \quad \text{.....(2.4)}$$

it can be seen that the rate of change of composition $\partial x/\partial t$ at a given height is proportional to the difference between $(L/Z)(\partial x/\partial z)$ and $K \frac{a}{G} S(f-y)$ at that level. At steady state, these terms are equal. Obviously if part of the column is in a pinch zone, where the operating and equilibrium lines are very close, then both terms on the right hand side of equation 2.4 must be small. Therefore the rate of composition change $\partial x/\partial t$ must also be small, since it depends on the difference between two small terms. If $(f-y)$ is large, then $\partial x/\partial z$ will also be large, so that when a change is made in the liquid rate, the difference between the two terms on the right hand side of the equation may also be large. This means that if the driving force is large for any level in the column at the start of a transient, but small at the end of it (e.g. $z=0.0$ in run 8), then the composition response at that level will initially be fast, but will slow as the transient proceeds. Conversely if the composition driving force is small at the start of a transient, but large at the end (e.g. $z=1.0$ for run 8), then the response will be slow at first, but will speed up as $f-y$ increases, and will eventually slow down as the new steady state is reached. This argument may be generalised as follows: the normalised composition response to a step change in reflux ratio will initially be fast at those levels which are moving into a pinch zone, and slow at those levels which are moving out of a pinch zone.

This is further illustrated in fig. 4.8 which shows the response at $z=1.0$ for a column going from initial reflux ratios of 1.0, 0.98, 0.96 and 0.94 to a final reflux ratio of 0.92 in each case. As expected,

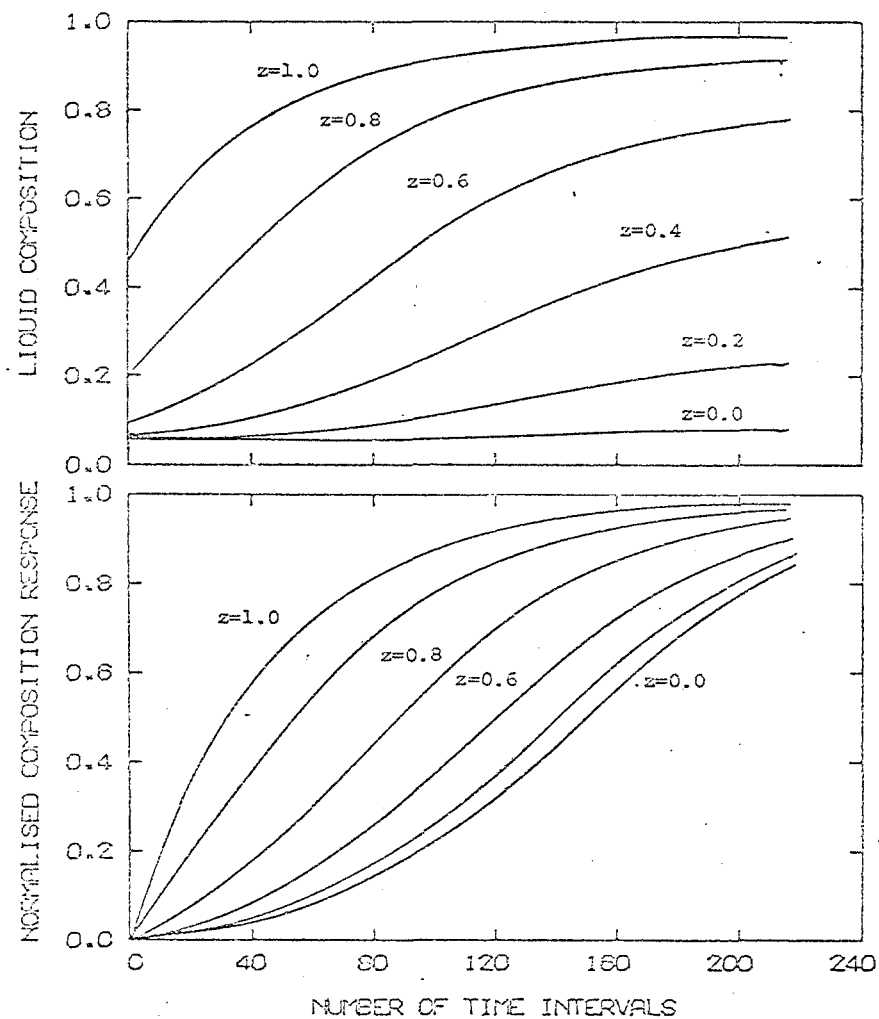


FIG 4.7 RUN 9

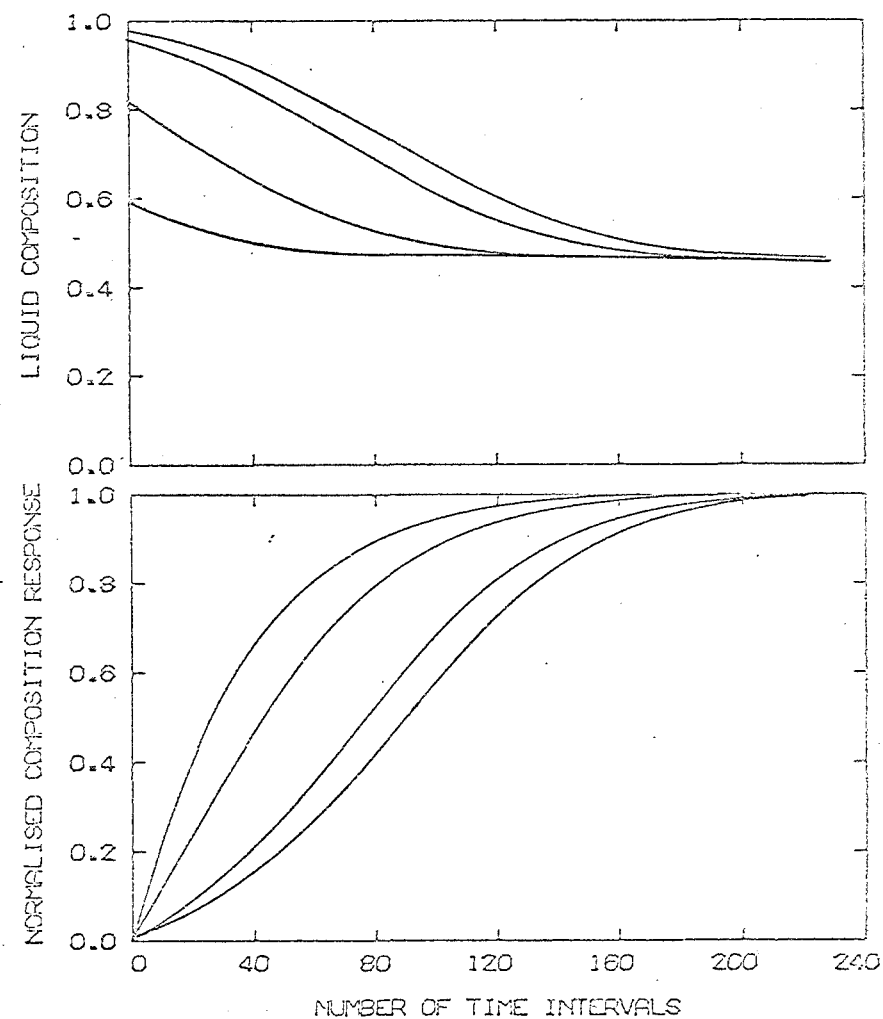


FIG 4.8 Z=1.0 VARIOUS INITIAL CONDITIONS

the response is slowest from the reflux ratio of 1.0 and fastest from that of 0.94. This is because for $R = 1.0$, $X_D = 0.981$ and the column must move out of a tight pinch zone at the top. For the initial reflux ratio of 0.94, $X_D = 0.588$ and the response was rapid in this case because the top of the column was not in a pinch zone.

The shape of the response curves has been shown to depend on the initial and final steady states as well as on the position in the column. Because of the large number of variables involved, there seems to be little point in trying to relate the coefficients and 'time constants' of an equation such as 4.3 to the parameters of the column being studied. Instead, if the composition at any level is required at a particular time, or as a function of time, this can be simply computed by the model as it stands. The computer solution is at least 100 times faster than the real time scale, so the model is suited to on-line work provided that the computer has sufficient storage. The time taken for the computer solutions, and the storage requirements, are discussed in appendix 3.

4.1.3 Comparison With Results Of Tomassi And Rice.

.....

The results of Tomassi and Rice(1970) are used as an example of the results of a model using a linear equilibrium relationship, in order to make a comparison with this study. Tomassi and Rice used an equilibrium curve linearised so that the computed compositions at the ends of the column at initial and final steady state matched their experimental values. This required prior knowledge of the final steady state. Their computed transients had the form:

$$x(z, \infty) - x(z, t) = \sum_{i=1}^n c_i \exp(s_i t) \quad \dots\dots(4.4)$$

This is similar to equation 4.3 except that in 4.4:

$$\sum_{i=1} c_i = x(z, \infty) - x(z, t) \quad \text{and} \quad s_i = -1/(\tau_i).$$

According to Tomassi and Rice, the coefficients c_i if normalised

so that $\sum_1 c_i = 1$, would depend only on z and the final steady state; while the first time constant τ_1 is either independent of, or a slowly varying function of, z . On the basis of three runs from different initial reflux ratios to the same final one, Tomassi and Rice concluded that the time constants depend on the final steady state, but not the magnitude of the disturbance or the initial steady state. We have already seen in section 4.1.1 that this need not be true. In runs 3 to 7 where the final steady state was the same in each case, the 'time constants' varied from 18 to 15 time intervals at $z = 1.0$, and from 11 to 23 time intervals at $z = 0.0$.

Tomassi and Rice state that linear theory predicts that the 'time constants' should be independent of z . They obtained this result when R was increased but not when R was decreased. Heinke et. al. (1965) found time constants practically independent of z , even when R was decreased. In the present study, this was found to be approximately true when the disturbances were small, but not for large disturbances. This is illustrated by the results in table 4.2 taken from runs 3 to 7.

TABLE 4.2 'TIME CONSTANTS' FOR RUNS 3-7. (FINAL $R = 0.80$).

Run	Initial R	'Time constants'		
		(Number of time intervals).		
		$z=1.0$	$z=0.6$	$z=0.0$
3	1.00	18.0	17.6	11.1
4	0.90	17.5	17.4	12.9
5	0.85	17.2	17.4	14.2
6	0.70	16.1	17.3	18.9
7	0.60	15.2	17.4	23.1

Table 4.2 shows that the 'time constant' depends on z more strongly for large disturbances than for small ones. The dependence of the 'time constant' on the initial steady state is also clearly seen for

$z=0.0$.

Both Heinke et. al. and Tomassi and Rice found, as the latter authors put it, "the relaxation time usually increased from top to bottom in experiments in which the reflux ratio was changed from a lower value to a higher value, and decreased when the reflux ratio was changed from a higher value to a lower one". These observations are explained by the column being in a pinch zone at the top for high reflux ratios but not for low reflux ratios.

4.2 FITTING OF 'TIME CONSTANTS' TO THE TRANSIENT RESPONSES.

There have been several schemes published for finding the time constants of a lumped-parameter system from its transient response. As an example, the method published by Thal Larsen (1955) is considered here. This will find up to three time constants representing a transfer function of the form:

$$G(s) = \frac{1}{(\tau_1 s + 1)(\tau_2 s + 1)(\tau_3 s + 1)}$$

To do this, it makes use of the times t_1 , t_2 , t_3 required for the normalised response to reach 0.1, 0.4 and 0.8 respectively. The ratio $(t_3 - t_1)/(t_2 - t_1)$ determines how many time constants are needed.

For one time constant, ratio = 3.725,

for two time constants, $3.725 > \text{ratio} > 2.92$,

for three time constants, $3.725 > \text{ratio} > 2.68$.

The evaluation of further ratios enables the actual values of the time constants to be found. The ratio given has been used to find how many time constants are needed to model the transient response curves of run 8. The numbers required appear in table 4.3. This shows that when $z=1.0$, more than three time constants would be needed to fit the

response, but at $z=0.0$ and $z=0.2$ the response is initially too rapid to be represented by even a single time constant.

TABLE 4.3 NUMBER OF 'TIME CONSTANTS' FOR TRANSIENTS OF RUN 8.

z	t_1	t_2	t_3	Ratio Number of time constants	
1.0	31	77	133	2.20	>3
0.8	18	56	107	2.34	>3
0.6	8	32	77	2.88	3
0.4	4	18	53	3.63	2
0.2	2	11	40	4.22	<1
0.0	1	8	33	4.57	<1

These results reinforce the conclusion drawn in section 4.1.2: that there is little point in trying to represent the non-linear distributed-parameter system as a linear lumped-parameter system, especially since the response of the distributed-parameter system can be obtained rapidly using a digital computer.

4.3 EFFECT OF COLUMN HOLDUPS.

For the runs described in section 4.1, the column was assumed to have zero vapour holdup, zero condenser holdup, and infinite reboiler holdup. Further runs were done to find the effect of including these holdups. Run 2 (fig. 4.2) was used as the basis for comparison. The total holdup in the packing for run 2 was 100 moles.

(1) Effect of vapour holdup. Runs were done for h ranging from 0.1 to 5.0 mol/m. I.e. from 1% to 50% of the liquid holdup. The effect of increasing vapour holdup was to increase the response time throughout the column, but the effect was more noticeable at the top of the column where the composition gradient was greatest.

Table 4.4 gives the 80% response time (i.e. the time at which the normalised response reaches 0.8) for different heights in the packing for various vapour holdups. It shows that the effect of the vapour holdup on the response time is small until the vapour holdup exceeds 10% of the liquid holdup. This is unlikely to happen in columns operating at atmospheric pressure.

TABLE 4.4 EFFECT OF VAPOUR HOLDUP ON RESPONSE TIME.

z	h = 0.0	0.1	0.5	1.0	2.0	5.0
0.0	17	17	17	18	19	21
0.6	19	19	19.5	20	21	25
1.0	19.5	19.5	20	21	22.5	27

(ii) Effect of condenser holdup. The condenser holdup H_C was varied from 1 to 20 moles. This increased the response times at the top of the column while having little effect further down. The 80% response time at some levels in the column for various values of condenser holdup is given in table 4.5. This clearly shows that the effect of condenser holdup decreases rapidly with distance down the column. It indicates that if the condenser holdup is small relative to the liquid holdup (say less than 5%), then the error introduced by ignoring it will be slight. However a condenser holdup of 10% of the total liquid holdup caused an increase in response time of 15% at the top of the column. Clearly the condenser holdup cannot be ignored if it is large compared with the holdup in the packing, as it may be if the condensate is taken to an external reflux divider. In such a case, it may also be necessary to include the effects of the distance-velocity lag in the condenser boundary condition equation.

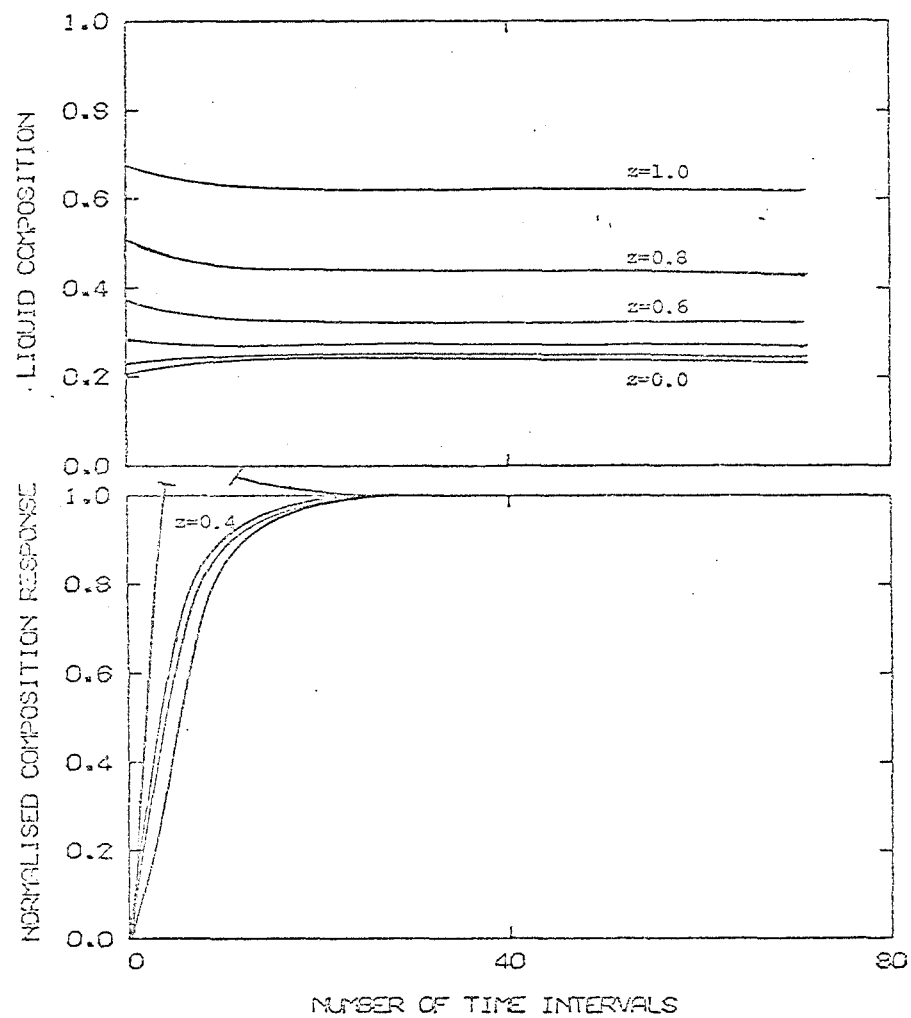


FIG 4.9 RUN 10

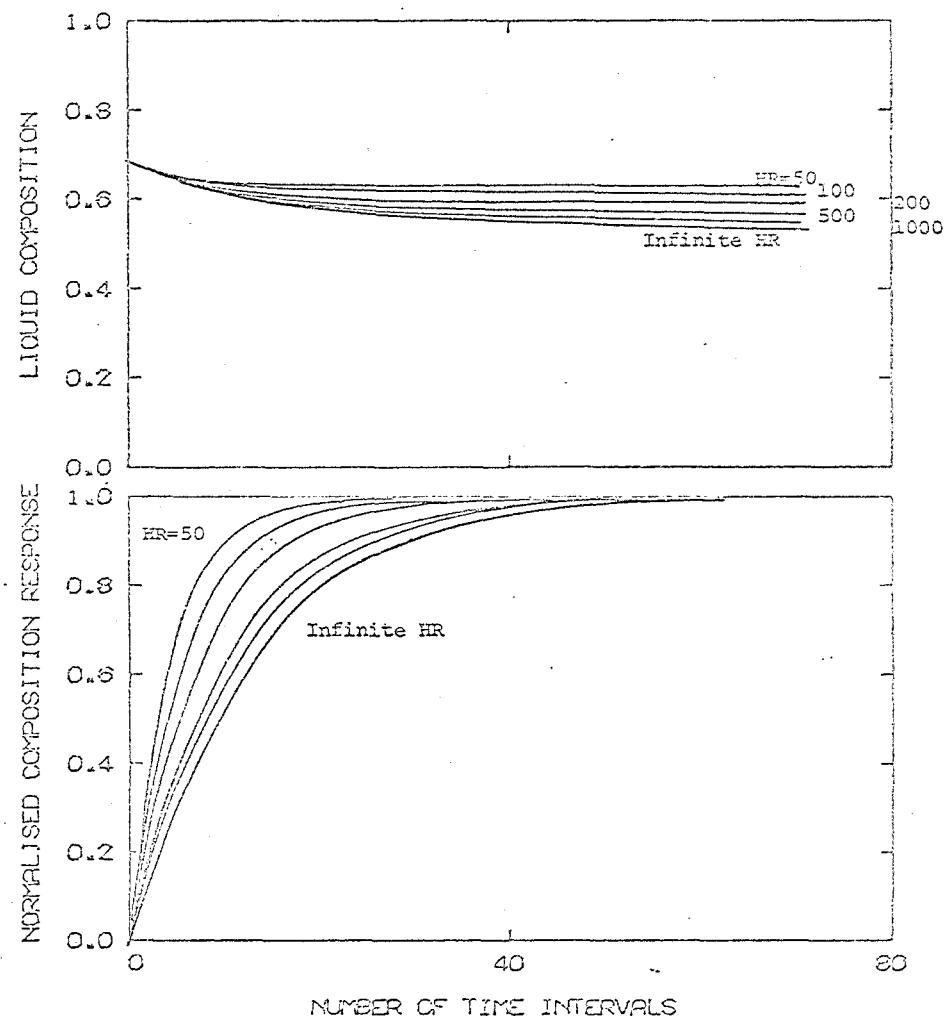


FIG 4.10 Z=1.0 VARIOUS REBOILER HOLDUPS

TABLE 4.5 EFFECT OF CONDENSER HOLDUP ON RESPONSE TIME.

z	HC = 0.0	1.0	2.0	5.0	10.0	20.0
1.0	19.5	20	20	20.5	22.5	25.5
0.6	19	19	19	19.5	20	22
0.0	17	17	17	17	17	18

(iii) Effect of reboiler holdup. For the basic column shown in fig. 2.1, the reboiler composition X_B will remain constant provided that the reboiler holdup is extremely large compared with that of the packing. For a column with finite reboiler holdup, the reboiler composition will change following an upset. E.g. following an increase in the reflux ratio, the liquid composition will begin to increase throughout the packing. Since the column is a closed system, this must be compensated for by a decrease in the reboiler composition. The size of the change in X_B will depend on the size of the reboiler holdup. These two changes tend to cancel out the effect each other has on the composition at any level. As a result, the time taken to reach a new steady state is less when the reboiler holdup is finite.

In fig. 4.9, the response is given for run 10 which was identical to run 2, except that the reboiler holdup was set to 50 moles instead of infinity. A comparison of fig. 4.9 with fig. 4.2 shows that the small reboiler holdup gave a much faster response and a different final steady state. The overshoot in the normalised response for $z=0.4$ in fig. 4.9 was because the composition at that level first decreased due to the change in the liquid rate, and then increased due to the change in reboiler composition.

Fig. 4.10 shows the response at $z=1.0$ for reboiler holdups ranging from 50 to infinity. Even with a reboiler holdup of 1000 moles, (i.e. 10 times greater than the holdup in the packing), there is a noticeable difference in the speed of the response and the final steady state compared with the case of infinite holdup.

The influence of the reboiler holdup will depend not only on its size in relation to the packing holdup, but also on the composition gradient at the bottom of the column. If the composition gradient is very small at $z=0.0$, but large further up the column, then a change of say 0.01 in X_B will give a large change in the compositions at levels above the bottom pinch zone. However, if the composition gradient is large at $z=0.0$, then a small change in X_B will have little effect on compositions further up the column.

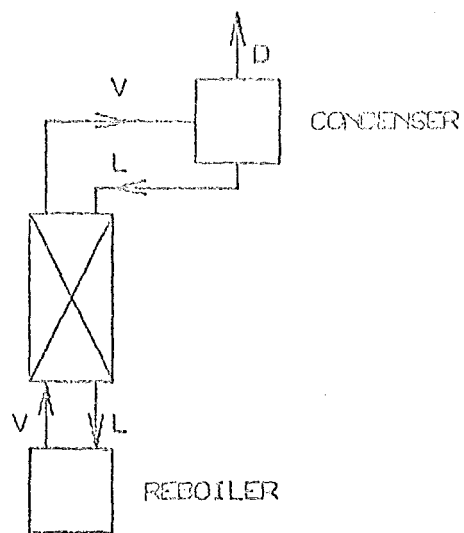
Previous workers have not taken into account the effect of reboiler composition changing during a run, despite the fact that it can be very important. They have expressed their reboiler boundary condition in terms of constant reboiler composition or constant vapour composition entering the bottom of the packing. This amounts to the same thing as infinite reboiler holdup.

(iv) Effect of liquid holdup. For a column with infinite reboiler holdup, zero condenser holdup, and zero vapour holdup, the response time is directly proportional to the liquid holdup and inversely proportional to the liquid rate. For other values of the reboiler, condenser and vapour holdups, the response will be identical and the response time will be proportional to the liquid holdup, provided that the ratio of the holdups is unchanged. If only the liquid holdup is changed, the response time will be proportional to the liquid holdup, but the final steady state will be different.

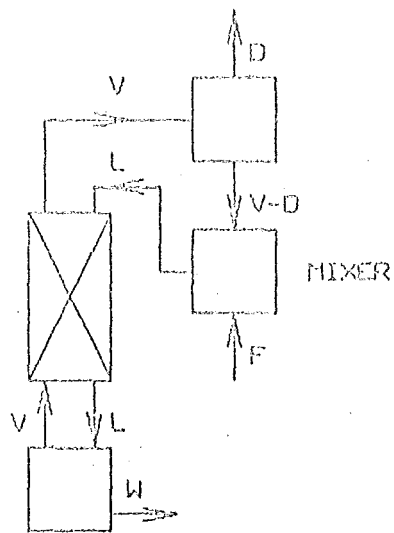
CHAPTER 5 MODIFICATIONS TO THE MODEL FOR OTHER COLUMN ARRANGEMENTS.

- 5.1 The Columns To Be Modelled.
- 5.2 The Dynamic Mass Balance Equations.
- 5.3 Boundary Conditions.
 - 5.3.1 Top Boundary Condition.
 - 5.3.2 Bottom Boundary Condition.
 - 5.3.3 Feed Point Boundary Conditions.
- 5.4 Initial Conditions.
- 5.5 Solution Of The Equations.
- 5.6 Unsteady State Responses From The Column Models.
 - 5.6.1 The Batch Column.
 - 5.6.2 The Stripping And Enriching Columns.
 - 5.6.3 The Continuous Column.

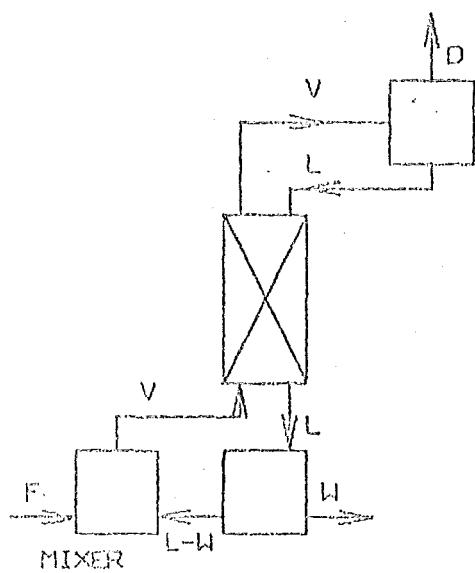
In this chapter, it will be shown how the mathematical model of the basic column, developed in chapter 2, can be modified to handle some columns of practical interest.



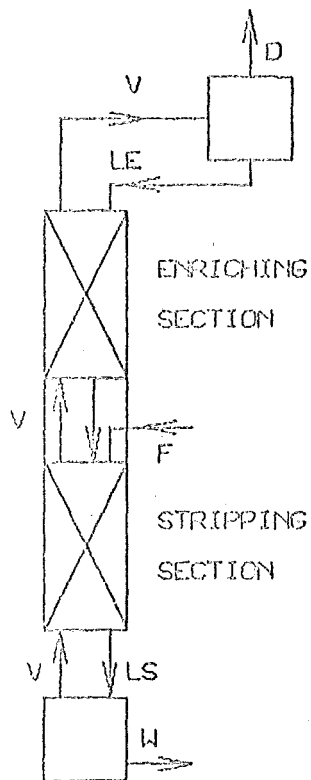
(A) BATCH COLUMN



(B) STRIPPING COLUMN



(C) ENRICHING COLUMN



(D) CONTINUOUS COLUMN

FIG. 5.1 THE COLUMNS MODELLED

5.1 THE COLUMNS TO BE MODELLED.

The column arrangements which will be considered are shown in fig.

5.1. They are:

Column 2.	A batch column.	Fig. 5.1(A)
Column 3	A stripping column.	Fig. 5.1(B)
Column 3A	A stripping column as in fig. 5.1(B), but with no condenser, so that all the vapour from the top of the column is removed as top product, and the liquid entering the top of the packing comes only from the feed.	
Column 4	An enriching column.	Fig. 5.1(C)
Column 4A	An enriching column as shown in fig. 5.1(C), but with no reboiler, so that the vapour entering the column comes only from the feed, and all liquid leaving the bottom of the packing is removed as bottom product.	
Column 5	A continuous column with a feed stream entering part-way up the packing.	Fig. 5.1(D)

Additional notation used in this chapter includes:

D	distillate rate	mol/s
F	feed rate	mol/s
XB	bottom product composition (reboiler composition)	
XD	top product composition (distillate composition)	
XF	feed composition	
W	bottom product rate	mol/s

In modelling the continuous column, the following new notation is needed:

y_e, y_s	equilibrium vapour composition in the enriching and stripping sections (respectively)	
x_e, x_s	liquid composition in the enriching and stripping sections	

y_e, y_s vapour composition in the enriching and stripping sections
 L_e, L_s liquid flowrate in the enriching and stripping sections
 V_e, V_s vapour flowrate in the enriching and stripping sections

5.2 THE DYNAMIC MASS BALANCE EQUATIONS.

For all the columns, the mass balance equations from section 2.2 still apply. Note however, that for the continuous column, there will usually be a different set of coefficients (equations 2.8 to 2.12) for each packing section, because of the differing flowrates and other variables in the two sections.

5.3 BOUNDARY CONDITIONS.

5.3.1 Top Boundary Condition.

=====

The equations from section 2.3.1 are directly applicable to the batch, enriching and continuous columns. For the stripping column, the mass balance of equation 2.13 will give $x_D(t)$ instead of $x(1,t)$. To compute $x(1,t)$, the further mass balance:

$$L \cdot x(1,t) = F \cdot x_F + (V-D) \cdot x_D \quad \dots\dots(5.1)$$

is needed.

For the stripping column with no condenser, the top boundary condition equations are:

$$x(1,t) = x_F ; L = F ; x_D = y(1,t) ; D = V \quad \dots\dots(5.2)$$

5.3.2 Bottom Boundary Conditions.

The reboiler boundary condition for the basic column cannot be applied directly to any of the columns in this chapter. However the boundary condition is still found in a similar manner.

(i) The batch column. The reboiler holdup in this case is always decreasing with time. The mass balance is thus:

$$\frac{d(HR.XB)}{dt} = L.x(0,t) - V.f(XB)$$

Since $dHR/dt = L-V$, then:

$$\frac{HR.dXB}{dt} + XB(L-V) = L.x(0,t) + V.f(XB) \quad \dots\dots(5.3)$$

Putting this in finite difference form at time $n+1/2$, and recalling that $XB = x_{1,t}$, gives:

$$x_{1,n+1} = x_{1,n} \frac{\left(\frac{HR}{\Delta t} - 0.5(L-V) \right) - 0.5V(f_{1,n+1} + f_{1,n}) + 0.5L(x_{2,n+1} + x_{2,n})}{\left(\frac{HR}{\Delta t} + 0.5(L-V) \right)} \quad \dots\dots(5.4)$$

where $HR_{n+1/2} = HR_n + 0.5(L-V)/\Delta t$

(ii) The stripping column and the continuous column.

Assuming constant reboiler holdup, the reboiler mass balance is:

$$\frac{HR.dXB}{dt} = L.x(0,t) - V.f(XB) - W.XB \quad \dots\dots(5.5)$$

This is similar to equation 2.15 and may be expressed in finite difference form in the same way as for equation 5.3. If the reboiler holdup varies, the term $XB.dHR/dt$ must be added to the left hand side of equation 5.5.

(iii) The enriching column. When there is a reboiler as shown in fig. 5.1(C), the mass balance is:

$$\frac{dX_B}{dt} = L \cdot x(0,t) - (L-W)f(X_B) - W \cdot X_B \quad \dots\dots(5.6)$$

A mass balance for the vapour mixer enables the vapour composition entering the packing to be found from:

$$y(0,t) = F \cdot X_F / V + (L-W)f(X_B) / V \quad \dots\dots(5.7)$$

If there is no reboiler, but only a vapour feed at its dew point, then the equations at the bottom of the column are:

$$y(0,t) = X_F ; V = F ; X_B = x(0,t) ; W = L \quad \dots\dots(5.8)$$

5.3.3 Feed Point Boundary Conditions.

For the continuous column, two further boundary condition equations are required at the feed point. These are found from liquid and vapour mass balances. Assuming that the feed is a liquid at its bubble point, we get:

$$L_S = L_E + F$$

$$L_S \cdot x_s(1,t) = L_E \cdot x_e(0,t) + F \cdot X_F$$

therefore:

$$x_s(1,t) = (L_E \cdot x_e(0,t) + F \cdot X_F) / (L_E + F) \quad \dots\dots(5.9)$$

The vapour from the top of the stripping section is then assumed to pass unchanged to the enriching section. Thus:

$$y_e(0,t) = y_s(1,t) \quad \dots\dots(5.10)$$

If the feed is not a liquid at its bubble point, then an enthalpy

balance is needed to compute the amount of saturated liquid and vapour leaving the feed zone.

5.4 INITIAL CONDITIONS.

In modelling all the columns in this chapter, it was assumed that steady state conditions prevailed up to zero time, at which point an upset was introduced.

The assumption that the batch column was at steady state at time zero, meant that the equations for the basic column could be used to find its initial composition profile. Thus the same computer subroutines were used to find the initial steady state for the batch column, as were used for the basic column.

For the other columns, the initial condition equations are the same as the dynamic equations, but with all time derivatives set to zero.

5.5 SOLUTION OF THE EQUATIONS.

Computer subroutines were written to find the initial composition profiles for the stripping, enriching and continuous columns. The variables chosen to be specified or computed in the subroutines were:

(i) Stripping column:

N , V , X_B , W , X_F and L were specified;
OG

X_D , F , D , $x(z)$, $y(z)$ and $f(z)$ were computed.

(ii) Enriching column:

N , V , X_B , D , X_F and L were specified;
OG

X_D , F , W , $x(z)$, $y(z)$ and $f(z)$ were computed.

(iii) Continuous column:

N for each section, all flows and XB were
OG
specified;
XD, XF x(z), y(z) and f(z) were computed.

The subroutines solved the equations by a similar approach to that of subroutine FINDXD, although no convergence forcing was needed. Listings of these subroutines can be obtained from the author.

The unsteady state equations for the batch, stripping, enriching and continuous columns were solved using mainline programs similar to MAINLINE1 for the basic column. Listings of these programs are also available from the author.

5.6 UNSTEADY STATE RESPONSES FROM THE COLUMN MODELS.

5.6.1 The Batch Column.

.....

The batch column model gave stable transient responses whether the model was run with a constant reflux ratio throughout a run, or with the reflux ratio altered according to some time-schedule, as is often done in batch distillation. To give a check on the validity of the solution, an inventory of the more volatile component was computed throughout the batch run. The total amount of the more volatile component in the reboiler, packing, condenser and product receiver, was found to vary by a trivial amount, typically about 0.01 per cent.

5.6.2 The Stripping And Enriching Columns.

.....

The response predicted by the models for these columns was studied for step change upsets in the feed rate, feed composition, distillate rate, and for combinations of these upsets. The transient response

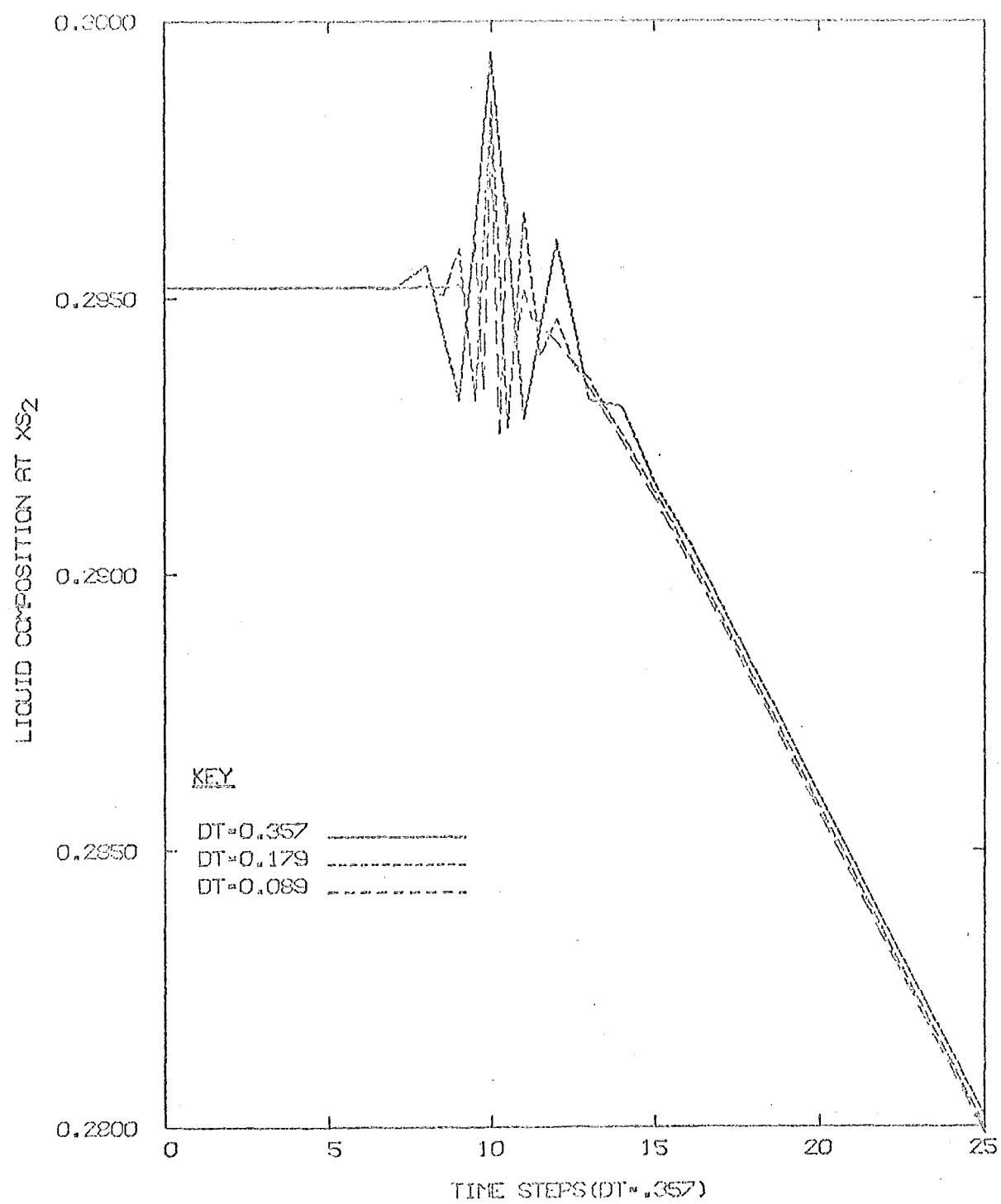


FIG. 5.2 OSCILLATION
IN THE NUMERICAL SOLUTION

curves are similar to those obtained for the basic column. The response again tends to be faster for the part of the column moving into a pinch zone, and slower for the part of a column moving from a pinch zone. The vapour holdup has a negligible effect on the dynamics if it is small, while the reboiler holdup again dominates the response. However these columns tended to respond to an upset more quickly than the basic column, presumably because the presence of a bottom product stream enabled the reboiler to respond more quickly.

For both types of column, a negative composition gradient (dx/dz) could exist in the packing for some time after a large upset. This could result from increases in XF or F for the enriching column; or from increases in D or F , or decreases in XF for the stripping column.

A dimensionless height interval of 0.1 was always found to be satisfactory for the stripping column. In some cases for the enriching column, an interval of 0.05 was needed to give stability in the steady state computation. The largest interval which gave stable steady state results was always found to give stable dynamic results.

An upset which caused a step change in conditions at the top of the packing also caused an oscillation in the numerical solution to be propagated down the packing. The oscillation usually had its greatest amplitude at the bottom of the packing. However, the oscillation in the numerical solution always quickly died away, and the solution was completely stable from then on.

To illustrate this effect, fig. 5.2 shows the early part of the response at the bottom of the packing in a stripping column to a decrease in distillate rate. The oscillation occurs as the effects of the upset are first felt at that point. The graph shows the response for three different step sizes ($dz=0.1$, $dt=0.357$; $dz=0.05$, $dt=0.179$; and $dz=0.025$, $dt=0.089$). Decreasing the step size is seen to decrease the time for which the oscillation lasts considerably, but to have little effect on the maximum amplitude. After the numerical oscillation has died away,

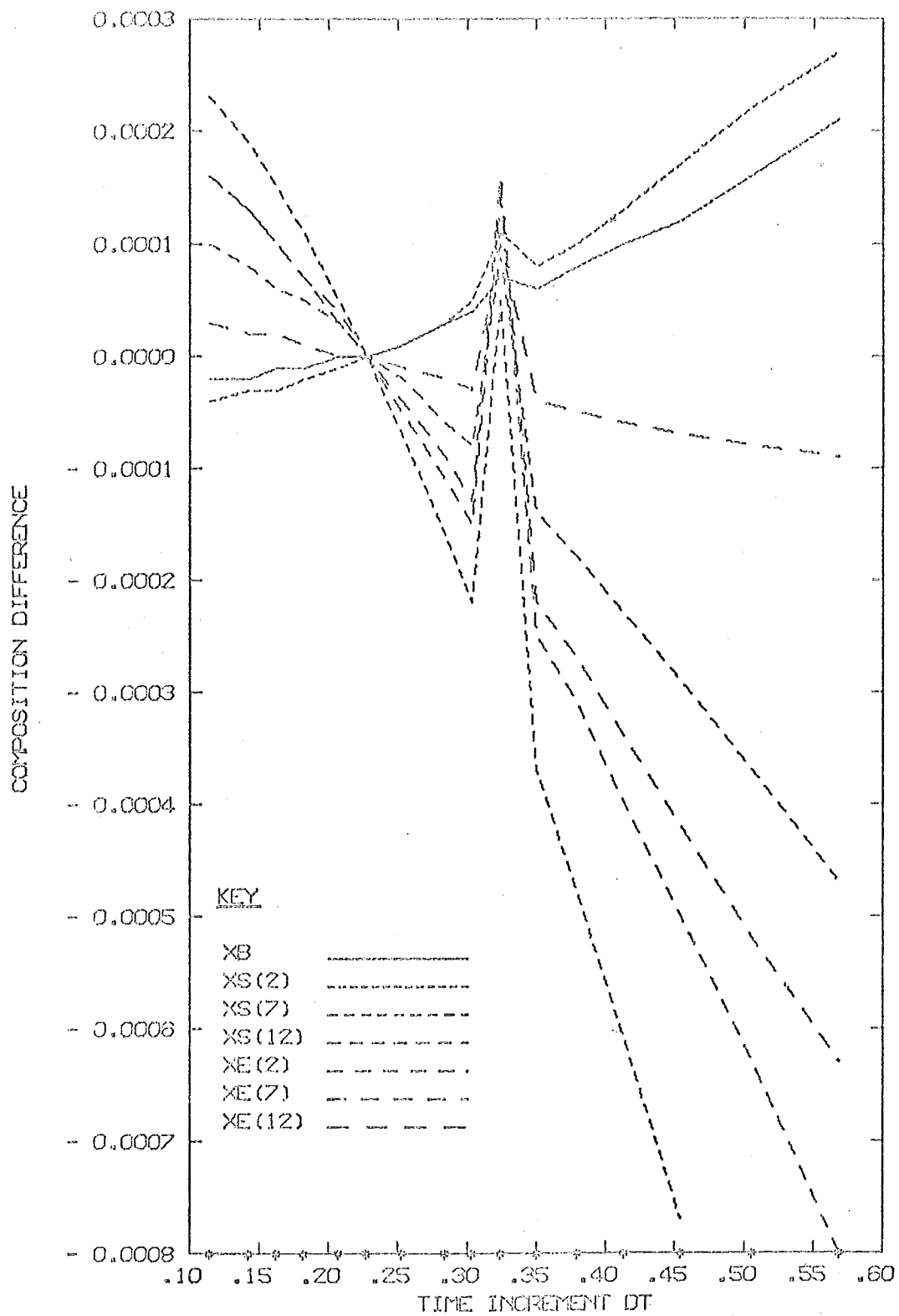


FIG. 5.3 EFFECT OF
DT ON TRUNCATION ERROR

the three curves in fig. 5.2 follow the same path, the difference between the lines being due to the slightly greater accuracy which is given by the smaller step sizes. Thus this brief initial period of numerical instability does not hinder the computation of the transient response at later times. The only situation in which it could be troublesome would be if the model were used in a digital control simulation. A filter would then be needed to reduce the noise effect of the numerical oscillation.

5.6.3 The Continuous Column.

The response of the continuous column model was studied for step change upsets in D, F, XF, and for combinations of these variables. A stable response was always obtained, with two iterations per time step being sufficient. As described in section 5.6.2, there was usually a short period of numerical oscillation in the computed liquid compositions in the stripping section after an upset. As before, these always died away naturally after a few time steps. Although the oscillations occurred in the stripping section for upsets in the distillate rate, as well as in the feed, no oscillation was observed in the enriching section compositions.

With differing parameters in each packing section, a choice had to be made on whether to set the time interval to $\Delta z/b$ for the enriching or $\frac{\Delta z}{2}$ for the stripping section. The value of b that gave the smallest time step was used. In order to test the effect of using other time intervals on the accuracy of the results, a number of runs were done for a feed composition upset with different time intervals. Fig. 5.3 shows the variations in liquid packed compositions with different time intervals at the time in the response when these variations were largest. The graph shows a maximum discrepancy of -0.0012 mole fraction. This was for a time interval of 0.568 compared with the recommended interval of 0.227. Thus the error introduced into the numerical solution by using a time interval 2.5 times greater than the recommended value was insignificant.

The errors introduced by using different time steps appear in fig. 5.3 to vary almost linearly with the time step. A startling exception to this, is the run done with a time step of 0.324. This is the time step which would have resulted if b_2 for the stripping section, rather than for the enriching section, had been used.

It has just been shown that the choice of the time interval for the numerical solution of the model is not critical. This is another aspect of the convenience and flexibility of using a numerical method of solution of the mathematical models of packed distillation columns.

CHAPTER 6 THE EXPERIMENTAL COLUMN AND MIXTURE.

- 6.1 The Column.
- 6.2 The Packing.
- 6.3 The Distillation Mixture.
 - 6.3.1 Properties Of The Pure Components.
 - 6.3.2 Properties Of Mixtures.
 - 6.3.3 Vapour-Liquid Equilibrium.
- 6.4 Flowrates And Pressure Drops.
 - 6.4.1 Flooding And Loading Rates.
 - 6.4.2 Variation Of Flow Rates With Height.
 - 6.4.3 Pressure Drops.
- 6.5 Holdup.
- 6.6 Mass Transfer.
 - 6.6.1 The Transfer Unit Approach.
 - 6.6.2 Effect Of The Operating Variables.
 - 6.6.3 Wetting Rate And Effective Area.
 - 6.6.4 Prediction Of The Height Of A Transfer Unit.
 - 6.6.5 Experimental Numbers Of Transfer Units.
 - 6.6.6 End Effects.
- 6.7 Experimental Measurements.
 - 6.7.1 Measurement Of Composition Profiles.
 - 6.7.2 Temperature Measurement.
 - 6.7.3 Vapour Flow Rate Measurement.
 - 6.7.4 Measurement Of The Distillate Rate.
 - 6.7.5 Measurement Of The Column Pressure Drop.
 - 6.7.6 Determination Of The Column Steady State.

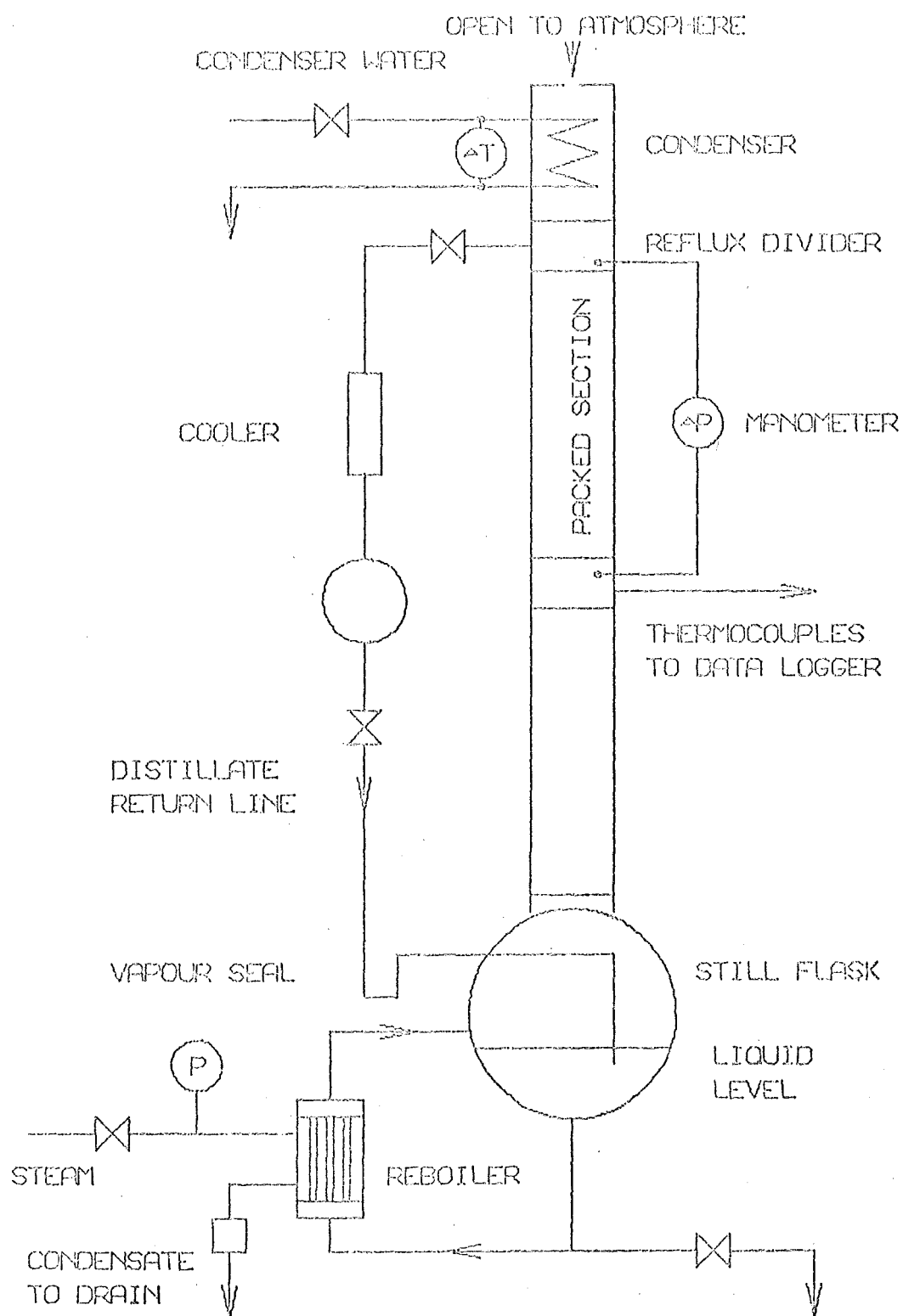


FIG. 6.1

THE EXPERIMENTAL COLUMN

6.1 THE COLUMN.

The experimental column was 152 mm in diameter. There was a 1.52 m high packed section above 1.8 m of unpacked column. The reboiler was a vertical shell and tube type with circulation by natural convection. The heat transfer area was 0.2 m^2 and the maximum available steam pressure was 450 kPa. The condenser was a water-cooled glass coil, 1.4 m^2 in area, with an overall heat transfer coefficient of $280 \text{ W/(m}^2 \cdot \text{K)}$. The reflux divider comprised a weir over which the condensate passed, and a collecting tray which could be positioned to collect any desired fraction of the condensate as distillate. The distillate return line to the still contained a liquid seal to prevent the flashing of vapour from the still back up the line.

Apart from the reboiler and the reflux divider, which were made from stainless steel, the main column components were items of Q.V.F. glassware. The packing section, reflux divider and condenser were lagged to minimise heat losses. The estimated surface heat losses were:

packing section 75 W; condenser + reflux divider 50 W.

A diagram of the column is given in fig. 6.1.

The liquid was distributed through four holes in a tray beneath the reflux divider. The vapour did not pass through these holes. In retrospect, it appears that the liquid distribution may have been inadequate, because the top 20 % of the packed height gave consistently less separation than did the rest of the packing. There is no consensus of opinion in the literature on the number of distribution points needed. Leva (1953) p.66 quotes results for a 12 inch column in which 4 points were found to give as good a distribution as 19 points. Since low fluid density and surface tension are thought to aid distribution, it was thought that 4 points would be adequate when methanol and isopropanol were distilled, as in this work. On the other hand, Eckert (1961)

recommends the use of 32 distribution points per square foot for a column of 1.25 feet diameter. This would require 6 or 7 points for a 152 mm column.

The literature also presents diverse opinions on the need for liquid redistributors in packed distillation columns. Eckert recommends redistribution every 20 feet or 2.5 to 3 column diameters. The latter recommendation, for a small diameter column, would result in virtually a plate column with packing between the plates. Perry (1963) offers suggestions of every 10 feet (p.13.29) or every 15 feet (p.18.32), while in Perry (1973), p.18.31, it is stated: "It is possible to design commercial packed columns for heights of 25 to 30 feet between distributors". As the packed height in this work was only 1.52 m (5 feet), no liquid redistribution was provided for.

6.2 THE PACKING.

The packing used in this work was 10 mm ceramic Raschig rings. The ratio of column to packing size was thus 15. Recommended values in the literature include:

>7 Leva (1953) p.67,

->8 Perry (1973) p.18.30,

>30 Eckert (1961); Backhurst and Harker (1973) p.138.

The choice of a ratio of 15 was a reasonable compromise because:

- (a) with a packed height of only 1.52 m, the liquid maldistribution caused by a large packing should not have been too serious;
- (b) pressure drops become excessive with smaller packing;
- (c) data for holdup, pressure drops and mass transfer coefficients are rarely reported for rings smaller than 3/8". Extrapolation would therefore often be needed in using literature data. E.g. Jesser and Elgin (1943) used packing sizes from 0.5" to 1" for holdup studies in a 6" column.

Data for the packing used are summarised in table 6.1. The three rows are data from: (a) Leva (1953) p.7; (b) Backhurst and Barker (1973) p.109; (c) measured in this work.

TABLE 6.1 PACKING DATA.

Source	Nominal size	Wall thickness	Number per m ³	Area a		Void e %	a/e ³ 1/m
				2 m ² /m	3 m ³ /m		
(a) Leva	3/8"	1/16" (1.6mm)	845000	440		68	1400
(b) Backhurst	3/8"	1/16" (1.6mm)	870000	481		67	1600
(c) measured	10mm	2.2mm	704000	427		70	1245

6.3 THE DISTILLATION MIXTURE.

The binary mixture used in the experimental work was methanol and isopropanol (IPA). The main reasons for choosing this system were the large boiling point range, and the nearly linear temperature-composition curve. This made it ideal for using the boiling temperature to find the composition.

6.3.1 Properties Of The Pure Components.

The physical properties of methanol and isopropanol are given in table 6.2. Figures in brackets were estimated or obtained by interpolation. The vapour viscosity figures given for isopropanol are the values reported in the reference for n-propanol.

TABLE 6.2 PROPERTIES OF METHANOL AND ISOPROPANOL.

Property	Temp	Methanol	IPA	Reference
molecular weight		32.04	60.09	Perry (1963) p.3-23
latent heat	64.7	35.201		Perry (1963) p.3-113
(kJ/mol)	82.3		40.022	
boiling point (F)		148.4	180.2	Ballard and van Winkle (1952)
boiling point (C)		64.66	82.33	converted from above
		64.50	82.2	Timmermans(1950)p.304,317
		to 64.75	to 82.44	
liquid viscosity	60	0.36	0.86	Perry (1963) p.3-199
(cp)	70	0.32	0.69	
	80	0.28	0.55	
vapour viscosity	65	0.011	0.0085	Perry (1973) p.3-211
(cp)	82	0.0115	0.0093	
surface tension	20	22.61	21.7	Weast(1968) p.F-32
(dyne/cm)	50	20.14		
	55		19.05	Timmermans (1950) p.303
liquid density	50	765.0		Timmermans (1950) p.303
³ (kg/m)	60	755.5		
	70	746.0		
	80	735.5		
	90	725.0		
	55	(760.5)	753.2	Timmermans (1965) p.256
	82.3		(725.8)	

Property	Temp	Methanol	IPA	Reference
saturated vapour	50	0.06739		Timmermans (1950) p.303
density (kg/m ³)	60	1.006		
	64.7	(1.196)		
	70	1.465		
	80	2.084		
	90	2.907		
	64.7	1.17	1.96	
	82.3	1.23	2.061	
liquid specific	40.5	0.6115		Timmermans (1950) p.305
heat (cal/g/K)	40		0.670	ibid. p.318
	60		0.742	
	80		0.798	
	100		0.848	
	40	0.62	0.70	Perry (1963) p.3-126
	60	0.63	0.76	
	70	0.65	0.79	
	80	0.66	0.82	
liq. diffusivity	65	$0.9(10^{-4})$	$1.3(10^{-5})$	Perry (1973)
(cm ² /s)	82	$1.15(10^{-4})$	$2.09(10^{-5})$	p.3-234, eqn.3.32
vap. diffusivity	65	0.086	0.086+/-8%	Perry (1973)
(cm ² /s)	82	0.096	0.096+/-8%	p.3-231, eqn.3.29
liquid Schmidt	64.7	50.3	810	
number	82.3	32.0	336	
vapour Schmidt	64.7	1.09	0.50	
number	82.3	0.97	0.47	

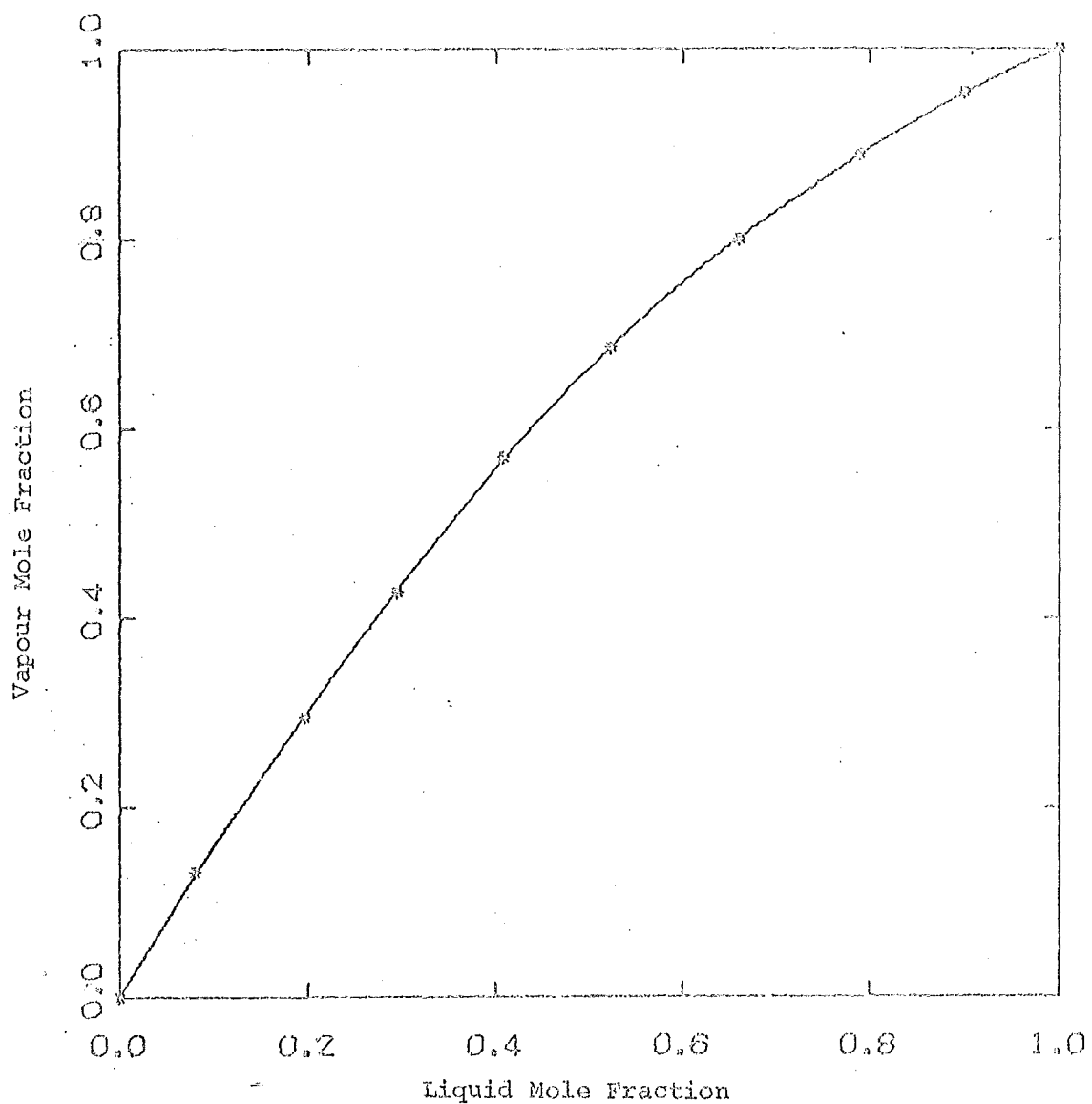


FIG 6.2 LIQUID-VAPOUR
EQUILIBRIUM DATA FOR IPA-MEOH

6.3.2 Properties Of Mixtures.

For many properties (e.g. liquid density, viscosity) the property for the mixture was estimated from an average of the pure component values, weighted according to the composition. For certain other properties, the following methods were used:

- (i) for vapour densities, the ideal gas law was applied.
- (ii) for liquid specific heats, the equation:

$$C_p = 202.1 - 126.6 x + 9.44 x^2 \quad \dots\dots(6.1)$$

was derived. Equation 6.1 was obtained by fitting a linear equation to the specific heat - temperature data for methanol and isopropanol. These were combined with the temperature - composition relationship (equation 6.3) to give equation 6.1.

(iii) saturated liquid enthalpies were found relative to pure methanol by using $\frac{dH}{dT} = C_p$ assuming that $\left(\frac{dH}{dx}\right)_L = 0$. I.e., constant T.

assuming no heat of mixing. No published heats of mixing were found for this system. Integrating this equation gives:

$$H_L(x=x_2) - H_L(x=x_1) = \int_{T_1}^{T_2} C_p \cdot dT \quad \dots\dots(6.2)$$

6.3.3 Vapour-Liquid Equilibrium.

The vapour-liquid equilibrium for methanol - isopropanol has been measured by Ballard and van Winkle (1952). Their data was fitted by least squares to give:

$$T = 180.205 - 27.868 x + 24.453 x^2 + 33.440 x^3 - 12.928 x^4 \quad \dots\dots(6.3)$$

where T is in degrees Fahrenheit and x is the mole fraction of methanol.

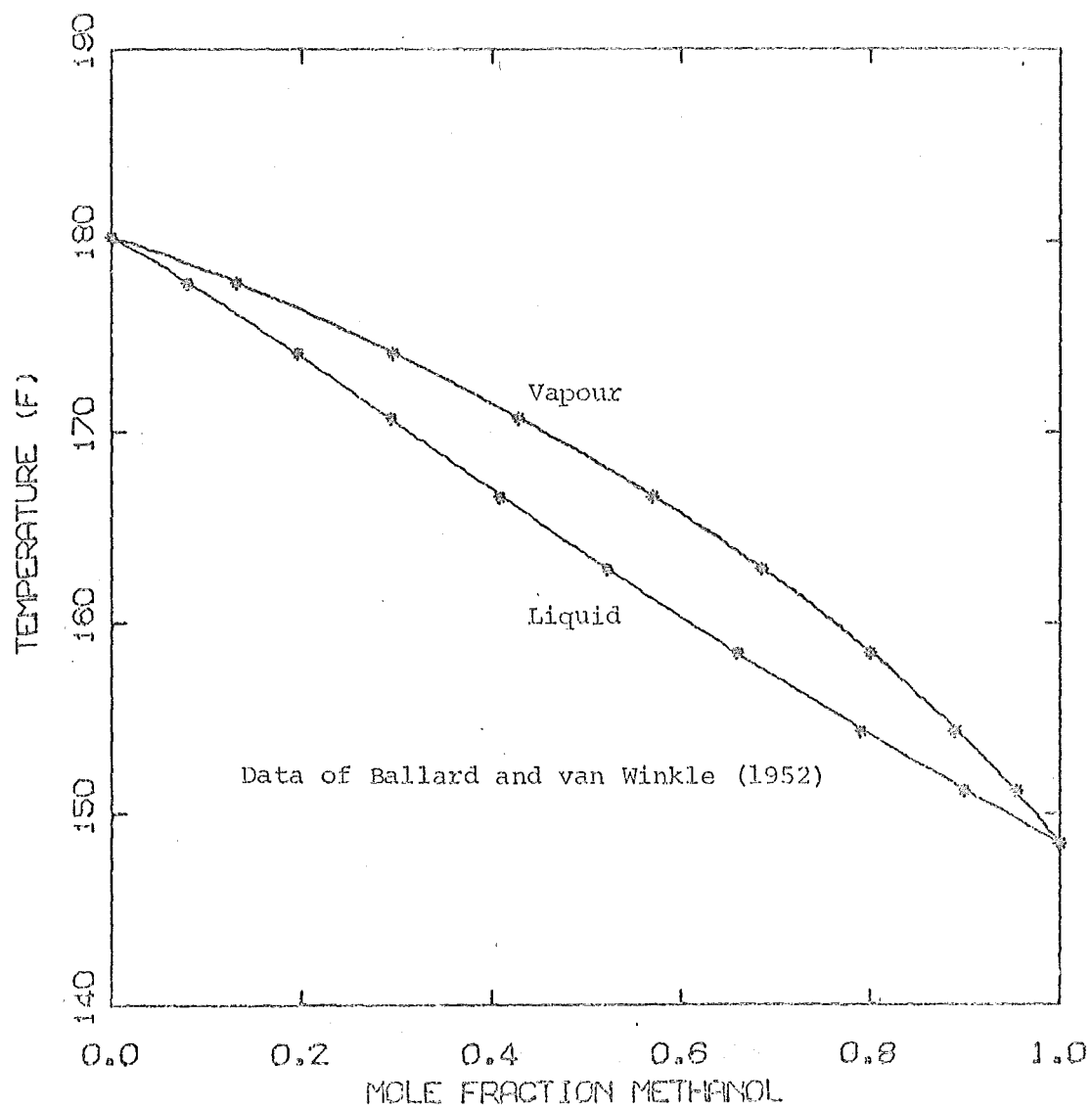


FIG 6.3 BOILING POINT
COMPOSITION CURVE IPA-MEOH

A least squares curve fit was also used to obtain a relationship between f and x for the published data. The equation is:

$$f = x + x(1-x) \left[A + \sum_{i=1}^n B_i (1-2x)^i \right] \quad \dots\dots(6.4)$$

where x and f are mole fractions. The values of A and B are:

$$\begin{aligned} A &= 0.659357 & B_1 &= 0.052195 \\ B_2 &= -0.175710 & B_3 &= -0.019018 \\ B_4 &= 0.210234 \end{aligned}$$

The values of f and T computed from equations 6.3 and 6.4 are included in table 6.3 together with the data of Ballard and van Winkle. Figs. 6.2 and 6.3 plot their data points and the fitted curves.

TABLE 6.3 EQUILIBRIUM DATA.

Ballard and van Winkle data. Computed from curve fits.

x	f	T	f	T
0.000	0.000	180.2	0.000	180.2
0.081	0.132	177.8	0.131	177.8
0.195	0.296	174.1	0.297	174.1
0.293	0.4285	170.7	0.4288	170.7
0.408	0.570	166.6	0.568	166.7
0.522	0.685	162.8	0.686	162.8
0.6605	0.800	158.4	0.801	158.3
0.790	0.891	154.3	0.889	154.4
0.901	0.9535	151.2	0.9545	151.2
1.000	1.000	148.4	1.000	148.4

The pressure dependence of the boiling point was estimated from the vapour pressure data. Antoine equation coefficients have been published by Boublík et. al. (1973) for the equation:

$$\log(P) = A - B/(T + C)$$

where P is the vapour pressure in mm Hg, and T is in Celsius. The coefficients given for methanol are: $A = 8.08097$; $B = 1582.3$; $C = 239.73$. For isopropanol, $A = 7.7402$; $B = 1359.5$; and $C = 197.53$.

For both pure components, this gave $(dP/dT) = 30$ mm Hg per degree Celsius at 760 mm Hg pressure. This converts to 4 kPa/K. It has been assumed that the effect of pressure on the boiling point of mixtures will be the same as the effect on the pure components.

6.4 FLOW RATES AND PRESSURE DROPS.

6.4.1 Flooding And Loading Rates.

These can be predicted from the generalised pressure drop correlation given in fig. 19 of Leva (1953). The following units were used for the variables:

G', L' kg/s/m^2 ; p_L, p_V kg/m^3 ; a m^2/m^3 ; μ centipoise.

When g (9.8 m/s^2) was used in place of g_c , the coordinates had the same numerical values as for the units Leva used.

When the physical properties and packing constants were substituted into the coordinates, they became:

for methanol, X axis = $0.040L'/G'$; Y axis = $0.152(G')$

for isopropanol, X axis = $0.053L'/G'$; Y axis = $0.102(G')$

Table 6.4 lists the vapour flow rates predicted to cause flooding for pure methanol and pure isopropanol at various reflux ratios.

TABLE 6.4 PREDICTED VAPOUR FLOW RATES FOR FLOODING.

L'/G'	METHANOL				ISOPROPANOL			
	X	Y	G'	V	X	Y	G'	V
1.0	0.040	0.178	1.08	0.615	0.053	0.158	1.24	0.378
0.9	0.036	0.188	1.11	0.633	0.048	0.165	1.27	0.386
0.8	0.032	0.193	1.13	0.641	0.042	0.176	1.31	0.398
0.7	0.028	0.201	1.15	0.654	0.037	0.185	1.35	0.409

Note that G' is the vapour rate in kg/s/m^2 and V is the vapour rate in mol/s for the 152 mm diameter column. The L'/G' ratio has little effect on the predicted flooding rates. However, the predicted molal vapour rate for flooding is very much less for isopropanol than for methanol, so the column can be expected to start flooding from the bottom.

Although the existence of loading points in packed columns is open to doubt, the loading limits predicted from the generalised pressure drop correlation (Leva (1953) fig. 19) are given in table 6.5.

TABLE 6.5 PREDICTED LOADING RATES AT TOTAL REFLUX.

	Upper loading limit				Lower loading limit		
	X	Y	G'	V	Y	G'	V
Methanol	0.040	0.090	0.77	0.438	0.045	0.54	0.309
IPA	0.053	0.087	0.93	0.280	0.043	0.65	0.196

In the experimental work described in chapters 7 and 8, the vapour rates ranged from 0.237 to 0.397 mol/s at the top of the packing. This was from 75% of the lower loading limit to 90% of the upper loading limit, or 65% of the flooding limit, based on Leva's predictions for methanol. For isopropanol, the range was from midway between the loading limits to 5% above the predicted flooding rate.

6.4.2 Variation Of Flow Rates With Height.

In appendix 1, equation A.1.2 was obtained from an enthalpy balance to give the variation of vapour rate with height. To illustrate the variation in flow rates in the experimental column, some typical values are now computed.

If $Q_S = 75 \text{ W}$; $V_T = 0.3 \text{ mol/s}$; $x(z=1.0) = 0.98$; and $x(z=0.0) = 0.2$;

then $H_{V,T} - H_{L,T} = 35.68 \text{ kJ/mol}$; $H_V - H_L = 39.06 \text{ kJ/mol}$;

and $H_{L,T} - H_L = -1.733 \text{ kJ/mol}$.

Case (i): $L_T = 0.3 \text{ (D = 0.0)}$.

$$V = (0.3 \times 35.68 + 0.075) / 39.06 = 0.276 \text{ mol/s}$$

Case (ii): $L_T = 0.24 \text{ (D = 0.06)}$.

$$V = (0.3 \times 35.68 + 0.06 \times (-1.733) + 0.075) / 39.06 = 0.273 \text{ mol/s}$$

The change in the vapour rate through the column was 8% and 9% for the two cases given. The change in reflux ratio is zero for the first case. In the second case, $R = 0.8$ at the top of the packing, and $R = 0.213 / 0.273 = 0.78$ at the bottom; a change of 2.5% compared with the 9% change in vapour rate.

The change in mass flow rate is much greater than the change in molal flow rate, mainly because of the large change in molecular weight with composition. For the previous total reflux example, the vapour mass rate changes from 0.0104 kg/s at the top of the packing to 0.0150 kg/s at the bottom, a 44% increase.

6.4.3 Pressure Drops.

A convenient form of the generalised pressure drop correlation for predicting pressure drops is that presented by Prähli (1969) fig.7. Pressure drops predicted from this diagram for 1.52 m of packed bed and

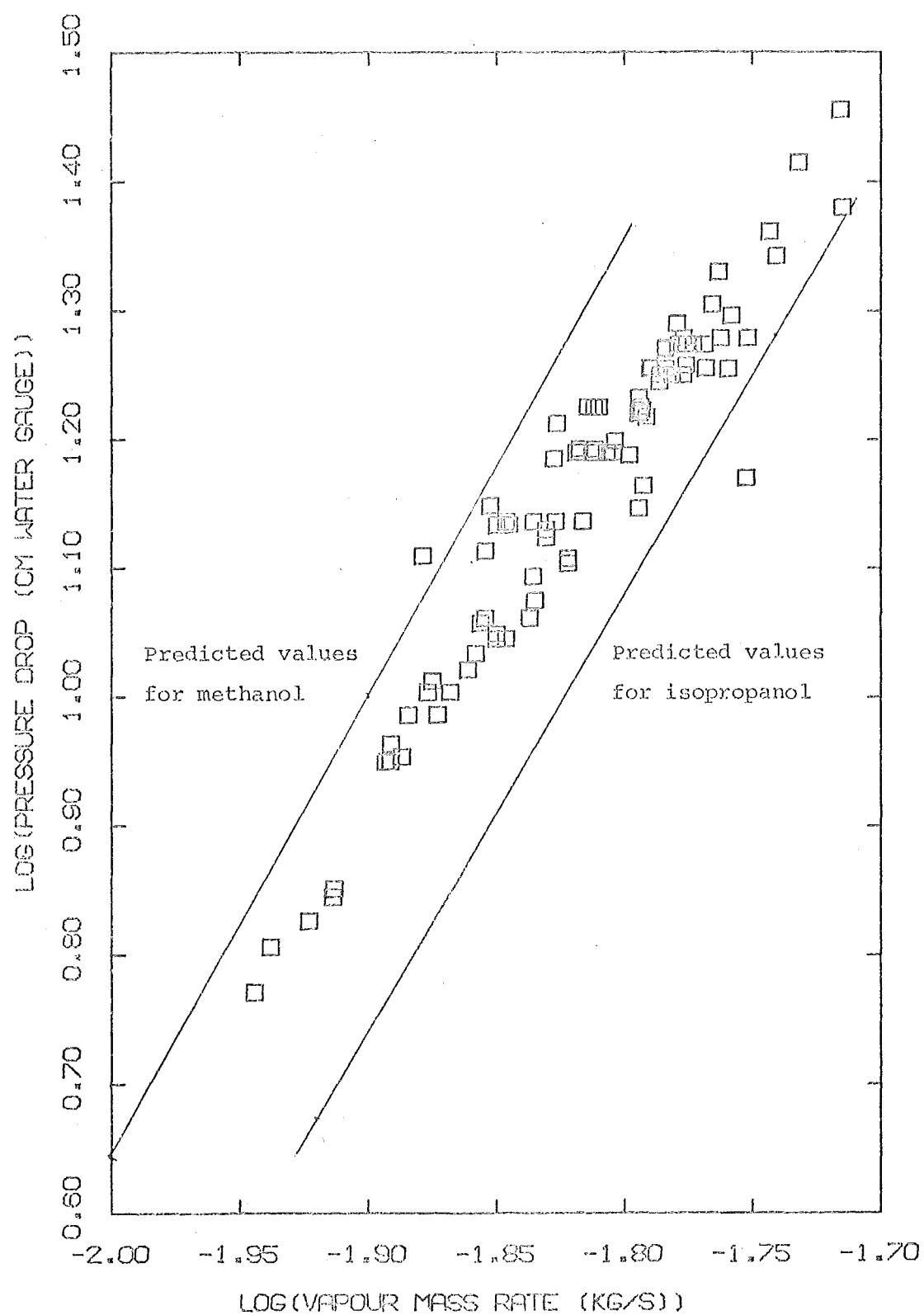


FIG 6.4

PRESSURE DROP VERSUS VAPOUR RATE

total reflux conditions are given in table 6.6.

TABLE 6.6 PREDICTED PRESSURE DROPS.

V	Methanol			Isopropanol		
	G'	Y	DP	G'	Y	DP
mol/s	² kg/s/m		mm water			
0.20	0.35	0.019	18	0.66	0.044	47
0.25	0.44	0.029	29	0.82	0.069	95
0.30	0.53	0.043	44	0.99	0.100	190
0.35	0.62	0.058	69	1.15	0.135	335
0.40	0.70	0.074	102	1.32	0.178	--

TABLE 6.7 REGRESSION ANALYSIS OF MEASURED PRESSURE DROPS.

Liquid rate	b	c	Correlation	Standard	Number of
kg/s			coefficient	error	points
all	7.06	2.695	0.966	0.036	89
<0.012	7.33	2.86	0.998	0.012	6
0.012 to 0.014	6.81	2.56	0.92	0.037	29
0.014 to 0.016	5.64	1.91	0.87	0.031	34
>0.016	6.82	2.56	0.94	0.026	20

The measured pressure drops from the experimental runs were fitted by a linear regression to the equation:

$$\log(DP) = b + c \cdot \log(G) \quad \text{.....(6.5)}$$

where DP is the pressure drop in mm water gauge, and G is the vapour rate in kg/s. The regression was done on all points together, and on points grouped according to the liquid rate. As can be seen from table 6.7, no consistent dependence on liquid rate was found.

Fig. 6.4 is a logarithmic plot of pressure drop versus vapour mass rate, with the experimental and predicted points shown.

6.5 HOLDUP.

(1) Liquid holdup.

This can be predicted by using equations 3 and 4 of Leva (1953) p.52.

These combine to give:

$$H' = 0.0004 (L'/Dp)^{0.6} u^{0.1} (62.3/p_L)^{0.78} (73/s)^n \dots\dots(6.6)$$

where:	H'	= liquid holdup	(m^3/m^3)
	L'	= liquid flow rate	$(lb/hr/ft^2)$
	u	= liquid viscosity	(cp)
	Dp	= equivalent spherical diameter of packing	(inch)
	p_L	= liquid density	(lb/ft^3)
	s	= surface tension	(dyne/cm)

For 10 mm Raschig rings, a value for Dp of 0.375 inches was obtained by interpolating in table 1, page 7 of Leva. For the range of liquid rates in this work, $n = 0.53 \pm 0.03$ (Leva p.55). Using equation 6.6 for both pure methanol and pure isopropanol in a 152 mm column gives:

$$H = 51.9 L'^{0.6} \text{ for methanol}$$

$$H = 42.85 L'^{0.6} \text{ for isopropanol,}$$

where H = liquid holdup (mol/m), and L = liquid flow rate (mol/s).

Table 6.8 summarises the predicted values of H for the pure components, and the mean value for a 50 mole percent mixture.

TABLE 6.8 PREDICTED LIQUID HOLDUPS.

L(mol/s)	Holdup (Methanol)		Holdup (IPA)		(50% mixture)
	$\frac{3}{m} \frac{3}{m}$	(mol/m)	$\frac{3}{m} \frac{3}{m}$	(mol/m)	(mol/m)
0.20	0.046	19.8	0.074	16.3	18.0
0.25	0.053	22.6	0.085	18.7	20.6
0.30	0.059	25.2	0.094	20.8	23.0
0.35	0.065	27.6	0.103	22.8	25.2

Note that the molal holdup for methanol is expected to be 21% greater than that for isopropanol at a given liquid flow rate, while the volumetric holdup is expected to be 60% less than for isopropanol.

(ii) Vapour holdup.

The maximum vapour holdup can be found by using the ideal gas law to compute the amount of vapour required to fill the voids in the packing. For a void fraction of 0.7 and a column cross-section area of 0.0182 m², the vapour holdup is 0.45 mol/m. This is about 5% of the liquid holdup and is almost independent of flow rates.

(iii) Condenser holdup.

The holdup in the condenser and reflux divider combined was estimated to be 5 moles +/- 1.5 moles.

(iv) Reboiler holdup.

This was large, because the column used had a large still flask designed for batch operations. The holdup ranged from 430 to 930 moles +/- 30 moles.

6.6 MASS TRANSFER.

6.6.1 The Transfer Unit Approach.

The accepted methods of expressing the separation achieved in a packed column are by the number of theoretical plates, or by the number of transfer units. The latter approach was proposed by Chilton and Colburn (1935). Colburn (1939) defines the number of transfer units as:

$$N_{OG} = \int_{Y_1}^{Y_2} \frac{dy}{(x-y)} \quad \dots\dots(6.7)$$

for equimolar counter-diffusion (as in distillation).

The transfer unit approach is more realistic than the theoretical plate approach, in that it treats the composition as a continuously varying function of height. This is suitable for the dynamic column model developed in chapter 2.

To compute the column height Z required for a particular separation expressed in N_{OG} , the height of a transfer unit H_{OG} must be known, since:

$$Z = N_{OG} \cdot H_{OG}$$

At atmospheric pressure, H_{OG} is defined as:

$$H_{OG} = V/(K a_G S) = H_G + m(V/L)H_L \quad \dots\dots(6.8)$$

$$\text{where } H_G = V/(k a_G S) \quad \dots\dots(6.9)$$

$$\text{and } H_L = L/(k a_L S) \quad \dots\dots(6.10)$$

TABLE 6.9 EFFECTS OF OPERATING VARIABLES ON THE HEIGHT OF A TRANSFER UNIT.

Increasing:	Leva (1953)		Perry (1973)
	H_L	H_G	H_{OG}
Gas mass velocity,	No effect below loading point. Increases above loading point.	Increases.	Increases. Minor effect.
Liquid mass velocity,	Increases.	Little or no effect.	Decreases.
Packing size,	Usually increases slightly.	Increases.	Increases but not a direct effect.
Packed height,	No effect.	Increases very little.	Increases slightly.
Temperature,	Decreases quite markedly.	Little or no effect.	Decreases.
Pressure,			Negligible effect.
Column diameter,			Possibly increases.
Liquid distribution,	Sensitive with some packings.	Less sensitive than H_L .	

H_G is the gas film resistance and $m(V/L)H_L$ is the liquid film resistance.

Most workers regard the majority of the mass transfer resistance in distillation to be in the gas phase. Thus "in distillation work the number of transfer units is usually calculated as N_{OG} , i.e. based on gas composition changes, even though considerable resistance may lie in the liquid phase" (Perry (1973) p.13.50).

Pratt (1951) quotes results of Suroweic and Furnas, who obtained liquid film resistances amounting to 30 to 40% of the total resistance; Johnstone and Pigford, who found liquid film resistances to be 8% of the total; and Jackson and Ceaglske, who found negligible liquid film resistances for distillation in wetted wall columns.

6.6.2 Effect Of The Operating Variables.

The effect of the operating variables on the height of a transfer unit have been summarised by Perry (1973) p.13.50 and Leva (1953) p.89. See table 6.9.

There is a major discrepancy between the statements of Leva and Perry on the effects of liquid mass velocity. This probably depends on whether or not the influence of the liquid velocity on the amount of wetted packing was considered. Chilton and Colburn (1935) state that "In packed columns, the useful area appears to vary with the liquor rate, and this variation may have as much importance as the vapour velocity or even more". When Chilton said that he would expect increased liquor rate to decrease H_{OG} , as long as it meant an increased amount of wetted surface, he anticipated the findings of Pratt (1951). Pratt concluded that H_{OG} was inversely proportional to the degree of wetting. Thus so long as the liquid rate is below the minimum effective liquid rate (MELR) which gives complete wetting, increasing L can be expected to increase the degree of wetting and thus decrease H_{OG} . At liquid rates above the minimum

effective liquid rate, L has no significant effect on H .
OG

6.6.3 Wetting Rate And Effective Area.

Pratt (1951) plotted the degree of wetting against the liquid flow, expressed as a fraction of the minimum effective liquid rate, for various operations. For distillation using Raschig rings, this shows that the degree of wetting is approximately equal to the fraction of the minimum effective liquid rate. Backhurst and Harker (1973) p.149 define the wetting rate as:

$$WR = \frac{\text{flow rate } (m^3/hr/m)}{\text{specific area } (m^2/m)} \quad \dots\dots(6.11)$$

The minimum effective liquid rate is quoted by Morris and Jackson (1953) p.22 as 0.85 ft³/hr/ft (0.08 m³/hr/m), below which columns should not be operated. However as Pratt points out, for small packing sizes with large specific area, it is impossible to achieve the minimum effective liquid rate without flooding. E.g. the maximum wetting rate that could be achieved in the column in this study is for isopropanol at total reflux. From section 6.4, $G = 0.0227$ kg/s at flooding. This leads to a wetting rate of 0.014 m³/hr/m, which is only 17% of the minimum effective liquid rate recommended by Morris and Jackson.

The value of the minimum effective liquid rate is however open to question. Yoshida and Koyanagi (1962) found the effect of surface tension on the minimum effective liquid rate to be important. Pratt recommends the use of MELR = 0.6 to 0.7 ft³/hr/ft for distillation and quotes an experimental value of 0.14 for methanol at high concentration. As this is close to the maximum possible wetting rate for the present column, it seems likely that the minimum effective liquid rate was not exceeded in this work.

Perry (1973) p.18.32 warns that the effective area is not necessarily the same as the wetted area, and quotes the results of Weisman and Bonilla who found that for vapourisation of water into air:

$$(\text{effective area})/(\text{total area}) = 0.44G'^{0.31} L'^{0.07}$$

The influence of L here is very slight, despite the fact that at the flow rates they used, the wetting rate ranged from only 20 to 80% of the minimum effective liquid rate recommended by Morris and Jackson.

6.6.4 Prediction Of The Height Of A Transfer Unit.

(1) Height of a liquid film transfer unit (H_L).

There are several correlations available in the literature for predicting H_L .

(a) Backhurst and Harker (1973) table 4-13, list values of H_L for distillation. Extrapolation from 12 mm to 10 mm Raschig rings gives a value of 0.15 ft (0.06 m). The effect of temperature or flow rates is not considered.

(b) Sherwood and Holloway (1940) use:

$$H_L = (L'/c.u.)^n (N_{Sc})^{0.5} \quad \text{at 25 degrees Celsius} \dots (6.12)$$

Using $c = 310$ and $n = 0.4$, and correcting for temperature gives:

$$H_L = 0.013(L')^{0.4} \quad \text{for methanol at 64.7 Celsius,}$$

and $H_L = 0.019(L')^{0.4}$ for isopropanol at 82.3 Celsius.

(c) Cornell (1960) generalised data from several sources with the equation:

$$H_L = b \cdot c(N_{Sc})^{0.5} (Z/10)^{0.15} \quad \dots\dots(6.13)$$

with $b = 0.035$ for 3/8 inch Raschig rings; $c = 1.0$ for $L < 50\%$ flooding rate; and $c = 0.6$ for $L = 80\%$ of the flooding rate.

For a column of 1.52 m packed height, this yields:

$$H_L = 0.0315c(N_{Sc})^{0.5} \quad (\text{ft}) \quad \dots\dots(6.14)$$

Note that this is independent of flow rates, apart from the effect of c as flooding is approached.

(d) Schulman et al (quoted by Perry (1973) p.18.33) suggest a relationship in which k_L is proportional to $(L')^{0.45}$. Since $H_L \propto L'/k_L$,

this means $H_L \propto (L')^{0.55}$.

Note the varying dependence on L' in these correlations. The values of H_L predicted by (a), (b) and (c) above are listed in table 6.10.

Apart from the single figure prediction of Backhurst and Harker, H_L is seen to be greater for isopropanol than for methanol because of the much higher Schmidt number for the former. Consequently, H_L may be expected to increase with distance down the packing as the concentration of isopropanol increases.

(ii) Height of a gas film transfer unit.

Correlations available for predicting H_G include:

(a) the nomograph in Backhurst and Harker (1973) p.132. Evaluating H_G for various vapour rates shows that this predicts that H_G is proportional to $(G')^{0.25}$. The effects of temperature and pressure are included, but no reference is made to vapour properties or liquid flow rate.

(b) Sherwood and Holloway (Perry (1973) p.18.36) suggest:

$$H_G = 1.01(G')^{0.31} (L')^{-0.33} \quad \dots\dots(6.15)$$

(c) Cornell (1960) correlated data published by several workers by:

$$H_G = c(N)^{0.5} (D/12)^{1.24} (Z/10)^{1/3} \dots\dots(6.16)$$

$$\frac{Sc_{gas}^{0.6}}{(L'_1 f_1 f_2 f_3)}$$

where the f terms involve the physical properties of the system. Using $c = 135$ for 3/8 inch Raschig rings gives:

$$H_G = 13.8/L^{0.6} \quad \text{for isopropanol at 82.3 Celsius,}$$

$$\text{and } H_G = 20.6/L^{0.6} \quad \text{for methanol at 64.7 Celsius.}$$

(d) from the Reynold's analogy, Chilton and Colburn (1935) propose:

$$H_G = V/k_a = (1/j.a)(N)^{2/3} \dots\dots(6.17)$$

$$G \quad G \quad Sc$$

$$\text{where } j = 0.023(N)^{-0.2}$$

$$Re$$

After considering the effects of wetting and examining the available data, Pratt (1951) proposes:

$$\left(\frac{k_p a_m e}{G} \right) / (G') = c (N_{Re})^{-0.25} (N_{Sc})^{-2/3} w_e^{b.L} \quad \dots (6.18)$$

with $b = 0$ for Raschig rings. Since $H_G = G' / (k_p a_m e)$, this leads to:

$$H_G = (e / (a_m c w)) (N_{Re})^{0.25} (N_{Sc})^{2/3} \quad \dots (6.19)$$

where $N_{Re} = (D_p G) / (u_e \mu)$ and D_p is the equivalent diameter of the packing

in feet.

Pratt (1951) suggests a value of 0.123 for c . Assuming that $w = L' / MELR$, this leads to:

$$H_G = 0.013 (G')^{0.25} / (L' / MELR) \quad \text{for methanol} \quad \dots (6.20)$$

$$\text{and } H_G = 0.016 (G')^{0.25} / (L' / MELR) \quad \text{for isopropanol} \quad \dots (6.21)$$

Values of H_G predicted by (b) and (c) are included in table 6.10 for total reflux conditions. Because of the uncertainty in the value of the minimum effective liquid rate, no values have been computed from (d).

TABLE 6.10 PREDICTED HEIGHTS OF FILM TRANSFER UNITS.

	L	L'	H (a) L	H (b) L	H (c) L	H (b) G	H (c) G
	mol/s	kg/s/m ²	(ft)	(ft)	(ft)	(ft)	(ft)
Methanol	0.20	0.35	0.15	0.12	0.22	0.90	0.73
	0.25	0.44	0.15	0.13	0.22	0.90	0.64
	0.30	0.53	0.15	0.14	0.22	0.90	0.57
	0.35	0.53	0.15	0.15	0.20	0.89	0.52
IPA	0.20	0.66	0.15	0.23	0.55	0.89	0.34
	0.25	0.82	0.15	0.24	0.46	0.89	0.30
	0.30	0.99	0.15	0.26	0.35	0.89	0.26
	0.35	1.15	0.15	0.28	0.17	0.88	0.24

(iii) Height of an overall transfer unit.

This is computed from equation 6.8 once H_G and H_L are known. The slope of the equilibrium curve, m , ranged from 1.61 (pure isopropanol) to 0.45 (pure methanol). For most of the experiments done in this work, V/L ranged from 1.0 to 1.25. Thus the term $m.V/L$ had values from 0.45 to 2.0.

Using the predictions for H_G and H_L from Cornell's equations, values of H_{OG} have been computed and are listed in table 6.11. From this table 6.11, it can be seen that H_{OG} is expected to vary by as much as a factor of 1.7 between the values for methanol and isopropanol at low liquid rates. At higher liquid rates, the differences between predicted H_{OG} values become much smaller. For isopropanol, the majority of the resistance comes from the liquid phase since $m.V/L$ ranges from 1.6 to 2.0, and $H_L > H_G$ for all but the highest liquid rates. For methanol, H_G

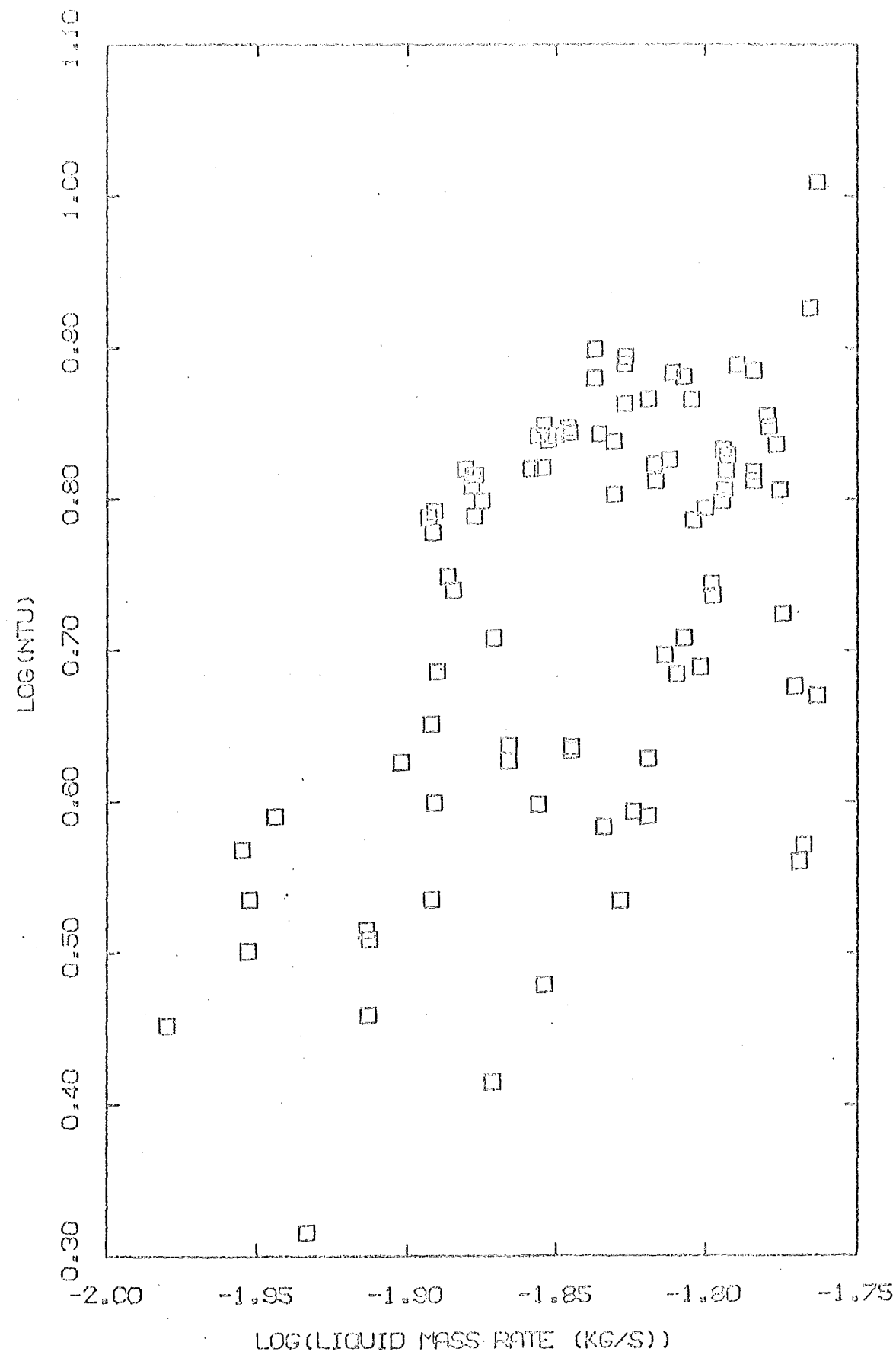


FIG 6.5

NTU VERSUS MASS LIQUID RATE

>> H_L and $m.V/L < 1.0$, so the gas phase resistance should predominate.

TABLE 6.11 VALUES OF H_{OG} PREDICTED BY CORRELATIONS OF CORNELL.

$L(\text{mol/s})$	H_{OG} (IPA, $m=1.61$)			H_{OG} (methanol, $m=0.45$)		
	$L/V=1.0$	0.9	0.8	$L/V=1.0$	0.9	0.8
0.20	1.22	1.32	1.45	0.83	0.84	0.85
0.25	1.04	1.12	1.23	0.74	0.75	0.76
0.30	0.82	0.89	0.96	0.67	0.68	0.69
0.35	0.51	0.54	0.58	0.61	0.62	0.63

As the experimental separations are expressed in N_{OG} , the predicted values of N_{OG} are listed in table 6.12. They are based on arithmetic mean values of H_{OG} for the two pure components, and a packed height of 1.52 m.

TABLE 6.12 PREDICTED VALUES OF N_{OG} .

L	$L/V=R$		
	1.0	0.9	0.8
0.20	4.88	4.63	4.35
0.25	5.62	5.35	5.03
0.30	6.71	6.37	6.06
0.35	8.93	8.62	8.26

6.6.5 Experimental Numbers Of Transfer Units.

The number of transfer units has been computed for the steady state conditions of all the experimental runs described in chapters 7 and

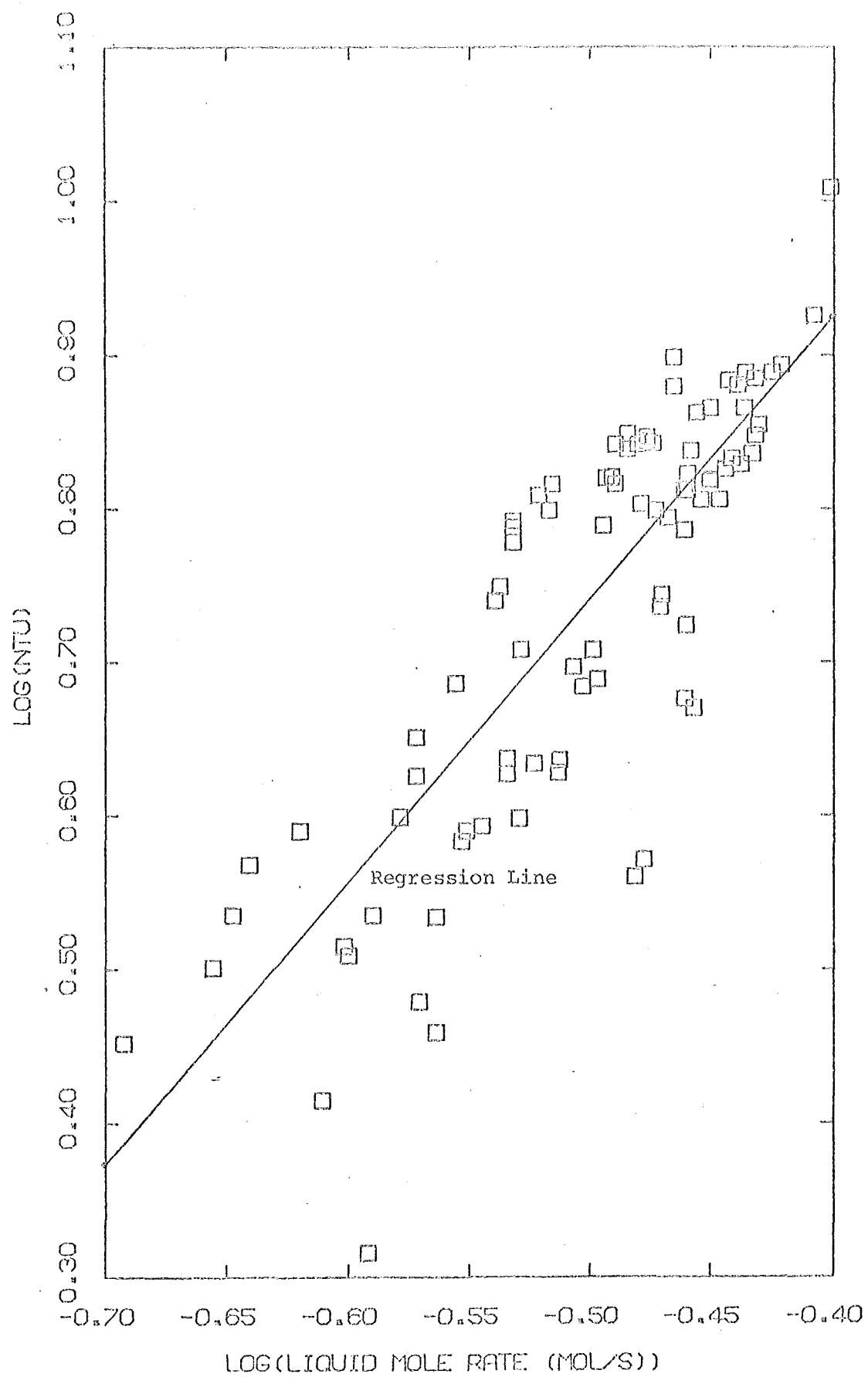


FIG 6.6

NTU VERSUS MOLE LIQUID RATE

8. N_{OG} is plotted against the mass liquid flow rate in fig. 6.5 and the molal liquid rate in fig. 6.6. The mass flow rate is based on conditions for the arithmetic mean of the two end compositions. These figures show that N_{OG} correlates much better with the molal than with the mass liquid rate. This is surprising since the correlations in the previous section have used mass rates.

Using a linear regression analysis, the following equations were fitted to the N_{OG} - liquid rate data:

$$N_{OG} = -4.39 + 31.73 L \quad \dots\dots(6.22)$$

$$r = 0.84 ; S.E. = 0.89$$

$$N_{OG} = -1.26 + 0.479 L_{\text{mass}} \quad \dots\dots(6.23)$$

$$r = 0.50 ; S.E. = 1.40$$

$$\log(N_{OG}) = 1.665 + 1.85 \log(L) \quad \dots\dots(6.24)$$

$$r = 0.83 ; S.E. = 0.076 \text{ on } \log(N_{OG}) = 20\% \text{ on } N_{OG}$$

where L = liquid rate mol/s
 L_{mass} = liquid rate kg/s
 r = correlation coefficient
 $S.E.$ = standard error

From equations 6.22 and 6.24, the correlation coefficient was almost identical for both the linear and logarithmic equations, even though 6.24 suggests that N_{OG} is proportional to $L^{1.85}$.

In an attempt to assess the effect of the vapour rate on N_{OG} , a multiple linear regression was done. This yielded:

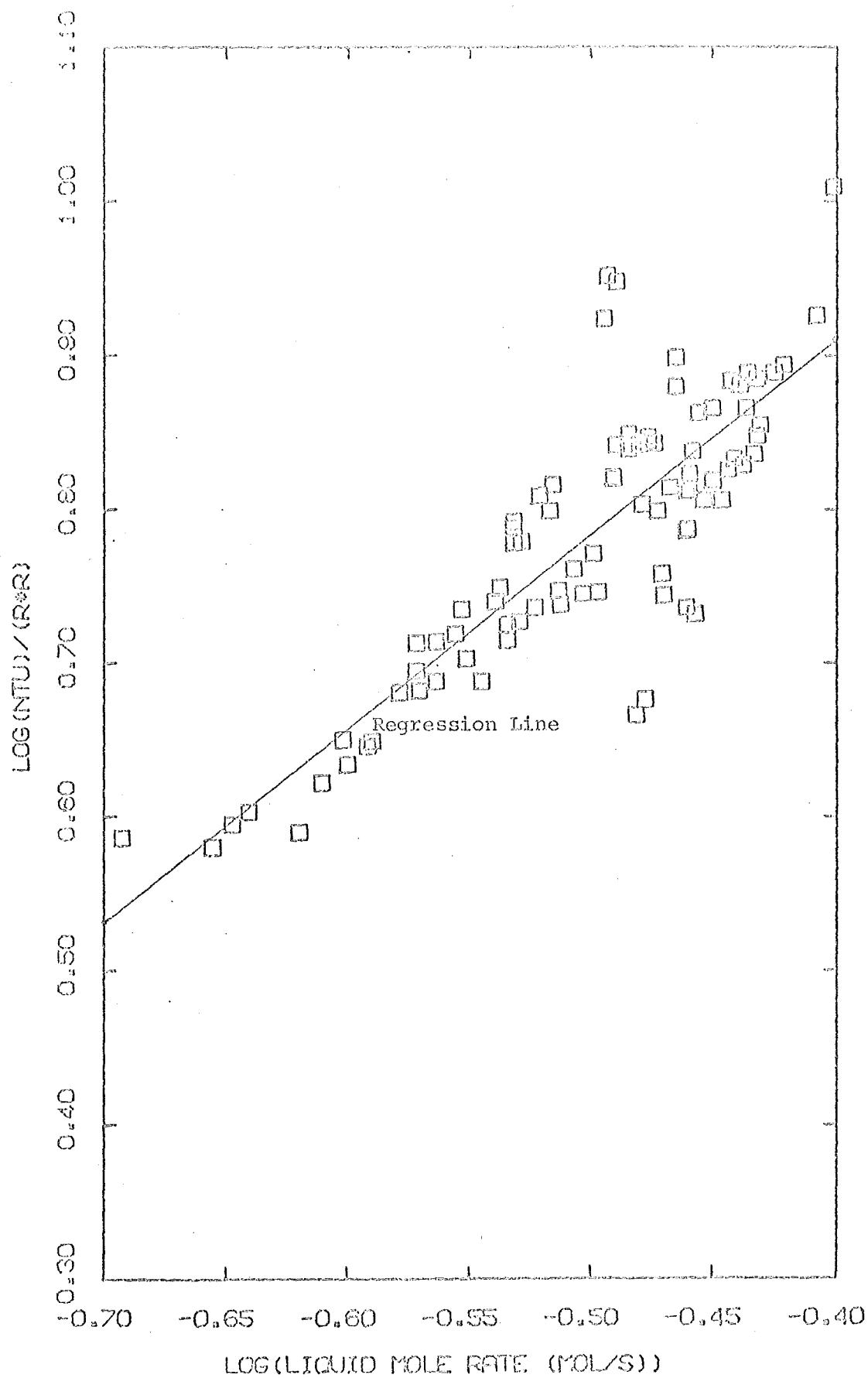


FIG 6.7

NTU/(R*R) VERSUS MOLE LIQUID RATE

$$\log(N_{OG}) = 1.39 - 2.15 \log(V) + 3.36 \log(L) \quad \dots\dots(6.25)$$

$$S.E. = 0.050 \text{ on } \log(N_{OG}) = 12\% \text{ on } N_{OG}$$

This suggests that $N_{OG} \propto L^{3.36} / V^{2.15}$. Since $L/V = R$, a plot of

$\log(N_{OG}^2 / R)$ versus $\log(L)$ was prepared (fig. 6.7). The linear regression

of $\log(N_{OG}^2 / R)$ against $\log(L)$ gave:

$$\log(N_{OG}^2 / R) = 1.41 + 1.253 \log(L) \quad \dots\dots(6.26)$$

$$r = 0.84 ; S.E. = 12\% \text{ on } (N_{OG}^2 / R)$$

Fig. 6.7 shows that equation 6.26 gives a better correlation at low liquid rates. Many of the runs done at high liquid rates were at total reflux (for which $R = 1.0$).

Because of the similar correlation coefficients for equations 6.22, 6.24 and 6.26, it does not seem to matter which equation is used to correlate the experimental number of transfer units, except that at low liquid rates, equation 6.26 seems preferable.

6.6.6 End Effects.

It was assumed that no significant mass transfer took place above the top of the packed bed. Because all the overhead vapour was condensed, any change in composition above the point where the product was withdrawn from the reflux divider could have no effect on the composition further down. Between this point and the top of the packing, there was very little liquid - vapour contact. The holes in the liquid distributor tray were only 2 cm above the top of the packing.

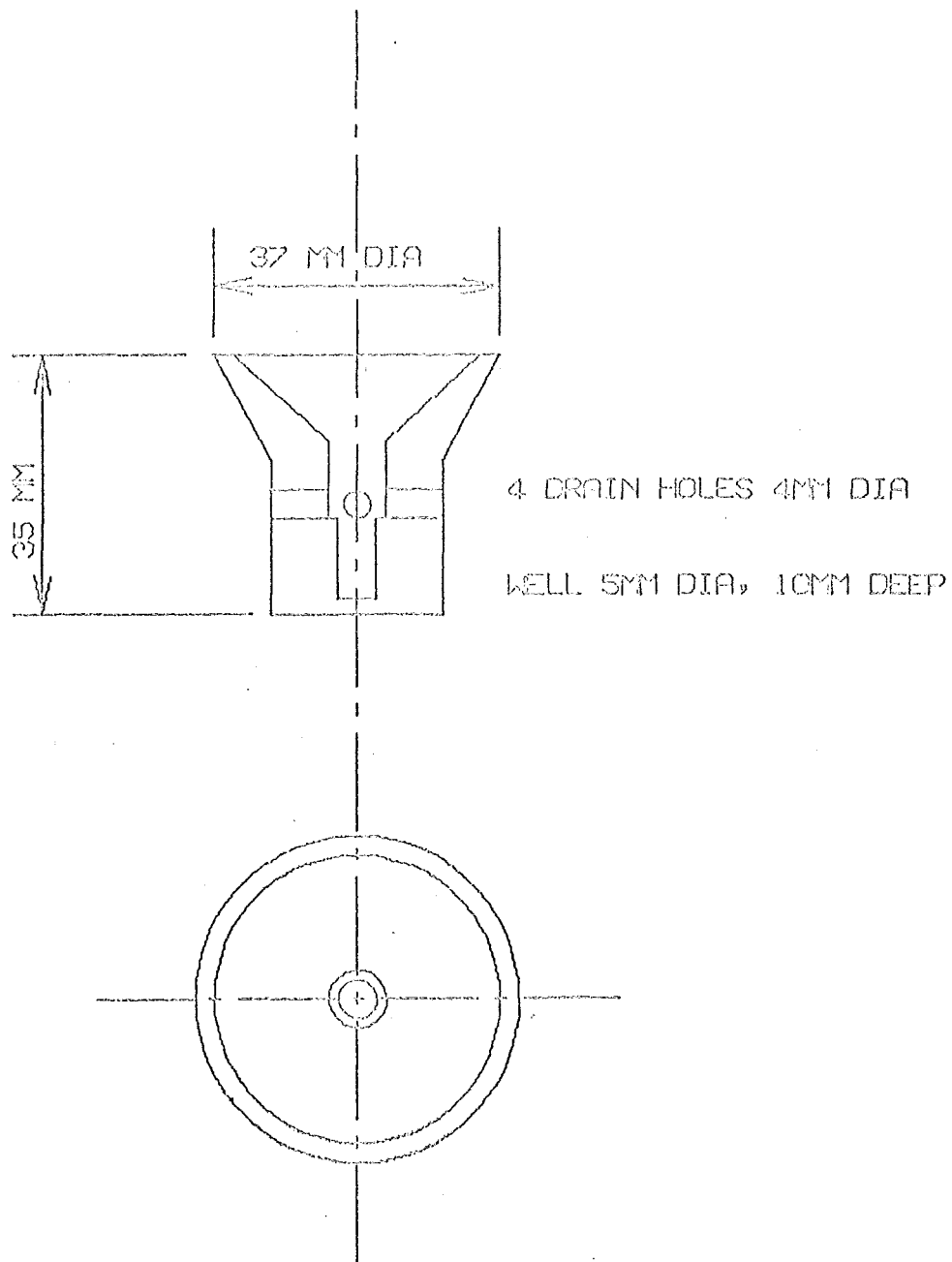


FIG. 6.8

THERMOCOUPLE LIQUID TRAPS

SCALE. FULL SIZE

TABLE 6.13 LOCATION OF THERMOCOUPLES.

Label	Height	Location
A	-	in the liquid condensate stream from the condenser
B	$z=1.0$	in the liquid from the top distributor
C	$z=0.8$	central
D	$z=0.6$	central
E	$z=0.6$	midway between centre and wall
F	$z=0.6$	adjacent to column wall
G	$z=0.5$	central
H	$z=0.4$	central
I	$z=0.2$	central
J	$z=0.0$	central, below bottom of packing
K	$z=0.0$	midway between centre and wall, below bottom of packing
L	$z=0.0$	adjacent to column wall, below bottom of packing
M	$z=0.0$	in total liquid stream below packing
P	-	calibration apparatus

Below the packed bed, there was a 1.8 m length of empty column which could act as a wetted wall column. The height of a transfer unit in such a column can be predicted using the Reynold's analogy (see Pratt (1951)).

$$\left(\frac{K_p H}{G_{bm} m} \right) \left(\frac{N}{Sc} \right)^{2/3} = c \left(\frac{N}{Re} \right)^{-0.2}$$

$$\text{hence } \frac{H}{G} = \frac{G'}{(K a_p M)} = \left(\frac{1}{(a.c)} \right) \left(\frac{N}{Re} \right)^{0.2} \left(\frac{N}{Sc} \right)^{2/3} \dots (6.27)$$

Using the value of 0.028 which Pratt recommends for c leads to:

$$\frac{H}{G} = 5.02 (G')^{0.2} \quad \text{for isopropanol at } 82.3^\circ \text{C in a } 152 \text{ mm}$$

column. (By comparison, the result $\frac{H}{G} = 5.02 (G')^{0.23}$ was obtained from Johnstone and Pigford (1942)).

The prediction from Pratt gives $\frac{H}{G} = 4.8 \text{ m}$ for $G = 0.01 \text{ kg/s}$, and an increased value at greater flow rates. Thus the maximum expected separation in the 1.8 m wetted wall section was about one third of a transfer unit. A separation of one theoretical plate was therefore assumed for the combined effects of the reboiler and the wetted wall section.

6.7 EXPERIMENTAL MEASUREMENTS.

6.7.1 Measurement Of Composition Profiles.

The composition, expressed in mole fraction of methanol, was obtained by measuring the liquid temperature at the required positions.

The relationship between liquid boiling temperature and composition is given by equation 6.3. For positions below the top of the packing, the pressure was above atmospheric pressure. A correction was made to the boiling temperatures (see section 6.3.3) assuming a linear change of pressure with height.

6.7.2 Temperature Measurement.

=====

The temperature of the liquid in the column packing was measured using copper-constantan thermocouples. To ensure that the measured temperature was that of the liquid, and not that of the vapour, the thermocouples were placed in liquid traps as shown in fig. 6.8. The liquid well had dimensions of 5 mm diameter and 10 mm depth, giving a volume of $2 \times 10^{-7} \text{ m}^3$. For 0.25 mol/s of methanol, this gave a mean liquid residence time of 0.3 seconds. This was short compared with the column dynamics.

The thermocouples were located and labelled as listed in table 6.13 and shown in fig. 6.9. Thermocouples B and M measured the temperatures of the total liquid stream at the top and bottom of the packing. All other thermocouples measured the temperature of only part of the liquid stream. The cold junctions of all thermocouples were soldered together and placed in an insulated icebath.

6.7.2.1 Thermocouple Calibration.

=====

Before they were mounted in the column, all thermocouples were calibrated together in a stirred hot water bath. The temperature was measured with a mercury in glass thermometer calibrated to $\pm 0.05 \text{ K}$. The thermocouple outputs were recorded on the data logger used to make the later measurements, and all thermocouples agreed within the resolution of the data logger (0.025 mV which represents approximately 1/16 K).

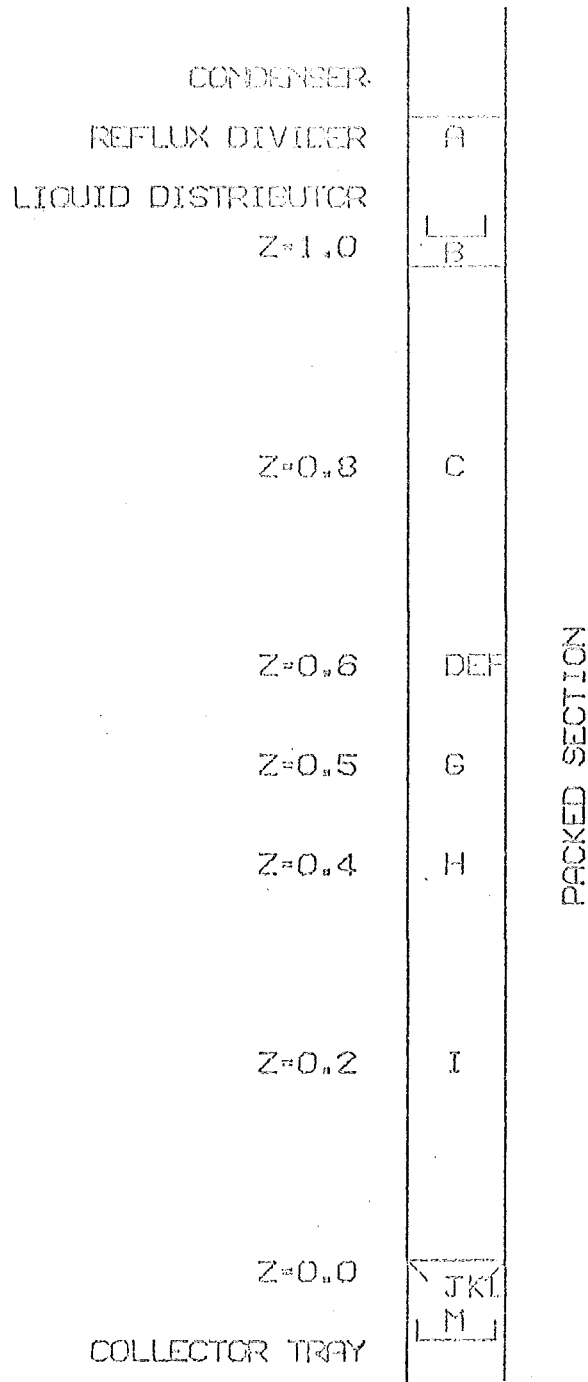


FIG. 6.9
 LOCATION OF THERMOCOUPLES
 SCALE. 1/12 FULL SIZE

The calibration data were fitted by least squares to the equation:

$$DVM = -6.0 + 15.616 T + 0.01556 T^2 \quad \dots\dots(6.28)$$

where DVM is the data logger digital voltmeter reading in units of mVx400, and T is in Celsius.

6.7.2.2 Calibration Of The Pure Component Boiling Points.

To allow for the effect of daily fluctuations in atmospheric pressure, and any possible changes in the thermocouple reference temperature and data logger calibration, a simple boiling point apparatus was used. This comprised an electrically heated flask and a reflux condenser. Thermocouple P was placed in the vapour space in the flask. The boiling point of either pure component could thus be monitored during a run. The constant, and coefficient of x, in equation 6.3 were adjusted for each day's run, so that equations 6.3 and 6.28 together gave the correct compositions for the measured boiling points of the pure components.

6.7.2.3 Measurement Of Thermocouple Voltage.

The thermocouple output voltages were measured using a SOLARTRON COMPACT SERIES 2 data logger on the 25 mV range. The resolution was 0.025 mV. The thermocouples listed in section 6.7.2 occupied 15 of the data logger's 20 channels, the remainder being unused. For the steady state and dynamic runs described in chapters 7 and 8, the thermocouple voltages were scanned every minute. They were displayed by the data logger on a digital voltmeter, and were also punched on paper tape in ASCII code.

6.7.2.4 Errors In Composition Measurement.

Uncertainties in measured compositions arose from two causes:

- (i) Noise in the thermocouple signals to the data logger, and lack of data logger resolution. The measured values of each thermocouple's output during a steady state period were assumed to be from a normal population whose mean was the true liquid boiling point. The error in the composition value was taken to be the 95% confidence limits of the mean value. These were found from the standard deviation of the observations and the statistical t parameter (see Davies (1957)). For many of the measurements made, this error was less than half the data logger resolution. In these cases, an error equal to half the resolution was assumed. This amounted to approximately 0.2 mole percent.
- (ii) From uncertainties in the measurement of the pure component boiling points used to fix the endpoints of the composition - temperature relationship for each day's run. The uncertainty in each boiling point measurement was usually ± 1 DVM unit, causing a further uncertainty in composition measurements of up to 0.3 mole percent.

6.7.3 Vapour Flow Rate Measurement.

The most accurate and convenient method of measuring the vapour flow rate through the packing, was by measuring the amount of heat removed from the column through the condenser. The vapour rate was given by:

$$V = (C_p \cdot W_r \cdot \Delta T + q) / \Delta H_v \quad \dots\dots(6.29)$$

where	V	= vapour rate at the top of the packing	mol/s
	C_p	= specific heat of water	J/(kg.K)
	W_r	= condenser water rate	kg/s
	ΔT	= temperature rise of condenser water	K
	ΔH_v	= latent heat of the vapour at the top of the packing	J/mol

q = surface heat loss from the condenser W

The water flow rate was measured using a bucket and stopwatch. The expected error in W_r was ± 0.2 sec in 30 sec = 0.7% in the time measurement, and ± 0.005 kg in 5 kg = 0.1% in the mass measurement.

The condenser water temperature rise was measured using a thermocouple with one junction in the inlet water, and the other junction in the outlet. The uncertainty in the thermocouple output measured on the data logger was ± 2 units in 300, i.e. 0.7%. The estimated surface heat loss q was 50 watts. The uncertainty in this was trivial compared with the heat flow of 10 to 12 kW. The latent heat ΔH_v depends on the distillate composition, but the error due to uncertainty in composition is no more than 0.05%. The total uncertainty in the measured vapour rate is thus $\pm 1.5\%$.

6.7.4 Measurement Of Distillate Flow Rate.

This was also measured with a bucket and stopwatch. The uncertainty was $\pm 1\%$ in most cases. From the measured vapour and distillate rates, the liquid rate was found from: $L = V - D$.

6.7.5 Measurement Of The Column Pressure Drop.

Whenever the column reached steady state conditions, the pressure drop across the packing was measured using an air-purged water manometer. The air was bubbled through isopropanol before reaching the pressure tappings to reduce the chance of introducing water vapour to the column. The uncertainty in the pressure drop measurements was usually 2 mm water gauge.

The pressure drop was measured to check whether experimental pressure drops matched those predicted in the literature (see section 6.4), to allow the measured boiling points to be corrected for the effect

of pressure, and also to indicate any fluctuation in the vapour flow rate.

6.7.6 Determination Of Column Steady State.

Like most physical processes, the conditions in a packed column should tend towards steady state without ever reaching that condition. The criteria for deciding when the column was essentially at steady state in this work were when, for a period of 15 minutes:

- (i) the condenser heat load was constant within experimental error,
- (ii) the pressure drop across the packing was steady,
- (iii) the temperature measured by each thermocouple in the column showed no long-term drift over that period.

Because small drifts in thermocouple outputs could be obscured by the noise level on the signals, the column was usually left for a further ten minutes after steady state had apparently been reached.

CHAPTER 7 EXPERIMENTAL COMPOSITION PROFILES AT STEADY STATE.

- 7.1 Operating Conditions.
- 7.2 Measured Compositions At Steady State.
- 7.3 Variation Of Composition At The Same Height.
- 7.4 Relative Separation At Different Levels In The Column.
 - 7.4.1 Experimental Variation Of H_{OG} With Packed Height.
- 7.5 Comparison Of Experimental And Predicted Composition Profiles.
- 7.6 Reproduceability Of Steady State Composition Profiles.
- 7.7 Conclusions.

Before considering how well the mathematical model predicts the dynamic behaviour of the column, it is desirable to know how well the measured compositions at steady state agree with those predicted by the model.

With this aim, the steady state composition profile was measured for 23 runs at total reflux. These initial runs were done at total reflux to eliminate any uncertainty in the value of the reflux ratio. The steady state profiles measured later as the initial and final steady states of transient runs are also considered in this chapter.

7.1 OPERATING CONDITIONS.

A summary of the operating variables for all measured steady states, both from the initial total reflux runs and the later dynamic runs, is provided as table A.4.1 in appendix 4.

In the total reflux runs, the operating conditions were changed between steady states by:

- (i) altering the reboiler steam pressure,
- (ii) adding some of one component to the reboiler, or by
- (iii) removing distillate from the column for some time to reduce the proportion of methanol in the system.

7.2 MEASURED COMPOSITIONS AT STEADY STATE.

The column was considered to be at steady state when the criteria given in section 6.7.6 were satisfied. The duration of the steady state conditions was later checked by plotting the measured compositions against time using a computer-driven plotter. The errors in the steady state composition measurements were considered in section 6.7.2.4.

7.3 VARIATION IN COMPOSITION AT THE SAME LEVEL.

At two levels in the column ($z=0.6$ and $z=0.0$), more than one thermocouple was located so that the effect of radial position on the composition could be observed. The mean and standard deviation of the composition differences between each pair of thermocouples have been computed for all the steady states. They are listed in table 7.1.

TABLE 7.1 VARIATION IN COMPOSITION FOR THERMOCOUPLES AT THE SAME LEVEL.

Height z	Thermocouples	Mean difference (mol %)	Standard deviation	95% confidence limits of mean
0.6	D-E	-1.4	4.5	1.0
0.6	D-F	-3.2	2.2	0.5
0.6	E-F	-1.8	5.0	1.1
0.0	J-K	+3.5	2.6	0.6
0.0	J-L	+0.4	1.2	0.3
0.0	J-M	+0.9	0.9	0.2
0.0	K-L	-3.1	2.9	0.6
0.0	K-M	-2.6	2.5	0.5
0.0	L-M	+0.5	0.7	0.2

The values of the mean differences in composition at thermocouples D, E and F suggest that at height $z=0.6$, there is an increase of composition from the centre of the packing to the wall. On average, the composition at E was 1.4 mol % greater than at D, while at F, the composition was an average of 1.8 mol % greater than at E. However, the results for individual runs were not consistent, and in many cases this apparent trend of increasing composition towards the wall was reversed. The possible reasons for a variation in measured composition at different points at the same level are:

(i) one or more thermocouples may not have measured a true liquid temperature owing to partial contact with the vapour.

(ii) the composition varied between one liquid rivulet and another because of differing local liquid and vapour rates. I.e., there was significant channeling in the flows in the packing. Each thermocouple measured the composition of only a sample of the liquid at its level. This may have varied from the mean composition at that level.

(iii) the liquid may have been subcooled on the column wall.

At $z=0.6$, the third possibility could have affected only

thermocouple F. The liquid trap of this thermocouple was touching the column wall. The estimated column heat loss was 100 W/m^2 . For a liquid film heat transfer coefficient of $100 \text{ W/(m}^2 \cdot \text{K)}$, this would have required a liquid film temperature drop of 1 K. However, only a small proportion of the liquid entering the trap of thermocouple F would have been in recent contact with the wall. Attempts to detect subcooling by adding cold liquid to the reflux stream, have shown that condensation of the vapour takes place very quickly to eliminate the subcooling. It is therefore unlikely that the liquid reaching thermocouple F was at all subcooled. Since thermocouples D, E and F were carefully installed upright in the packing, it is certain that they were entirely submerged in the liquid during all runs. Thus it would appear that the observed differences in composition at these thermocouple positions show a real variation in liquid composition across the packing owing to channeling of the liquid. As each thermocouple trap had an area equal to the projected area of about 10 packing pieces, and hence would have collected 10 or more liquid streams, it seems likely that the variation in composition between individual rivulets would be found to be even greater if it could be measured.

Below the packing, thermocouples J, L and M had average differences in composition of less than 1 mol %. At thermocouple K, the measured composition was an average of 2.5 to 3.5 mol % less than at the other thermocouples. This was due to the liquid trap for K being installed at an angle so that the thermocouple was partly in contact with the vapour. This resulted in a higher temperature being recorded and thus giving an apparently low liquid composition. In the total reflux runs, it was noted that the difference between the composition measured by K, and that measured by the other thermocouples, increased as the composition increased. Increased composition causes an increase in the difference between the liquid and vapour temperatures.

When thermocouple K is discounted, it is seen from table 7.1 that the mean and standard deviation of the differences in the composition is

much less at $z=0.0$ than at $z=0.6$. This is not surprising since the composition gradient is usually smaller at $z=0.0$ where the column is operating in a pinch zone.

7.4 RELATIVE SEPARATION AT DIFFERENT LEVELS IN THE COLUMN.

In the model developed in chapter 2, the assumption was made that the height of an overall mass transfer unit, H_{OG} , does not change with height in the column. In section 6.6.4, it was seen that the correlations in the literature predict that the height of a transfer unit will be influenced by the physical properties of the system, and by the temperature, so that it can be expected to vary as the composition varies with height.

To investigate the variation of the height of a transfer unit with height, the following steps were carried out. For each steady state, the separation, measured in number of transfer units, at each thermocouple relative to the bottom of the column (thermocouple M) was computed by numerical integration. This separation was then expressed as a percentage of the total column separation (i.e. the separation between thermocouples B and M). The maximum, minimum, mean, and confidence limits of the mean percentage separation for each thermocouple over all the steady state runs are listed in table 7.2. The differing number of observations for different thermocouples occurs because some thermocouples were not monitored for all runs. The separations at B and M for each run are 100 % and 0 % by definition. Runs in which the top composition exceeded 98 mol % were not included in this analysis. The "ideal" separation is that implied by the assumption of constant height of a transfer unit.

TABLE 7.2 RELATIVE SEPARATIONS AT EACH THERMOCOUPLE.

Thermocouple	Number of observations	Max %	Min %	Mean %	S.D.	95% limits	"Ideal" %
B	88	0.0	100.0	100.0	0.0	0.0	100.0
C	85	99.0	75.1	88.8	4.8	1.0	80.0
D	84	67.0	52.1	60.9	3.0	0.6	60.0
E	83	80.8	50.4	63.7	7.4	1.5	60.0
F	88	76.0	57.0	66.2	4.1	0.9	60.0
G	71	51.6	36.1	42.4	4.1	1.0	50.0
H	88	47.9	27.7	38.6	4.0	0.8	40.0
I	88	26.5	9.8	16.7	3.9	0.8	20.0
J	60	6.8	-1.4	2.0	2.2	0.6	0.0
K	69	4.1	-11.6	-6.0	3.2	0.7	0.0
L	71	7.4	-1.9	1.7	2.0	0.5	0.0
M	88	0.0	0.0	0.0	0.0	0.0	0.0

At thermocouples D, E, H, J and L, the mean separation is within 4 % of that which would occur if the height of a transfer unit was constant. However, there is a wide scatter in the percentage separations at these points for individual runs: e.g. from 26.5 to 9.8 % at I. At the other thermocouples, the mean separation varied from the "Ideal" by up to 8.8 % (at C). The figure for C means that on average, only 11 % of the separation (expressed in number of transfer units), was obtained in the top 20 % of the packing. This was probably due to the liquid distribution not being complete, and resulting in some dry packing in the top two column diameters. At thermocouple G, the separation was consistently only a few percent greater than at H, but considerably below that at D, E and F. As G was located midway between H and D, this means that either thermocouple G gave incorrect readings, or that the column achieved much better separation between $z=0.6$ and $z=0.5$ than between $z=0.5$ and $z=0.4$. The latter explanation seems totally improbable.

The large variation in the fraction of the total separation which

is achieved in a particular part of the packed height, means that even if the total number of transfer units of separation could be accurately predicted for a particular set of operating conditions, the composition at a particular level in the column could still not be predicted with any certainty.

7.4.1 Experimental Variation Of H_{OG} With Packed Height.

The average value of H_{OG} over a part of the packing height, z , may be computed from:

$$H_{OG} = \Delta z / N_{OG} = \int_{Y_1}^{Y_2} \frac{dy}{(f-y)} \quad \dots\dots(7.1)$$

where N_{OG} is the number of transfer units for the element Δz , and y_1 and y_2 are the mean vapour compositions at the bottom and top of the element.

The accuracy of the computed H_{OG} is limited by the uncertainty in composition measurement at each end of the element. A worse difficulty is that the measured composition, except at the column ends, is only a sample of the mean composition at that level, and may differ from the mean by several mol % as was shown in section 7.3.

To illustrate the results obtained when equation 7.1 was used to compute H_{OG} for experimental steady states, the results for two runs (steady states 12 and 20) are listed in table 7.3.

TABLE 7.3 LOCAL VALUES OF H_{OG} FOR TWO STEADY STATES.

		Steady state 12	Steady state 20
Reflux ratio		1.00	1.00
L (mol/s)		0.37	0.24
N (whole column)		7.05	3.89
H_{OG} (m)	B ~ C	0.61 +/- 0.13	0.40 +/- 0.16
	C ~ D	0.13 +/- 0.01	0.43 +/- 0.04
between	C ~ E	0.15 +/- 0.01	0.45 +/- 0.05
	C ~ F	0.14 +/- 0.01	0.26 +/- 0.01
	D ~ H	0.17 +/- 0.01	0.34 +/- 0.03
	E ~ H	0.15 +/- 0.01	0.22 +/- 0.01
	F ~ H	0.18 +/- 0.01	0.22 +/- 0.01
	H ~ I	0.24 +/- 0.02	0.35 +/- 0.03
	I ~ M	0.25 +/- 0.02	0.44 +/- 0.02

Reference to table 6.11 shows that for $L > 0.35$, H_{OG} should increase slightly as the methanol composition increases. For steady state number 12 (table 7.3), the reverse is shown to be the case except for the very top interval of packing. For $L = 0.24$ mol/s, table 6.11 predicts that H_{OG} should decrease by 30 % for pure methanol compared with pure isopropanol. However, in table 7.3 for steady state number 20, no definite trend in H_{OG} with height is apparent. Here the effect of uncertainty in composition at intermediate levels is clearly shown. The computed height of a transfer unit between $z = 0.8$ and $z = 0.6$ varies from 0.45 ± 0.05 m to 0.26 ± 0.01 m depending on whether thermocouple E or F is taken to give the mean composition at $z = 0.6$. Because thermocouple C may also give a composition which is not the mean composition at $z = 0.8$, the uncertainty in the height of a transfer unit over this interval is even greater. This problem applies to the other intervals in the column as well.

These examples show that without an accurate measurement of the mean composition at intermediate levels in the column, the variation of H with height cannot be reliably estimated using equation 7.1. Even OG with the limitations of the present measurements, it appears that the correlations considered in section 6.6.4 and summarised in table 6.11 cannot be relied on to predict even qualitatively how the height of a transfer unit will vary with height for a particular set of conditions.

7.5 COMPARISON OF THE EXPERIMENTAL AND PREDICTED COMPOSITION PROFILES.

TABLE 7.4 EXPERIMENTAL AND PREDICTED COMPOSITIONS FOR STEADY STATE 12.

Thermocouple	z	Experimental (mol %)	Separation (%)	Predicted (mol %)
B	1.0	93.4 +/- 1.1	100.0	93.4
C	0.8	91.2	1.0	85.7
D	0.6	73.3	0.9	71.9
E	0.6	76.0	1.0	71.9
F	0.6	71.5	1.1	71.9
H	0.4	46.3	0.8	51.2
I	0.2	27.0	1.0	29.3
M	0.0	14.2	1.0	14.2

The experimental and predicted composition profiles for a sample run (steady state number 12) are listed in table 7.4. For this steady state, the experimental composition agrees with that predicted only at thermocouple F, apart from the column ends (B and M) where the agreement is forced. At the other thermocouples, the difference is up to 5.5 mol % (at C). This result is typical of that found for all steady states.

Agreement may occur between the experimental and predicted compositions at one or more thermocouples, but at the others there may be a large disagreement, in some cases by more than 10 mole %.

7.6 REPRODUCEABILITY OF THE STEADY STATE COMPOSITION PROFILES.

Steady state runs number 39 to 41 were done to test whether steady state composition profiles were reproducible. For these runs, all the operating conditions agreed within the experimental errors. Between the steady states, large upsets were introduced by: (i) turning off the steam to the reboiler for 2 minutes, (ii) increasing the steam pressure for 4 minutes. The compositions, with errors, at each thermocouple are given in table 7.5 for these steady states.

TABLE 7.5 REPRODUCEABILITY OF STEADY STATE COMPOSITIONS.

		Steady State 39	Steady State 40	Steady State 41
Thermocouple	B	97.5 +/- 0.2	97.1 +/- 0.3	97.6 +/- 0.3
	C	-	-	97.0 0.2
	D	88.0 0.3	87.0 0.5	87.2 0.2
	E	90.6 0.4	89.3 0.3	90.3 0.3
	F	90.3 0.2	88.1 0.4	89.4 0.2
	G	76.2 0.5	73.4 0.2	74.3 0.2
	H	72.2 0.4	68.3 0.4	69.5 0.3
	I	44.2 0.3	42.9 0.3	43.2 0.2
	J	27.0 0.2	27.3 0.2	26.9 0.2
	L	25.9 0.2	26.4 0.2	26.2 0.2
	M	25.0 0.2	25.3 0.3	25.3 0.3

The composition errors tabulated include only the errors due to the uncertainty in the data logger measurements of thermocouple outputs. Errors due to the pure component boiling points have no effect on this

comparison since their effect is identical for each run. Apart from the thermocouples measuring mean compositions at the column ends, only at J was the composition the same within experimental error for all three runs. At the other thermocouples, the composition varied by up to 3.9 ± 0.8 mol % (at H).

These results show that even with the same operating variables, the compositions measured at a particular point at steady state may vary considerably. This supports the opinion expressed in section 7.3: that variations in measured compositions at different points at the same height indicate a random variation of composition in the individual liquid streams, rather than a consistent radial composition gradient.

7.7 CONCLUSIONS.

The important points regarding the steady state composition profiles are:

(i) the composition measured at one point in the packing may vary considerably from the compositions at other points at the same level, and hence from the mean composition at this level. This variation is more pronounced at the central packing heights.

(ii) the composition measured at a particular point in the packing is not reproduceable. It depends not only on the operating conditions, but also on the liquid flow pattern previously set up in the packing.

(iii) the total column separation, in number of transfer units, was found for most runs to be less than that predicted by the literature correlations (see section 6.6.4).

(iv) the height of a transfer unit was found to vary with height in the column, but the variation could not be accurately determined because of the uncertainty in measuring mean compositions at intermediate column heights. The height of a transfer unit is expected to depend on liquid rate, composition (and hence physical properties and temperature), and liquid distribution. It was shown in chapter 2, that if the dependence

of the height of a transfer unit on x , L and z is known, the incorporation of this dependence into the model is not difficult. However it is unlikely that the relationship between the height of a transfer unit and these variables will be known well enough to make this worthwhile. In most practical situations, the precise knowledge of intermediate column compositions should be unnecessary. If the mean composition at a particular column level is required for automatic control purposes, the average composition at several points across the column should be used. If possible, the collection of all the liquid at that level for composition measurement before redistribution would be an even better procedure.

(v) because the composition in the packing is not predicted by the model to better than ± 10 mol % in some cases at steady state, it can be expected that no better prediction of the compositions under dynamic conditions will be obtained.

CHAPTER 8 EXPERIMENTAL COMPOSITION PROFILES AT UNSTEADY STATE.

- 8.1 Introduction.
- 8.2 Plots Of Experimental Responses.
- 8.3 Comparison Of Experimental And Predicted Response
 Curves.
- 8.3.1 The Shape Of The Composition Response Curves.
- 8.3.2 The Speed Of The Composition Responses.
- 8.4 Conclusion.

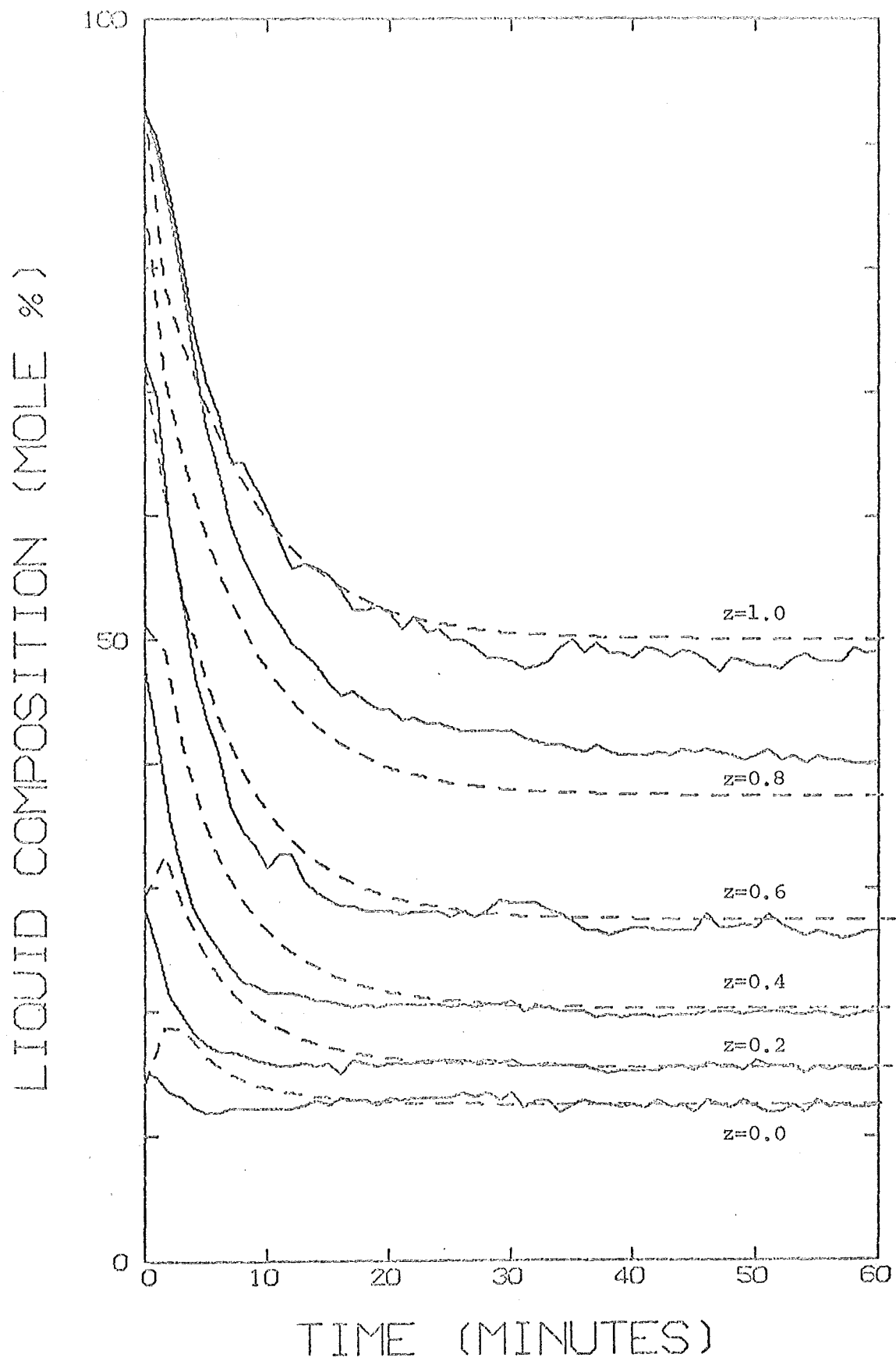


FIG 8.1 TRANSIENT NUMBER 11.

8.1 INTRODUCTION.

This chapter presents the results of the dynamic response measurements made on the column, and compares them with the responses predicted by the model described in chapter 2. The aim of this experimental work was to test the effectiveness of the model in predicting the response of the column to step changes in the liquid reflux rate, this being the easiest variable in which to introduce and measure upsets. Where shortcomings in the model become apparent, the possibility of overcoming them is considered.

8.2 PLOTS OF EXPERIMENTAL RESPONSES.

Transient responses were measured between the steady states listed in table 8.1. Operating variables for all steady states are listed in table A.4.1, appendix 4.

8.2.1 Change In NTU During A Transient.

In the model developed in chapter 2, it was assumed that the separation, in number of transfer units (NTU), would not change during a transient. To handle the large changes in NTU found experimentally from the initial steady state to the final steady state, two methods were tried. In the first, NTU was set to the final value immediately after the liquid reflux rate upset occurred. Fig 8.1 plots the measured and predicted responses for transient number 11 using this method. The second method was to vary NTU linearly between the required initial and final values as XD varied from its initial to its final value. Transient number 11 is again plotted in fig 8.2 using this method of varying NTU.

In figs. 8.1 and 8.2, the time scale plotted is the time for the experimental response. So that the shapes of the experimental and

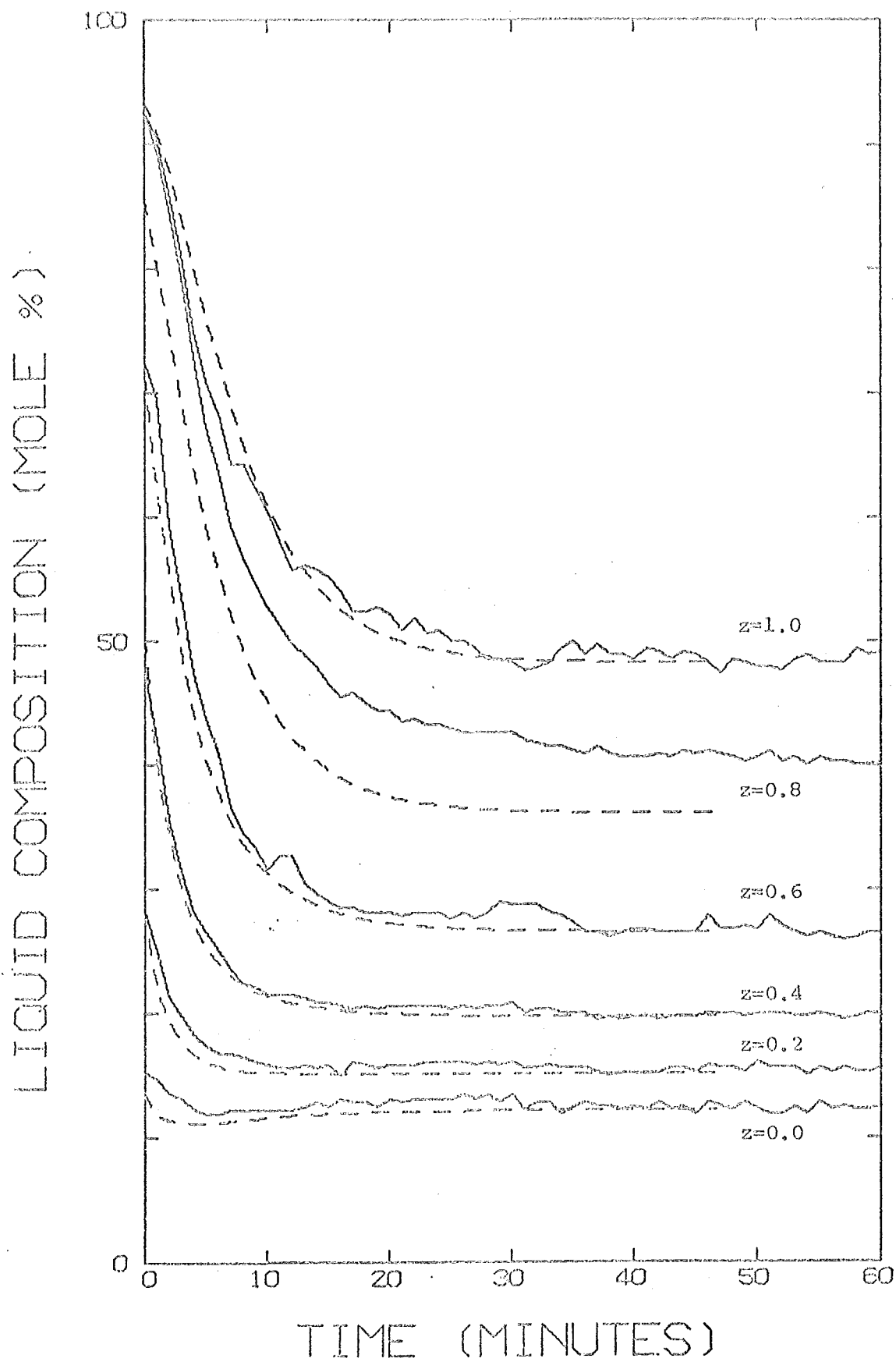


FIG 8.2 TRANSIENT NUMBER 11

TABLE 8.1 EXPERIMENTAL TRANSIENTS AND RESPONSE TIME RATIOS.

Transient number	Initial st. state	Final st. state	Response time ratio	Initial H (mol/m).	Final H (mol/m)
1	1	2	-	20,7	23,0
2	2	3	-	23,0	20,6
3	3	4	-	20,6	16,4
4	4	5	1,2	16,4	20,5
5	5	6	1,3	20,5	17,4
6	6	7	1,6	17,4	22,9
7	8	9	1,8	19,9	22,3
8	9	10	1,2	22,3	19,7
9	10	11	0,9	19,7	18,4
10	11	12	1,5	18,4	22,2
11	12	13	0,9	22,2	18,2
12	13	14	0,7	18,2	19,6
13	14	15	1,4	19,6	21,4
14	16	17	0,7	15,3	14,9
15	17	18	1,4	14,9	13,6
16	18	19	0,8	13,6	14,5
17	21	22	1,9	18,0	18,9
19	23	24	0,9	17,1	16,0
20	24	25	0,7	16,0	16,7
21	25	26	1,4	16,7	18,8
22	27	28	2,0	19,3	16,0
23	28	29	1,6	16,0	19,3
24	29	30	1,9	19,3	16,6
25	30	31	0,6	16,6	17,7
26	31	32	2,2	17,7	19,3
27	34	35	1,9	18,8	20,7
28	37	38	1,8	18,2	20,6
29	43	44	1,9	18,1	21,8
30	45	46	1,8	18,7	21,9

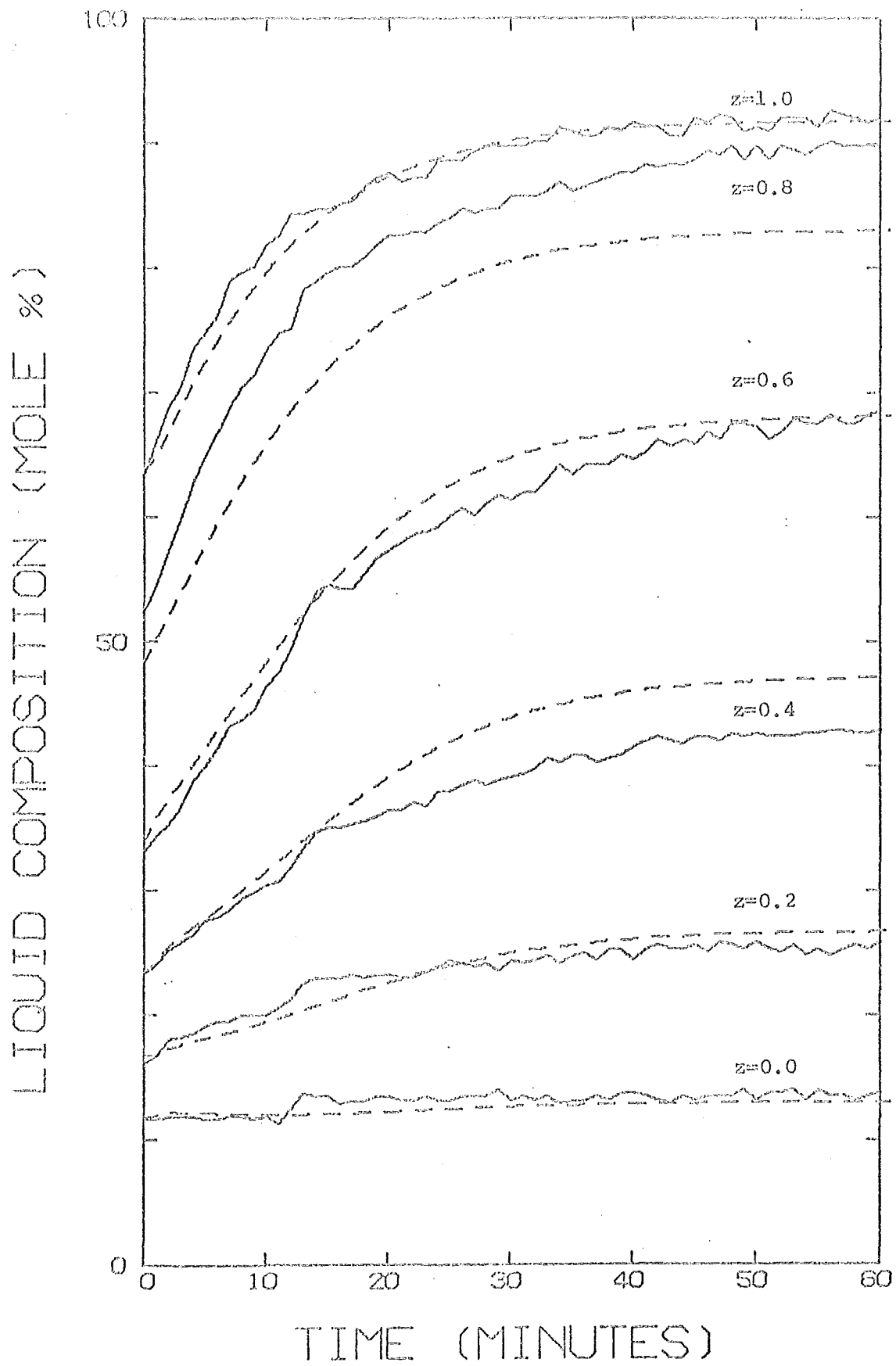


FIG 8.3 TRANSIENT NUMBER 13.

predicted response curves can be compared, the time scale of the predicted response has been normalised. This has been done by scaling the predicted response so that the time for 75 % of the total change in XD matches the 75 % XD response time of the experimental transient. This has also been done in fig. 8.3 and figs. A.5.1 to A.5.10. In all these plots, the continuous lines give the experimental response and the dashed lines give the predicted response.

It can be readily seen from figs. 8.1 and 8.2, that the use of NTU varying linearly with XD gave a response which agreed much more closely with the measured response than did the response using a step change in NTU. This was found to be true for all transients for which a comparison was made. A major difference in the results of the two approaches, is that the step change in NTU produced an overshoot in the response in the lower part of the column whenever there was a significant change in NTU for a run. This overshoot was much greater than any observed experimentally. Consequently, the method of using a gradually changing NTU was adopted. The NTU was computed from:

$$NTU = NTU(\text{initial}) + \frac{(NTU(\text{final}) - NTU(\text{initial})) \cdot (XD - XD(\text{initial}))}{(XD(\text{final}) - XD(\text{initial}))} \quad \dots\dots(8.1)$$

This is a very simplified approximation to the way in which NTU changes during a transient. As discussed in section 6.6, NTU is expected to vary not only with liquid composition, but also with liquid rate (vapour rate was kept constant during the transients). In view of the lack of success in correlating the values of NTU at steady state, there seems to be no justification for trying to make a more sophisticated prediction of NTU under dynamic conditions.

Both methods for setting the variation of NTU during a transient share a serious drawback. They require the final NTU to be known before the composition response to an upset can be predicted. Thus, unless the dependence of NTU on flow rates and compositions can be accurately

established, so that NTU can be predicted in advance to better than $\pm 5\%$, it is not possible to use the model to predict what the new steady state compositions will be after an upset. Instead, it will only be possible to predict how the compositions will change with time once the final steady state compositions are known.

In fig. 8.3, the response of transient number 13 is given for a change in liquid rate in the opposite direction to that of transient number 11 (fig. 8.2). The response curves of 10 other transients selected to cover a range of liquid rates and reboiler compositions are given in figs. A.5.1 to A.5.10, appendix 5.

8.3 COMPARISON OF EXPERIMENTAL AND PREDICTED RESPONSE CURVES.

To enable a comparison of the experimental and predicted response curves to be made, some criteria of "goodness of agreement" are needed. The criteria will depend on the end use of the model, so a definitive set of conditions to be met before a model can be considered satisfactory for all applications cannot be defined. For on-line control, the early part of the response to an upset may be of major importance, and the approach to the final steady state may be of less interest. For off-line design of control systems, the shape and speed of the response at some height may be needed. This would enable a time-constant type of transfer function to be fitted to the response for small upsets from a normal operating level. For batch column prediction, the ability of a model to predict the distillate composition at all times through a run is the most important consideration. This would require the dependence of the column separation on composition to be known. For policies other than constant reflux, the effect of changing the liquid rate on the separation (in NTU) would also be needed. The difficulty in predicting the dependence of NTU on liquid rate and composition has been discussed in section 6.6.

The comparison between the experimental and computed responses has

been made in two stages. Firstly, a comparison of the shape of the responses, and secondly, a comparison of the speed of the responses has been made.

8.3.1 The Shape Of The Composition Response Curves.

To enable the shape of the experimental and predicted responses to be compared, the time scale of the predicted response curve was normalised for each run. This was done by multiplying the time scale for the predicted response by a factor so that the 75 % XD response time for the predicted response equalled the 75 % response time for the experimental response. The figure of 75 % was chosen arbitrarily. It was decided to concentrate on a comparison of the distillate composition curves because:

- (i) the distillate composition is the composition most frequently of interest in practical columns.
- (ii) the change in distillate composition was usually much greater than the change in composition at the bottom of the packing (where the noise in composition measurement made comparison more difficult).
- (iii) it was found at steady state, that the compositions sampled at intermediate levels in the packing may differ widely from the mean composition at those levels. Thus there was little point in comparing a predicted average composition at some level with an experimental composition which was not the average composition at that level.

The first stage of the comparison was to check whether or not the final values of XD and $x(0)$ predicted by the model matched those observed experimentally. This need not occur, despite the use of the observed final values to compute the final NTU before the predicted response was computed. In the event of errors in the holdups used in predicting the response, a different final steady state would be obtained with the same NTU separation as the experimental final steady state.

For the 12 transients plotted in figs. 8.2, 8.3 and appendix A.5, table 8.2 summarises the predicted and observed final values of XD and

x(0).

TABLE 8.2 PREDICTED AND EXPERIMENTAL FINAL STEADY STATE VALUES FOR XD AND x(0).

Transient	XD		x(0)	
	Predicted	Experimental	Predicted	Experimental
1	99.2	99.2 +/- 0.4	47.8	48.2 +/- 0.3
2	96.0	95.9 +/- 0.4	40.3	39.9 +/- 0.3
4	94.4	94.4 +/- 0.4	37.3	38.3 +/- 0.3
10	93.2	93.3 +/- 0.8	14.0	14.2 +/- 0.6
11	48.0	48.3 +/- 0.6	12.2	11.9 +/- 0.6
13	91.8	91.9 +/- 0.8	13.0	13.0 +/- 0.6
15	46.0	45.9 +/- 0.5	14.6	14.6 +/- 0.4
16	53.4	53.5 +/- 0.5	14.9	14.9 +/- 0.4
19	55.8	56.0 +/- 0.4	16.0	16.0 +/- 0.3
20	64.5	64.4 +/- 0.4	16.0	16.1 +/- 0.3
21	87.6	87.9 +/- 0.5	18.1	18.3 +/- 0.3
26	93.4	93.5 +/- 0.4	22.8	22.9 +/- 0.3

The final values of XD agreed well for all runs compared with the uncertainty of the experimental measurements. At x(0), there was also agreement, except for transients 1, 2 and 4. For these runs, the reboiler composition was very high (>30 mol %) compared with the other runs. This led to a large difference between XB and x(0), and so a small error in the assumption of one theoretical stage of separation for the reboiler and wetted-wall column section combined, could have produced the small discrepancies observed.

To test the effect of errors in reboiler and packing holdups on final steady state predictions, responses were computed with 10 % errors in reboiler holdup and packing holdup for transients 4 and 11. From table 8.3, it can be seen that the effect of a 10 % change in reboiler or packing holdup on transient number 4 is negligible, but for transient 11,

there is a significant variation in XD. For transient 4 with a high reboiler composition and reboiler holdup, there was much more methanol in the reboiler than in the packing. This large quantity of the more volatile component meant that the reboiler composition did not change much as a result of the changed amount of the more volatile component in the packing. For transient 4, the top of the packing was also approaching a pinch zone situation. This tended to make XD insensitive to any change in XB caused by a different value of the holdup. For transient number 11, the reboiler composition and holdup were much lower than for transient 4, and hence an error in the holdup had a greater effect on the reboiler composition. Since the pinch zone was at the bottom of the packing for transient 11, the effect of a small change in XB on XD was greater. The composition change in XD for transient 11 was 45 mol %. Had the change in XD been smaller, the influence of holdup errors could have been expected to have been less.

TABLE 8.3 EFFECT OF ERRORS IN HOLDUPS ON PREDICTED FINAL VALUES OF XD AND $x(0)$.

Transient	Holdup change	Change in XD	Change in $x(0)$
4	10% decrease in HREB	0.0	-0.1
4	10% increase in HL	0.0	-0.1
11	10% decrease in HREB	+0.9	+0.1
11	10% increase in HL	+1.0	+0.1

The good agreement obtained between predicted and experimental final values of XD (table 8.2) does not confirm that the holdup values used were accurate. As an example, using a change in reboiler or packing holdup of 10 % for transient 11, a change of approximately 3 % in the predicted final NTU would have brought the predicted final XD back into agreement with the experimental value. Note that changing the value of a holdup used in the prediction moves the final value of both XD and $x(0)$ in the same direction, while changing the predicted final NTU moves them in opposite directions.

From the normalised response plots for the 12 transients presented, it was found that only for transients 4 and 11 were there discrepancies between the experimental and predicted values of XD of more than 2 mol % at any time during a transient. In the early part of these transients, the discrepancies were approximately 3 mol % and 4 mol % respectively. Since the total changes in XD for these transients were 30 and 40 mol % respectively, a maximum discrepancy of 10 % of the total change is considered to be satisfactory. Thus the model can be said to make a satisfactory prediction of the shape of the composition response for XD .

At intermediate levels in the packing, a quantitative comparison was not possible because average compositions at each level could not be measured. However, one phenomenon observed is worthy of note. For several transients (numbers 4, 10, 13, 21, 26) for which the liquid rate was increased, the composition response curves at more than one level showed a distinct change of slope at about the same time, usually 10 to 20 minutes after the upset. This was not observed for transients resulting from decreased liquid rate, nor from all increased liquid rate transients. For transients 4, 10 and 13, the change in slope appears to be related to a sudden change in $x(0)$ after some time, whereas the model predicts a much more gradual change in $x(0)$.

For transients 4 and 10, the predicted response at $z=0.0$ and $z=0.2$ showed a kink in the first few minutes. The fluctuating slope of the early part of these responses was not observed experimentally, and was probably caused by the method of relating NTU to XD in the model not accurately representing the change in NTU in the experimental column.

Apart from these effects, the shape of the predicted response in $x(0)$ matched the shape of the observed response. However, in some cases (e.g. transients 2 and 11) the time scales of the predicted and experimental responses at $x(0)$ did not agree when the time scales were normalised using the response for XD .

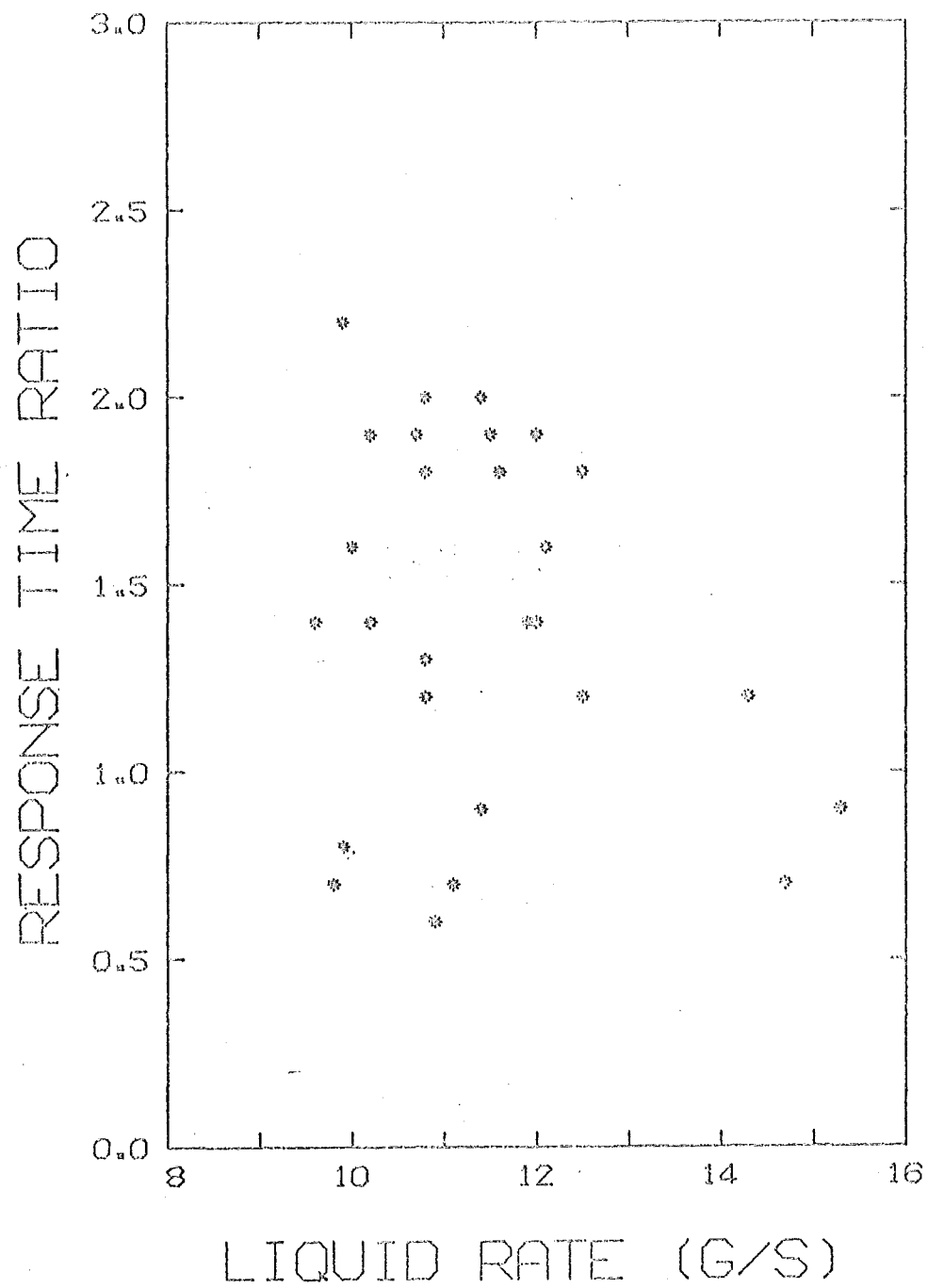


FIG 8.4
EFFECT OF LIQUID RATE
ON RESPONSE TIME RATIO

8.3.2 The Speed Of The Composition Responses.

As explained in the previous section, the time scale of the predicted transient response was scaled so that the 75 % response times for XD agreed for the experimental results and the model prediction. The required scale factor is used as a measure of the ability of the model to predict the correct time scale of the experimental transient response. The time scale factor, or response time ratio, is defined as:

$$\begin{aligned} &\text{response time ratio} \\ &= \frac{\text{time for 75 \% of total change in XD to occur in experimental transient}}{\text{time for 75 \% of total change in XD to occur in predicted transient}} \\ &\dots\dots(8.2) \end{aligned}$$

Thus a response time ratio of unity would show complete agreement between the response time of the model and the experimental column. The response time ratios for the transients are included in table 8.1. They range from 0.6 to 2.2. An attempt was made to correlate the response time ratios with column parameters such as the initial and final values of liquid rate (see fig. 8.4), vapour rate, liquid holdup, pressure drop, NTU, molal liquid rate, and also with the change in these variables during the transients. The scatter of points in fig. 8.4 is typical of the lack of correlation found with all these parameters. In fig. 8.5, the response time ratio is plotted against the change in liquid holdup from initial to final steady state. The holdup was based on conditions at the top of the packing and was computed from equation 6.6. This graph suggests that the response time ratio may be low when there is a small change in liquid holdup through a run. However, there is a considerable scatter in the points on the plot, so no firm conclusions can be drawn from it. Attempts were made to plot several variables (liquid rate, initial and final XD, initial and final NTU) as parameters in fig. 8.5, but for none of these was any correlation obtained.

The fact that in some cases, the experimental column responded more than twice as slowly as predicted, points to a serious shortcoming

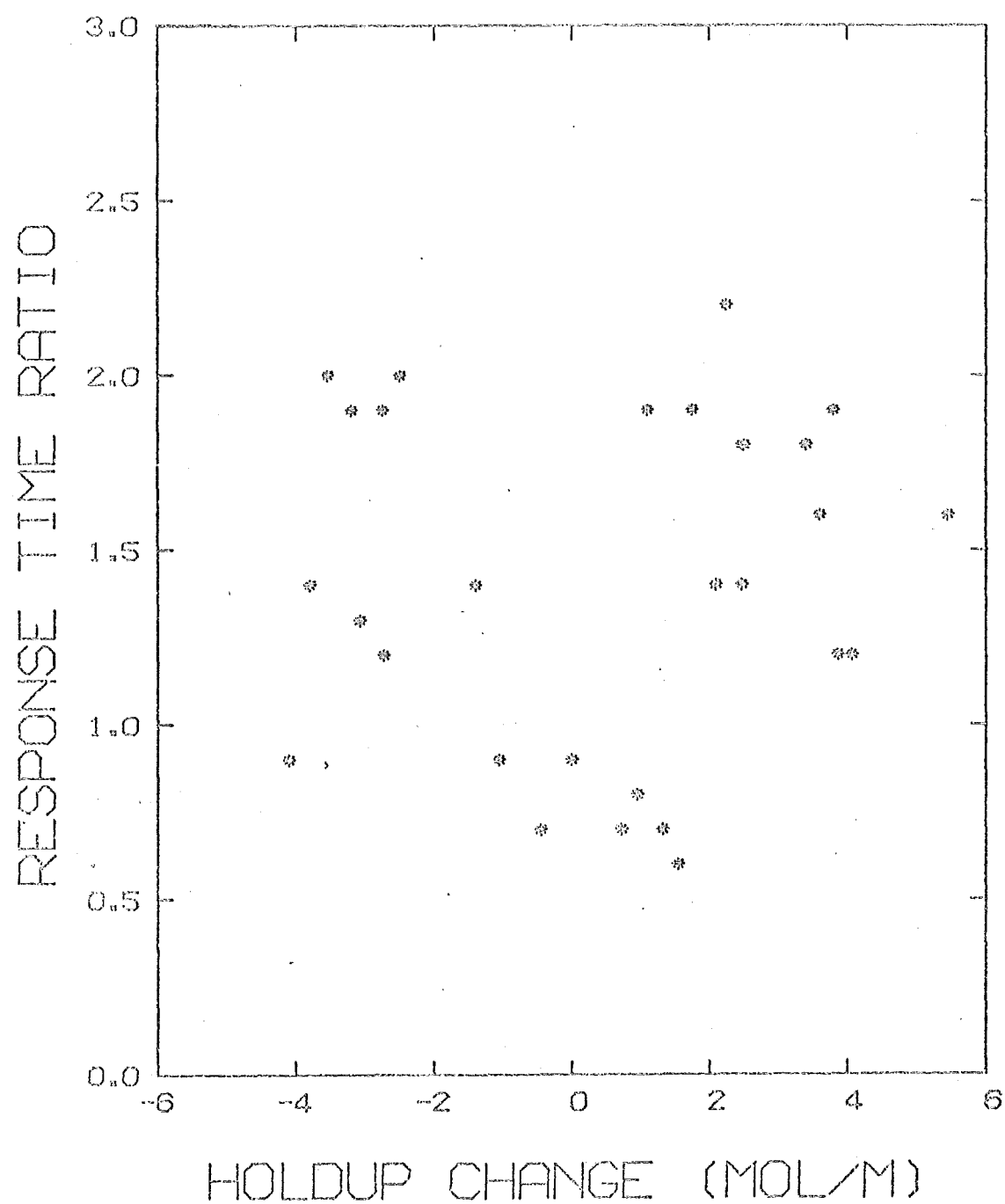


FIG 8.5.

EFFECT OF HOLDUP CHANGE
ON RESPONSE TIME RATIO

in the model. The possible reasons for the discrepancy in the predicted response times will now be considered.

(i) The liquid holdups predicted by equation 6.6 may be in error. Because the time intervals for the predicted response are given by:

$$\Delta t = H \cdot Z \cdot \Delta z / L$$

any error in the value used for H will give a corresponding error in the time scale. However, an error of as much as 100 % in H would be needed for some runs in order for this to explain the time scale discrepancies; compared with an expected error of perhaps ± 25 % in the correlation. Such an error would have caused a large discrepancy between the predicted and experimental final values of X_D and $x(0)$ (see table 8.3). Any error in the reboiler holdup large enough to account for the observed response time ratios would similarly cause large errors in the predicted final values of X_D and $x(0)$. The reboiler holdup was known to better than ± 10 %.

Any error in the predicted value of H could be expected to be mainly systematic. In particular, it could be expected that the predicted holdup would become progressively low at flow rates approaching flooding. Yet no systematic dependence of the response time ratio on liquid flow rate or composition (which determine the holdup) was found.

The other factors in the Δt term, namely L , Z and Δz , were subject to uncertainties of not more than 3 % for L , and even less for Z and Δz . It is thus concluded that neither errors in the liquid holdup, nor errors in the other factors which determine the predicted time scale, could have resulted in the observed values of the response time ratio.

(ii) The condenser holdup figure of 5 moles may have been in error by as much as 30 %. The effect of such an error on the response time ratio was computed to be 10 % for transient 4 (increasing liquid rate) and 7 % for transient 11 (decreasing liquid rate). Thus the error in the condenser holdup could not account for the response time ratios differing from unity. The greater influence of condenser holdup on the response time

when the liquid rate was increased, as seen here for transients 4 and 11, was found to occur in most cases computed.

The condenser holdup (in moles) may be expected to vary to a slight extent with vapour rate, and much more strongly with the distillate composition (because of the large difference in the molecular weights of methanol and isopropanol). To correct for these effects, the condenser mass holdup could be assumed to be constant, or it could be computed from the vapour rate if the dependence of holdup on vapour rate was known. The molal condenser holdup could then be found by using the molecular weight of the distillate mixture. By replacing $HC \cdot dx/dt$ in equation 2.13 with $HC \cdot dx/dt + x \cdot dHC/dt$, the influence of changing condenser holdup can readily be accounted for. For modelling a column with an external reflux drum, especially when the flows from the drum are manipulated to control the column, the use of a variable condenser holdup would be essential.

(iii) The way in which NTU varied throughout a transient may not have been adequately described by a linear dependence on the change in XD between the initial and final values. The use of this method of varying NTU in the model implies that the change in NTU depends on changes in composition, and ignores the effect of changes in the liquid rate. From table 6.12, it can be determined that when the liquid rate is decreased, NTU will decrease. Decreasing liquid rate also decreases the composition over most or all of the packing, and this is predicted in table 6.12 to cause a decrease in NTU except at the highest liquid rates. Thus, to take account of the effect of changing liquid rate on NTU, the value of NTU should be made to change even more rapidly during the initial part of a transient. This would cause the time scale of the predicted response to be even faster, and so the response time ratios would be greater than with the method used.

(iv) The vapour holdup was ignored in computing the predicted transients plotted in this work. However, when the results were recomputed using a vapour holdup of 0.5 mol/m, the effect on the response time ratio was of

the order of 1 to 2 %.

(v) The change in liquid holdup between initial and final steady states was not accounted for in the model. In line with the approach of previous workers, the dynamic mass balance in equation 2.4 was written:

$$\frac{H\partial x}{\partial t} = \frac{L\partial x}{\partial z} - K \frac{a.s(f-y)}{G} \quad \dots\dots(2.4)$$

This assumes that H is constant. The value of H used in computing the predicted transients was the value for the final steady state. However, for the experimental transients, the change in H from initial to final steady state as predicted by equation 6.6 varied by from 2.6 % (transient 14) to 32 % (transient 6). The initial and final values of H are included in table 8.1.

To include the effect of varying H, equation 2.1 should be used in expanded form:

$$\frac{H\partial x}{\partial t} + \frac{x\partial H}{\partial t} = \frac{L\partial x}{\partial z} - K \frac{a.s(f-y)}{G} \quad \dots\dots(8.3)$$

At the initial steady state, the right hand side of equation 8.3 (which represents the driving force for change) will be zero, as will $\partial x/\partial t$ and $\partial H/\partial t$. When the liquid reflux rate is changed, the initial driving force will be $\Delta L\partial x/\partial z$. The change in both H and x have the same sign as the change in L. Thus both $\partial x/\partial t$ and $\partial H/\partial t$ compete for a share of the same driving force. This means that the response of x to the change will be slower if there is also a change in H. Thus including the term for the rate of change of liquid holdup with time in the model, would result in the predicted transient response being slower than when the change in H is ignored. However, this requires knowledge of $\partial H/\partial t$; i.e. how the holdup in a particular section of the packing changes with time when a change is made in the liquid flow rate. The maximum possible value of $\partial H/\partial t$ for a packed height interval $Z\Delta z$ is given by:

$$\partial H / \partial t = \Delta L / (Z \cdot \Delta z) \quad \dots (8.4)$$

This is true if there is no increase in the liquid flow out of the bottom of the height interval until the steady state holdup corresponding to the new liquid rate has been established. In practice, it is certain that the liquid rate from the bottom of the packing interval under consideration will begin to increase before this occurs, so that the value of $\partial H / \partial t$ will be less than that predicted in this way. This can be confirmed by examining the figures for a particular transient.

For transient number 10, the initial liquid flow of 0.327 mol/s was changed to 0.370 mol/s. In modelling the transient, the initial value of x at $z=0.9$ was 0.4366, and at $z=1.0$ it was 0.5010. The column height was 1.52 m. The initial driving force for the addition of more volatile component to the interval $z=0.9$ to $z=1.0$ in the packing was

$$(\Delta L / Z)(\partial x / \partial z) = ((0.37 - 0.327) / 1.5) * ((0.501 - 0.4366) / 0.1) = 0.0185$$

The dynamic mass balance at $t=0$ for this section is thus:

$$H(\partial x / \partial t) + x(\partial H / \partial t) = 0.0185$$

For $H = 22.4$ mol/m, this gives an initial value of 0.00082 for $\partial x / \partial t$ if $\partial H / \partial t = 0$. The average value of $\partial x / \partial t$ at $z=1.0$ predicted by the model for the first two time intervals (with $H_C=0$) was 0.00097. (When a value of 5.0 moles was used for H_C , the retarding effect of the condenser holdup reduced the initial value of $\partial x / \partial t$ at $z=1.0$ to 0.00029).

However, if $\partial x / \partial t$ was initially zero, the maximum initial value of $\partial H / \partial t$ would be:

$$\partial H / \partial t = 0.0185 / 0.5010 = 0.037 \text{ mol/(m.s)}$$

This is only 13 % of the maximum possible value of 0.287 computed from equation 8.4. Since $\partial x / \partial t$ at $z=1.0$ is initially non-zero, the actual value of $\partial H / \partial t$ computed from mass transfer driving force considerations, must be an even smaller fraction of the maximum value obtained from considering the change in the liquid flow rate.

While it cannot be readily computed, it is obvious from the preceeding paragraphs that the effect of the change in liquid holdup in

the packing can have a significant retarding effect on the transient response to a step change in the liquid reflux rate. The rate of change of the liquid holdup is the key to knowing how large the effect is. It would be reasonable to expect that $\partial H/\partial t$ would be largest for transients in which the total change in H from the initial to the final steady state was the largest. Fig. 8.5 supports this theory to some extent, in that, with one exception, the transients with a response time ratio of less than 1.0 all had a change in H of less than 1 mol/m. However, the scatter in the points was such that no firm conclusions can be drawn.

(vi) The plug flow model assumed did not adequately describe the liquid flow behaviour. From the variation in the composition at a particular level in the packing, (see section 7.3), it was concluded that the liquid plug flow behaviour assumed by the model was not a true representation of the real column. As a further check on the liquid flow behaviour, the dead time in the response to changes in the liquid flow rate was measured. Assuming plug flow behaviour and no significant change in liquid holdup, the dead time at level z should be:

$$\text{dead time} = H \cdot Z \cdot (1-z)/L \quad (\text{seconds}) \quad \dots\dots(8.5)$$

This is equal to the mean liquid residence time from the top of the packing to the level z . Table 8.4 compares measured dead times in the experimental column with mean residence times (based on the use of equation 6.6 to predicted the liquid holdup) for $z=0.0$.

TABLE 8.4 COMPARISON OF EXPERIMENTAL DEADTIMES AND MEAN LIQUID RESIDENCE TIMES AT $z = 1.0$

Test	L'	V'	L	Dead time	Mean residence
	(g/s at $z=1.0$)			(seconds)	time (seconds)
1	7.2	13.3	decreasing	19 +/- 6	112
2	12.4	12.4	increasing	30 +/- 8	90
3	6.7	10.5	decreasing	20 +/- 6	116
4	9.6	9.6	increasing	40 +/- 12	100
5	4.6	10.5	decreasing	22 +/- 6	134
6	10.7	10.7	increasing	34 +/- 6	96

The results in table 8.4 show that the dead time was approximately one sixth of the mean residence time when the liquid rate was decreased, and one third of the mean residence time when the liquid rate was increased. These results show that the plug flow model is quite inadequate for predicting the dead time in response to liquid rate upsets, and support the suggestion that there is considerable channelling in the liquid flow in the packing. How important this is in the prediction of the time scale of the dynamic response to an upset is, however, unclear. Because some liquid passes through the column several times faster than the mean flow rate, there must be liquid which passes through several times slower than the mean rate. The incorporation of a statistical residence time distribution into the model, to account for this, would add considerably to the complexity of the computation involved in modelling a column. Intuitively, the column dynamics are more likely to be retarded by the existence of stagnant pools of liquid in the packing at low liquid rates. However, the lack of correlation between the response time ratios and the liquid rate, means that this cannot be proposed as the major cause of variation in the response time ratios.

CHAPTER 9 CONCLUSIONS AND SUGGESTIONS FOR FURTHER WORK.

9.1 The Model.

9.2 Experimental Results.

9.3 Further Work.

9.3.1 Model Development.

9.3.2 Experimental Testing.

9.1 THE MODEL.

It was seen in chapters 1 to 5 that a dynamic model for a packed distillation column, based on the mass balance equations used by previous workers, could be readily solved using a digital computer. The computer solution was fast, accurate and stable. The use of a digital computer to solve the equations had some important advantages when compared with previous analytical solutions of the model.

(i) An equilibrium curve representing reported experimental liquid-vapour equilibrium data was used. Analytical solutions of the model require a linear equilibrium relationship, or the assumption of constant relative volatility.

(ii) An analytical solution requires constant coefficients in the mass balance equations. It was shown in chapter 3 how variable coefficients can be used with only a slight increase in the amount of computation needed in the numerical solution. This means that it is not necessary to assume that flow rates, holdups and mass transfer coefficients are constant throughout a column.

(iii) As was shown in chapter 5, the boundary conditions of a numerical solution can be easily adapted to model any column of practical interest, including a continuous column.

9.2 EXPERIMENTAL RESULTS.

The conclusions concerning the experimental steady state results are given in section 7.7. From the results and discussion given in chapter 8, the following conclusions can be drawn regarding the ability of the model to predict the dynamic response of the experimental column.

(i) The use of a value of NTU which varied linearly with XD through a transient, was found to give a satisfactory prediction of the shape of the response of XD. In modelling some transients, it gave changes in the slope of the early part of the response at some lower levels in the packing. This is unlikely to cause practical problems.

(ii) Because the effect of changing the liquid rate on NTU could not be adequately predicted, the experimental final steady state had to be known before the dynamic response to an upset could be predicted by the model.

(iii) In modelling the transients, the final value of NTU could be adjusted so that the predicted final values of XD and $x(0)$ agreed with the measured values, within experimental error, except for $x(0)$ when the reboiler composition was high.

(iv) When the predicted and experimental dynamic responses were compared on a normalised time scale, there was good agreement between the curves for XD.

(v) The agreement between the predicted and experimental response curves at other levels was not so close. This was predicted in chapter 7, and was due mainly to the experimental measurements not giving the mean compositions at intermediate levels.

(vi) The factor by which the time scale of the predicted response had to be multiplied to make it match the experimental response, (the response time ratio), was found to vary between 0.6 and 2.2. No correlation between the response time ratio and column parameters such as liquid flow rate or holdup, was found to help in explaining these widely varying response time ratio values.

(vii) Errors in assumptions in the model which may have contributed to the response time ratio values found were: (a) no account being taken of the rate of change of liquid holdup, (b) the variation of NTU during the

transient not being as described, and (c) the liquid not following plug flow behaviour as was assumed.

(viii) Errors in holdup predictions alone could not account for the wide variation in the response time ratios. The effect of such errors should have been systematic.

(ix) Whether the model is considered to be satisfactory in describing the dynamic behaviour of a packed distillation column will depend on the requirements of the user. The composition changes in the transients used to test the model were much greater than can be expected in a production column, except perhaps in a batch column. With smaller upsets, the changes in NTU and H become less, and the problems of how these vary with time are therefore less important. The vital factor in the model's performance is how well the time scale of the response it predicts matches reality. If a column is kept within a reasonably small operating region, one or two calibration transients may suffice to give an adequate time-scale conversion factor.

9.3 FURTHER WORK.

9.3.1 Model Development.

=====

Implementation of the use of variable coefficients is a minor step which can be readily taken if sufficient information is available, particularly concerning the variation in mass transfer coefficients. Use of a variable holdup through the transient is also prevented only by the lack of knowledge of how the holdup varies with time following a change in the liquid flow rate. There seems to be little point in trying to develop a more sophisticated dynamic packed distillation column model, until it can be proved that inadequacies in the predicted dynamic responses are due to defects in the model, and are not due to lack of knowledge of such factors as the rate of change of holdup with time.

The introduction of a further dimension to the problem, by considering the radial composition variation, should be considered only if it can be proved experimentally to be a significant effect. The radial composition measurements in this work (see section 7.3) do not provide evidence for a consistent variation of composition with radial position. Modelling the radial composition variation would require a model for the radial liquid and vapour flow rate variation which included the effect of channelling. The extra computation involved in solving a model which includes these features would probably not be justified by the improvement in the results.

9.3.2 Experimental Testing.

.....

Further testing of the model under the most favourable possible experimental conditions would be useful in assessing its performance. The components of the binary system used in this study had widely differing molecular weights, molal latent heats and boiling points. The choice of a system in which these factors are close for each component, should lead to smaller variations of liquid holdup, flow rates and mass transfer coefficients with composition. Close attention to the initial liquid distribution, and choice of a packing which will maintain even liquid distribution, should help to eliminate any influence of the liquid distribution on the dynamic column behaviour.

It would be desirable to have available liquid holdup data measured under distillation conditions, rather than at ambient temperatures. Data on the rate of change of liquid holdup with time following a change in the liquid flow rate, would be of great use in determining how important the change in holdup is on the transient response time.

There is scope for a detailed study of the variation of composition across the packing, and of the relationship between this and the liquid distribution.

Measurements of the mean composition at various levels in the column would enable the dependence of the overall mass transfer coefficient on the liquid flow rate, liquid composition and liquid distribution to be correlated better. Unfortunately, measurement of the composition at a large number of positions at the same level is not easy if the operation of the packing is not to be disturbed. It was not possible using the composition measuring method of this work. Most published mass transfer coefficient data are based on compositions measured only at the ends of the packing.

SYMBOLS

a	interfacial area per unit volume	$\frac{m^2}{m^3}$
A, B, C, b, c	constants with various uses	
b_1, b_2, c_1, c_2	constants defined in chapter 2	
C_p	specific heat	J/(kg.K)
D_p	equivalent diameter of the packing	m
D	column diameter	m
D	distillate rate	mol/s
DP	column pressure drop	mm water
DTC	condenser dead time	s
DVM	data logger reading	mVx400
e	void fraction	
f	equilibrium vapour composition	
f_e, f_s	equilibrium vapour composition in the enriching and stripping sections	
F	feed rate	mol/s
g	acceleration due to gravity	$m.s^{-2}$
G	vapour flowrate	kg/s
G'	vapour flowrate	$kg/(s.m^2)$
h	vapour holdup per unit packing height	mol/m
H	liquid holdup per unit packing height	mol/m
H_G	height of a vapour film transfer unit	m
H_L	height of a liquid film transfer unit	m
H_L	liquid enthalpy	kJ/mol
H_{OG}	height of an overall gas-phase transfer unit	m
H_V	vapour enthalpy	kJ/mol
HC	condenser holdup	moles
HR	reboiler holdup	moles

k_G	mass transfer coefficient based on the vapour composition driving force	$\text{mol}/(\text{s.m}^2)$
k_L	mass transfer coefficient based on the liquid composition driving force	$\text{mol}/(\text{s.m}^2)$
K_G	mass transfer coefficient based on the overall vapour composition driving force	$\text{mol}/(\text{s.m}^2)$
K_L	mass transfer coefficient based on the overall liquid composition driving force	$\text{mol}/(\text{s.m}^2)$
L	liquid rate	mol/s
L'	liquid rate	$\text{kg}/(\text{s.m}^2)$
LE, LS	liquid flowrate in the enriching and stripping sections	mol/s
m	slope of equilibrium curve	
M_m	mean molecular weight	
$MELR$	minimum effective liquid rate	$(\text{m}^3/\text{s})/\text{m}$
N	mass transfer rate per unit packing height	$\text{mol}/(\text{s.m})$
N_{OG}, NTU	number of overall gas-phase transfer units	
N_{Re}	Reynold's number (packed bed)	
N_{Sc}	Schmidt number	
ρ	density	kg.m^{-3}
P	vapour pressure	mm Hg
P_{bm}	bulk pressure	atm
Q_s	surface heat loss	W
r	correlation coefficient	
R	internal reflux ratio ($=L/V$)	
σ	surface tension	dyne/cm
s	Laplace Transform variable	
S	cross sectional area of the column	m^2

S.E.	Standard error	
t, t'	time	s
T	temperature	K, C or F
μ	viscosity	centipoise
V	vapour flowrate	mol/s
VE, VS	vapour flowrate in the enriching and stripping sections	mol/s
w	fractional wetting rate	
W	bottom product rate	mol/s
Wr	wetting rate	$\frac{2}{m/s}$
x	mole fraction of the more volatile component in the liquid	
x_e, x_s	liquid composition in the enriching and stripping sections	
x_N	normalised liquid composition response	
X, Y	coordinates for generalised pressure drop correlation	
XB	liquid mole fraction in the reboiler	
XD	liquid mole fraction in the distillate	
XF	feed composition	
y	mole fraction of the more volatile component in the vapour	
y_e, y_s	vapour composition in the enriching and stripping sections	
z	dimensionless height from the bottom of a packed section	
Z	total height of the packed section	m
τ	time constant	
z	dimensional height from the bottom of a packed section	m
Δt	time interval	
Δz	dimensionless height interval	

SUBSCRIPTS

G	vapour
i	height subscript
L	liquid
m	maximum height subscript
n	time subscript
T	top of the packing
V	vapour

SUPERSSCRIPTS

*	equilibrium composition
---	-------------------------

REFERENCES

- Archer D.H. and Rothfus R.R., Chem Eng Prog Symposium Series vol 57, number 36, p.2 (1961)
- Backhurst J.R. and Harker J.H., Process Plant Design, London, Heinemann Educational Books (1973)
- Ballard L.H. and van Winkle M., Ind Eng Chem vol 44, p.2450 (1952)
- Bogart M.J., Trans A I Chem E vol 33, p.139 (1937)
- Borchardt E. and Wagner H.G., Chem Ing Techn vol 43, p.956 (1971)
- Boublik T., Fried V. and Hala E., The Vapour Pressures of Pure Substances, Amsterdam, Elsevier (1973)
- Bowman J.R. and Briant R.C., Ind Eng Chem vol 39, p.745 (1947)
- Boyle J.D. and Palmer A., in "International Symposium on Measurement and Control", London, Inst. of Measurement and Control, p.189 (1973)
- Chilton T.H. and Colburn A.P., Ind Eng Chem vol 27, p.255 (1935)
- Cohen K., J Chem Phys vol 8, p.588 (1940)
- Colburn A.P., Trans A I Chem E vol 33, p.211 (1939)
- Cornell D. et al, Chem Eng Prog vol 58, p.68 (July 1960)
- Davies O.L. (Ed.), Statistical Methods In Research and Production, London, Oliver and Boyd (1957)
- Eckert J.S., Chem Eng Prog vol 57, p.54 (1961)
- Heinke P. et al, Chem Ing Techn vol 37, p.681 (1965)
- Heinke P. and Wagner H.G., Chem Ing Techn vol 38, p.1252 (1966)
- Jawson M.A. and Smith W., Proc Roy Soc (London) vol A225, p.226 (1954)
- Jesser B.W. and Elgin J.C., Trans A I Chem E vol 39, p.277 (1943)
- Johnstone H.F. and Pigford R.L., Trans A I Chem E vol 38, p.25 (1942)
- Kropholler H.W. et al, Measurement and Control vol 1, p.T55 (1968)
- Larsen T.H., AIEE Transactions Part II vol 74, p.109 (May 1955)
- Leva M., Tower Packings and Packed Tower Design, 2nd Edn. Akron Ohio, U.S. Stoneware Co. (1953)

REFERENCES

- Marshall W.R. and Pigford R.L., The Application of Differential Equations to Chemical Engineering Problems, Newark Delaware, Univ. of Delaware (1948)
- Morris G.A. and Jackson J., Absorption Towers, London, Butterworths (1953)
- Perry J.H. (Ed.), Chemical Engineer's Handbook, 4th Edn. New York, McGraw-Hill (1963).
- Perry R.H. and Chilton C.H (Eds.), Chemical Engineer's Handbook, 5th Edn. Tokyo, McGraw-Hill Kogakusha (1973)
- Prahl W.H., Chem Eng vol 76, p.89 (Aug 11, 1969)
- Pratt H.R.C., Trans Inst Chem Engrs vol 29, p.195 (1951)
- Rose A. and Welshans L.M., Ind Eng Chem vol 32, p.668 (1940)
- Rosenbrock H.H., Trans Inst Chem Engrs vol 40, p.376 (1962)
- Sherwood T.K. and Holloway F.A.L., Trans A I Chem E vol 36, p.39 (1940)
- Timmermans J., Physico-Chemical Constants of Pure Organic Compounds, vol 1, New York, Elsevier (1950)
- Timmermans J., Physico-Chemical Constants of Pure Organic Compounds, vol 2, Amsterdam, Elsevier (1965)
- Tomassi G. and Rice P., Ind Eng Chem Process Des Dev vol 9, p.234 (1970)
- von Rosenberg D.U., Methods for the Numerical Solution Of Partial Differential Equations, New York, Elsevier (1969)
- Weast R.C. (Ed.), Handbook of Chemistry and Physics, 49th Edn. Cleveland, The Chemical Rubber Co. (1968)
- Williams T.J., Chem Eng Prog Symposium Series vol 59, number 46, p.1 (1963)
- Yoshida F. and Koyanagi T., A I Chem E J vol 8, p.309 (1962)

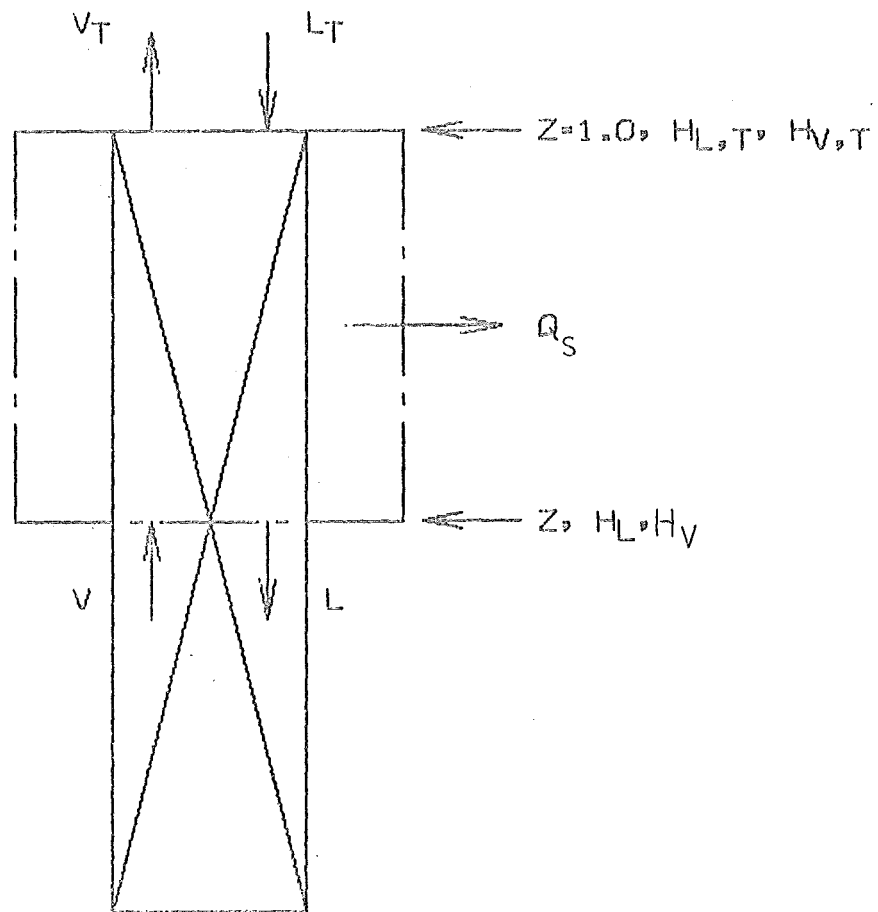


FIG A.1.1 ENTHALPY
BALANCE IN THE PACKING

The purpose of this enthalpy balance is to allow the variation of liquid and vapour flow rates with height in the packing to be computed. Taking a balance over the packing from the top down to height z (see fig. A.1.1) gives:

$$V_{T,V,T} \cdot H_{V,T} + L_{L,T} \cdot H_{L,T} + Q_S (1-z) = L_{T,L,T} \cdot H_{L,T} + V_{T,V} \cdot H_{V,T}$$

where H_V = vapour enthalpy kJ/mol

H_L = liquid enthalpy kJ/mol

Q_S = surface heat loss over total packing length W

T = subscript denoting condition at the
top of the packing ($z=1.0$)

and variables without the T subscript are at height z .

Using the mass balances:

$$L_T = V_T - D$$

and $L = V - D$ (A.1.1)

to eliminate L and L_T leads to:

$$V(z) = \frac{V_T (H_{V,T} - H_V) + D (H_{L,T} - H_L) + Q_S (1-z)}{(H_V - H_L)} \quad \text{.....(A.1.2)}$$

The liquid rate may then be computed for any height z from (A.1.1).

APPENDIX 2

COMPUTER SUBROUTINES

A.2.1 SUBROUTINE YSTAR.

This subroutine finds the equilibrium vapour composition, y^* or f , for any given liquid composition x . Any desired relationship can be used. In this study, the equilibrium data of Ballard and van Winkle (1952) for isopropanol-methanol was fitted by a least-squares curve fit to the equation:

$$f = x + x(1-x)(A + \sum_{i=1}^n B_i (1-2x)^i)$$

No improvement in the closeness of fit was found for values of n greater than 4. A listing of subroutine YSTAR follows.

```

SUBROUTINE YSTAR(Y,X)
C   THIS SUBROUTINE EVALUATES THE EQUILIBRIUM VAPOUR COMPOSITION
C   Y FOR ANY LIQUID COMPOSITION X
C   DIMENSION B(4)
C   THESE COEFFICIENTS ARE FOR THE ISOPROPANOL-METHANOL SYSTEM
DATA B/0.052195,-0.17571,-0.019018,0.210234/,A/0.659357/
C   TEST FOR OFF-RANGE X
IF(X.GT.1.0)GO TO 2
IF(X.LT.0.0)GO TO 3
C   EVALUATE Y. THE EXPRESSION IS Y=X+X(1-X)(A+SIGMA(B(I)*(1-2X)**I))
XX=1.-2.*X
SUM=0.
Z=1.
DO 1 J=1,4
Z=Z*XX
1 SUM=SUM+B(J)*Z
Y=X+X*(1.-X)*(A+SUM)
RETURN
2 Y=1.0
X=1.0
GO TO 6
3 Y=0.
X=0.0
6 PRINT 9,X

RETURN
9 FORMAT(' YSTAR ERROR  X= ',E14.4)
END

```

A.2.2 SUBROUTINE SSTATE.

This coordinating subroutine calls another subroutine to find whichever variable is unspecified, and the steady state composition profile in the column. The subroutine called is chosen using the parameter ICLASS as shown in table A.2.1.

TABLE A.2.1 SUBROUTINES CALLED TO FIND UNKNOWN PARAMETERS.

ICLASS	Unknown parameter	Subroutine called to find it	Subroutine used to get composition profile
0	XD	FINDXD	FINDXD
1	N OG	FINDTU	FINDXB
2	XB	FINDXB	FINDXB
3	R	FINDR	FINDXB

The parameters in the argument list for SSTATE are as follows:

TABLE A.2.2 ARGUMENT LIST FOR SSTATE.

Parameter	Origin	Use
ICLASS	specified in MAINLINE	see table A.2.1
XB	<div style="display: inline-block; vertical-align: middle;"> <div style="display: inline-block; vertical-align: middle; font-size: 2em; line-height: 1;">[</div> <div style="display: inline-block; vertical-align: middle;"> 3 of these will be specified in MAINLINE. The other will be computed in a subroutine called by SSTATE </div> </div>	reboiler composition
XD		top product composition
R		reflux ratio
FNTU		number of transfer units
DZ	defined in MAINLINE	height increment
Y	<div style="display: inline-block; vertical-align: middle;"> <div style="display: inline-block; vertical-align: middle; font-size: 2em; line-height: 1;">[</div> <div style="display: inline-block; vertical-align: middle;"> computed in FINDXD or FINDXB </div> </div>	vapour composition
X		liquid composition
F		equilibrium vapour composition
M	computed in SSTATE	2+ number of height increments
IFLAG	SSTATE	flag set if impossible separation specified

A listing of subroutine SSTATE follows.

```

C      SUBROUTINE SSTATE(ICLASS,XB,XD,R,FNTU,DZ,Y,X,F,M,IFLAG)
C      THIS SUBROUTINE WILL CALL ANOTHER TO FIND THE STEADY STATE
C      CONCENTRATION PROFILE AND WHICHEVER OPERATING PARAMETER IS UNSPECIFIED
C      THE VALUE OF ICLASS DETERMINES WHICH ROUTINE IS USED
C
C      THE VALUES WHICH ICLASS MAY TAKE ARE AS FOLLOWS:
C
C      ICLASS      UNKNOWN      ROUTINES USED
C
C      <=0         XD          FINDXD
C      1           NTU         FINDTU & FINDXB
C      2           XB          FINDXB
C      3           R           FINDR & FINDXB
C
C      DIMENSION X(1),Y(1),F(1)
C              INITIALISE COUNTER USED IN FINDXB
C      IFACT=1
C      IF ICLASS.GE.3 USE FINDR TO EVALUATE R AND RETURN
C      IF(ICLASS.GE.3)CALL FINDR(XB,XD,R,FNTU,DZ,Y,X,F,M,IFACT,IFLAG)
C      IF(ICLASS.GE.3)RETURN
C      EVALUATE COEFFICIENTS
C      1 M=1.001/DZ+2.
C      FN=FNTU*DZ/2.
C      A=(1-FN)/(1+FN)
C      B=FN/(1+FN)
C      C=(1.-R)*XD/R
C      IF(ICLASS.GE.1)GO TO 11
C      IF ICLASS.LT.1 USE FINDXD TO EVALUATE XD
C      CALL FINDXD(A,B,XB,R,FNTU,DZ,XD,Y,X,F,M)
C      RETURN
C      11 IF(ICLASS.GE.2)GO TO 12
C      IF ICLASS.EQ.1 USE FINDTU TO EVALUATE FNTU
C      THEN USE FINDXB TO GET CONCENTRATION PROFILE
C      IFLAG=0
C      CHECK THAT THE SPECIFIED SEPARATION IS POSSIBLE FOR THE
C      SPECIFIED R. IF NOT PRINT MESSAGE, SET IFLAG TO 1 AND RETURN
C      CALL YSTAR(Y(2),XB)
C      X(2)=Y(2)/R-C
C      IF(X(2).GT.XB)GO TO 6
C      IFLAG=1
C      PRINT 97,X(2),XB,XD,R
C      RETURN
C      6 CALL FINDTU(XB,XD,X,Y,F,R,C,FNTU,M)
C      41 ICLASS=2
C      12 CONTINUE
C      IF ICLASS.EQ.2 USE FINDXB TO EVALUATE XB
C      CALL FINDXB(M,A,B,C,DZ,IFACT,XD,XB,X,Y,F,R,FNTU,ICLASS)
C      IF DZ HAS BEEN HALVED, RECALCULATE COEFFICIENTS
C      IF(IFACT.GT.1)GO TO 1
C      RETURN
C      97 FORMAT(/60X,'*****'/30X,'IMPOSSIBLE CONDITION
C      1 X(1)='F10.6,' XB='F10.6,' XD='F10.4,' R='F10.4/)
C      END

```

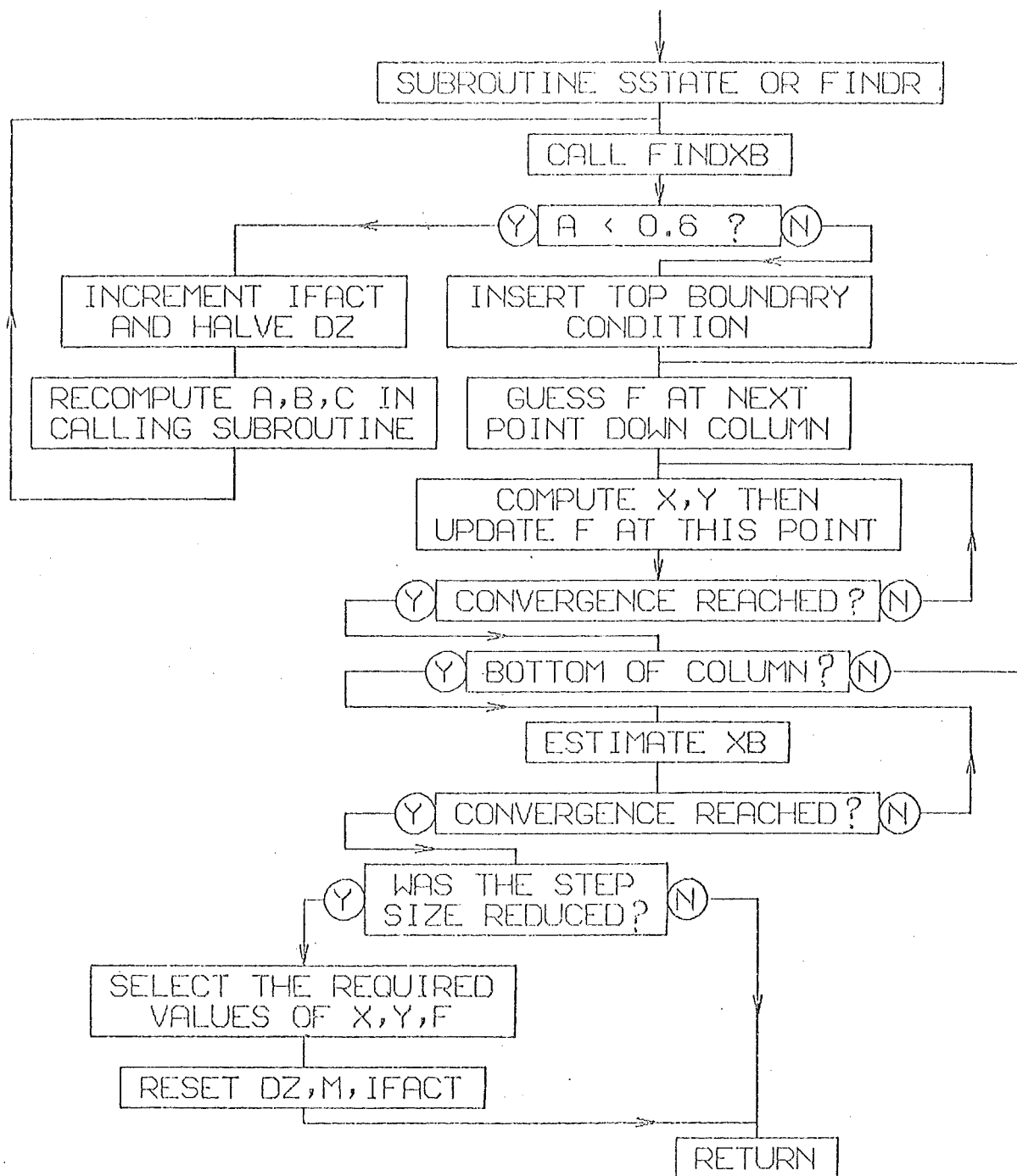


FIG A.2.1 FLOW
DIAGRAM FOR FINDXB

A.2.3 SUBROUTINE FINDXB.

The purpose of this subroutine has been outlined in section(3.2.1). The parameters in the argument list are the same as for SSTATE with the addition of:

TABLE A.2.3 ARGUMENTS FOR FINDXB.

Parameter	Origin	Use
A	<div style="display: inline-block; vertical-align: middle;"> <div style="display: inline-block; vertical-align: middle;">[</div> <div style="display: inline-block; vertical-align: middle;">calculated in SSTATE</div> <div style="display: inline-block; vertical-align: middle;">]</div> </div>	<div style="display: inline-block; vertical-align: middle;"> <div style="display: inline-block; vertical-align: middle;">[</div> <div style="display: inline-block; vertical-align: middle;">coefficients in equations (3.10) and (3.11)</div> <div style="display: inline-block; vertical-align: middle;">]</div> </div>
B		
C		
IFACT	initialised in SSTATE	counter

IFACT gives the number of times by which M has been increased for calculations in FINDXB. M is successively doubled (up to the maximum dimension for X of 162) until the value of A exceeds 0.6. For lower values of A, the subroutine may not converge to XB. If M has been increased by a factor of 4 for instance (IFACT=4), then at the end of FINDXB it is returned to its previous value. Every fourth value of X, Y and F is then selected to be returned to SSTATE.

A listing of subroutine FINDXB has been included along with a flow diagram.

SUBROUTINE FINDXB(M,A,B,C,DZ,IFACT,XD,XB,X,Y,F,R,FNTU,ICLAS)

SUBROUTINE FINDXB FINDS THE UNKNOWN XB AND THE CONCENTRATION
PROFILES FOR THE BASIC COLUMN AT STEADY STATE WHEN XD, R AND
NTU ARE SPECIFIED.

DIMENSION X(1),Y(1),F(1)

IF A.LT.0.6, HALVE STEP SIZE AND RETURN TO RECALCULATE
COEFFICIENTS UNLESS THE MAXIMUM 161 STEPS WILL BE EXCEEDED

IF(M.GT.82)GO TO 2

IF(A.GE.0.6)GO TO 2

IFACT MEASURES TOTAL REDUCTION IN STEP SIZE

IFACT=IFACT*2

DZ=DZ/2.

RETURN

2 BA=B/A

PRINT HEADING IF ICLASS.EQ.2

IF(ICLAS.EQ.2)PRINT 103,XD,R,FNTU

FIX VALUES OF X,Y AND F AT TOP OF COLUMN

X(M)=XD

Y(M)=XD

CALL YSTAR(F(M),X(M))

IN THIS LOOP THE VALUES OF X,Y AND F ARE FOUND

AT EACH SUCCEEDING POINT WORKING DOWN THE COLUMN

DO 26 I=3,M

L=M-I+1

APART FROM THE FIRST POINT,THE VALUE OF F AT EACH POINT IS ESTIMAT ED BY

EXTRAPOLATING FROM THE TWO PREVIOUS POINTS

F(L+1)=F(L+2)

IF(I.GT.3)F(L+1)=2.*F(L+2)-F(L+3)

BEGINNING OF ITERATION LOOP

DO 21 J=1,10

YSTOR IS THE LATEST VALUE OF Y. Y IS SET EQUAL

TO YSTOR AFTER CONVERGENCE IS TESTED

YSTOR=Y(L+2)/A-BA*(F(L+1)+F(L+2))

X(L+1)=YSTOR/R-C

CALL YSTAR(F(L+1),X(L+1))

IF(J.EQ.1)GO TO 25

GO ON TO NEXT POINT IF CONVERGENCE REACHED

IF(ABS(Y(L+1)-YSTOR).LE.0.00005)GO TO 26

IF(J.EQ.10) GO TO 21

25 Y(L+1)=YSTOR

21 CONTINUE

PRINT MESSAGE IF NO CONVERGENCE AFTER 10 ITERATIONS

PRINT 106,I,YSTOR,Y(L+1)

26 Y(L+1)=YSTOR

FIRST GUESS FOR XB BY EXTRAPOLATING FROM X(2) AND X(3)

XB=X(2)-(F(2)-Y(2))*(X(3)-X(2))/(F(3)-F(2))

CALL YSTAR(YSTOR,XB)

ITERATE XB UNTIL YSTOR = Y(2)

DO 23 J=1,10

IF(ABS(Y(2)-YSTOR).LE.0.0001)GO TO 24

XB=XB*Y(2)/YSTOR

CALL YSTAR(YSTOR,XB)

23 CONTINUE

IF NO CONVERGENCE FOR XB, PRINT MESSAGE

PRINT 91,XB,(X(I),I=2,M)

GO TO 3

PRINT VALUE OF XB AFTER CONVERGENCE

24 PRINT 105,XB,J

IF STEP SIZE REDUCED AT START OF THIS ROUTINE CONVERT BACK TO OLD STE P SIZE

3 IF(IFACT.LE.1)GO TO 4

DZ=DZ*IFACT

M=1.0001/DZ+2.

DO 30 I=2,M

X(I)=X(2+(I-2)*IFACT)

F(I)=F(2+(I-2)*IFACT)

30 Y(I)=Y(2+(I-2)*IFACT)

IFACT=1

4 RETURN

105 FORMAT(60X,'XB CONVERGED TO',F10.4,'AFTER J=',I4,' ITERATIONS')

91 FORMAT(' XB FAILED TO CONVERGE',12F8.4)

106 FORMAT(' NO CONVERGENCE FOR I=',I4,' LATEST AND PREVIOUS VALUES

OF Y ARE ',2F10.4)

103 FORMAT(/40X,'SUBROUTINE FINDXB',8X,'XD',8X,'R',9X,'FNTU' /

160X,3F10.4/)

END

A.2.4 SUBROUTINE FINDR.

This subroutine is used to compute the reflux ratio at steady state when X_B , X_D and N_{OG} are known. The minimum reflux ratio is computed from:

$$R_{\min} = (X_D - y_2) / (X_D - X_B)$$

where: $y_2 = f(X_B)$

The parameters in the argument list for FINDR are defined as for SSTATE and FINDXB. A listing of FINDR follows.

A.2.5 SUBROUTINE FINDTU.

The purpose of this subroutine was described in section(3.2.3). The number of transfer units is found by a trapezoidal integration rule based on equation (3.15). To test the accuracy of the integration, the number of steps is doubled and the number of transfer units recalculated. This is repeated until convergence is obtained, or the maximum dimension of X , Y and F is reached. The value of N_{OG} (represented by FNTU in the program) is printed each time so that the convergence can be seen.

The parameters in the argument list have the same meaning as for SSTATE and FINDXB. Subroutine FINDTU is listed below.

```

SUBROUTINE FINDR(XB,XD,R,FNTU,DZ,Y,X,F,M,IFACT,IFLAG)
C
C SUBROUTINE FINDR FINDS THE REFLUX RATIO R FOR THE BASIC COLUMN
C WHEN XB, XD AND NTU ARE SPECIFIED. IT USES A STEPHALVING PROCESS
C TO FIND R AND USES FINDXB TO COMPUTE THE CONCENTRATION PROFILES
C FOR EACH TRIAL R.
C CONVERGENCE IS REACHED WHEN THE COMPUTED XB EQUALS THAT SPECIFIED.
C
C DIMENSION X(1),Y(1),F(1)
C PRINT HEADING
C PRINT 103,XB,XD,FNTU
C SET ITERATION COUNTER
C K=0
C FIND MINIMUM VALUE OF R(RMIN) AND SET INITIAL STEP SIZE DR=(1-RMIN)/2
C CALL YSTAR(Y(2),XB)
C RMIN=(XD-Y(2))/(XD-XB)
C DR=(1.-RMIN)/2.
C TAKE FIRST VALUE OF R AS 1.0 AND STORE REQUIRED VALUE OF XB AS XSTOR
C R=1.0
C XSTOR=XB
C EVALUATE COEFFICIENTS AND NUMBER OF STEPS
C 1 M=1.001/DZ+2.
C 2 FN=FNTU*DZ/2.
C A=(1-FN)/(1+FN)
C B=FN/(1+FN)
C C=(1.-R)*XD/R
C USE FINDXB TO EVALUATE XB
C 15 CALL FINDXB(M,A,B,C,DZ,IFACT,XD,XB,X,Y,F,R,FNTU,ICLASS)
C IF FINDXB HAS HALVED DZ, REEVALUATE CONSTANTS
C IF(IFACT.GT.1)GO TO 1
C OTHERWISE UPDATE VALUE OF R, HALVE STEP SIZE AND REPEAT
C IF R HAS CONVERGED (SO THAT XB=XSTOR),PRINT RESULTS AND RETURN
C IF(ABS(XSTOR-XB).LE.0.001)GO TO 17
C IF(XB.GT.XSTOR)R=R+DR
C IF R EXCEEDS 1.0, PRINT THAT AN IMPOSSIBLE CONDITION EXISTS AND RETURN
C IF(R.GT.1.0)GO TO 19
C IF(XB.LT.XSTOR)R=R-DR
C K=K+1
C IF(K.GE.10)GO TO 18
C DR=DR/2.
C GO TO 2
C 17 PRINT 94,R,K
C RETURN
C 18 PRINT 93,R
C RETURN
C 19 PRINT 92,XSTOR,XD,FNTU
C IFLAG=1
C RETURN
C 92 FORMAT(60X,'*****'/,40X,'IMPOSSIBLE CONDITION XB=',F10.
C 14,' XD=',F10.4,' NTU=',F10.4)
C 94 FORMAT(/60X,'R CONVERGED TO ',F10.5,' AFTER K=',I4,' ITERATIONS')
C 93 FORMAT(60X,'R=',F10.5,' FAILED TO CONVERGE')
C 103 FORMAT(/40X,'SUBROUTINE FINDR',9X,'XB',8X,'XD',6X,
C 1'FNTU'/60X,3F10.4/)
C END

```

```

SUBROUTINE FINDTU(XB,XD,X,Y,F,R,C,FNTU,M)
C
C   THIS ROUTINE FINDS THE REQUIRED NUMBER OF TRANSFER UNITS WHEN
C   XB,XD AND R ARE SPECIFIED FOR THE BASIC COLUMN AT STEADY STATE.
C
C   ON RETURN TO SSTATE, FINDXB IS CALLED TO COMPUTE THE X, Y AND F
C   PROFILES IN THE COLUMN.
C
C   DIMENSION X(1),Y(1),F(1)
C   PRINT HEADING
C   PRINT 103,XB,XD,R
C   TOTAL NTU IS FOUND BY INTEGRATING 1/(F-Y)DY USING TRAPEZOIDAL RULE
C   THE NUMBER OF STEPS(INCR) IS SET INITIALLY TO INCR(=1/DZ)
C   6 INCR=M-2
C   FNSTOR=0.
C   42 FNTU=0.
C   FM=INCR
C   THE RANGE IN Y BETWEEN XD AND Y(2) IS DIVIDED INTO EQUAL INCREMENTS OF SIZE (
C   DY=(XD-Y(2))/FM
C   INCR=INCR+2
C   IN THIS LOOP THE INTEGRAL IS SUMMED
C   DO 40 I=2,INCR
C   FI=I-2
C   Y(I)=Y(2)+DY*FI
C   X(I)=Y(I)/R-C
C   CALL YSTAR(F(I),X(I))
C   IF(I.EQ.2)GO TO 40
C   DF=(Y(I)-Y(I-1))*(1./(F(I)-Y(I))+1./(F(I-1)-Y(I-1)))/2.
C   FNTU=FNTU+DF
C   40 CONTINUE
C   THE INTEGRAL AND NUMBER OF INCREMENTS IS PRINTED
C   PRINT 96,FNTU,INCR
C   IF FNTU HAS NOT CONVERGED TO A LIMIT AND IF THE
C   MAXIMUM DIMENSION WILL NOT BE EXCEEDED, DOUBLE THE
C   NUMBER OF INCREMENTS AND REPEAT. OTHERWISE RETURN.
C   IF(ABS(FNTU-FNSTOR).LE.0.05)GO TO 41
C   IF(INCR.GT.82)GO TO 41
C   INCR=2*(INCR-2)
C   FNSTOR=FNTU
C   GO TO 42
C   41 RETURN
C   96 FORMAT(60X,'FNTU=',F10.4,' NUMBER OF POINTS=',I5)
C   103 FORMAT(/40X,'SUBROUTINE FINDTU',8X,'XB',8X,'XD',9X,
C   1'R'/60X,3F10.4/)
C   END

```

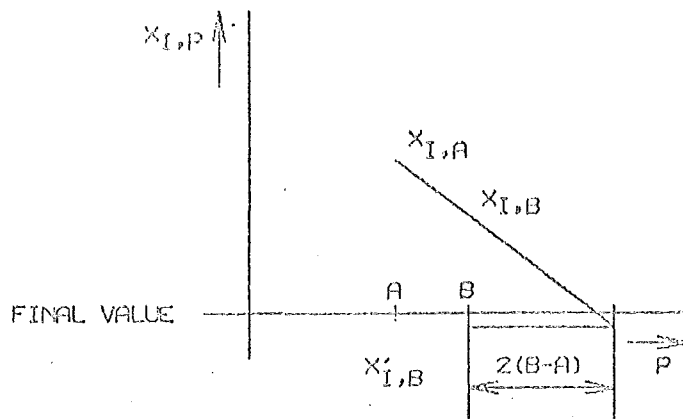



FIG A.2.2

CONVERGENCE FORCING ROUTINE

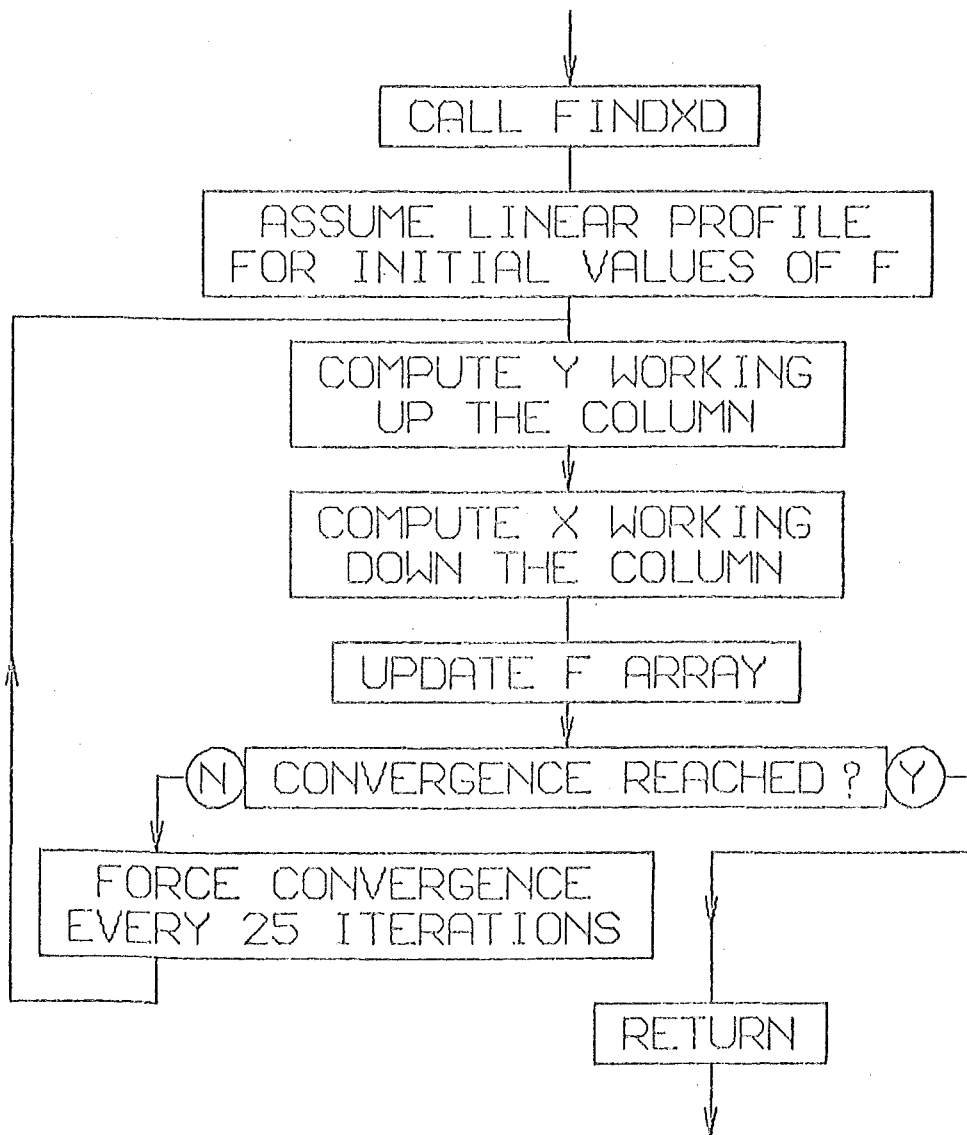


FIG A.2.3 FLOW

DIAGRAM FOR FINDXD

A.2.6 SUBROUTINE FINDXD.

This subroutine finds the top composition XD and the composition profile when R, N_{OG} and XB are specified. An initial estimate for XD is needed, but the method will converge from any initial estimate greater than XB. The approach to convergence may be slow if the composition profile is strongly non-linear. This is overcome by extrapolating the approach to the solution after a certain time. This speeds the convergence markedly. The method is illustrated in fig. A.2.3.

The dotted line in fig.A.2.3 shows the value of X (at point I after P iterations) plotted against P. This is denoted here by $X_{I,P}$.

After B iterations, the value of $X_{I,B}$ is replaced by:

$$\begin{aligned} X'_{I,B} &= X_{I,B} - 2(X_{I,A} - X_{I,B}) \\ &= 3X_{I,B} - 2X_{I,A} \end{aligned}$$

where $X'_{I,B}$ is the new value given to $X_{I,B}$. This is done for X at each point up the column after every B iterations. The value used for B was 25 and A was set at 15. A test of the average improvement for all X values was used to decide when sufficient convergence was obtained. An average change in the x values of 0.0001 between one convergence forcing and the next was usually used as the test.

A flow diagram for subroutine FINDXD is given in fig. A.2.3, and a listing follows.

```

SUBROUTINE FINDXD(A,B,XB,R,FNTU,DZ,XD,Y,X,F,M)
C
C SUBROUTINE FINDXD FINDS STEADY STATE CONCENTRATION PROFILES FOR
C THE BASIC COLUMN WHEN NTU,XB AND R ARE SPECIFIED AND XD IS
C UNKNOWN. AN INITIAL GUESS FOR XD IS NEEDED.
C
  DIMENSION F(1),X(1),Y(1),STX(42)
  DZI=1./DZ
C PRINT HEADING
  PRINT 103,XB,R,FNTU
C EVALUATE CONSTANT
  C=FNTU*DZ/R/2.
C EVALUATE Y(2) USING BOTTOM BOUNDARY CONDITION
  CALL YSTAR(Y(2),XB)
C ASSUME LINEAR PROFILE AS FIRST GUESS FOR F
  CALL YSTAR(F(M),XD)
  F(2)=Y(2)+0.01
  DO 8 I=3,M
    FI=I-2
  8 F(I)=F(2)+(F(M)-F(2))*FI*DZ
C BEGIN ITERATION LOOPS
  DO 17 K=1,10
    DO 6 IM=1,25
C FIND VALUES FOR Y UP THE COLUMN
      DO 1 I=3,M
  1 Y(I)=A*Y(I-1)+B*(F(I-1)+F(I))
C PUT IN TOP BOUNDARY CONDITION
      X(M)=Y(M)
C UPDATE F(M)
      CALL YSTAR(F(M),X(M))
C FIND VALUES FOR X DOWN THE COLUMN
      DO 5 I=3,M
        J=M-I+2
  4 X(J)=X(J+1)+C*(Y(J)+Y(J+1)-F(J+1)-F(J))
C UPDATE F
      5 CALL YSTAR(F(J),X(J))
C IF IM=15 STORE VALUES OF X
      IF(IM.NE.15)GO TO 6
      DO 7 I=2,M
  7 STX(I)=X(I)
  6 CONTINUE
C TEST FOR CONVERGENCE
      ERROR=0.
      DO 10 I=2,M
  10 ERROR=ERROR+ABS(X(I)-STX(I))
C IF SUFFICIENTLY CONVERGED OR K=10, EXIT FROM ITERATION LOOP
      IF(ERROR.LE.DZI*0.0001)GO TO 21
C CONVERGENCE FORCING ROUTINE
      DO 9 I=2,M
        X(I)=3.*X(I)-2.*STX(I)
  9 CALL YSTAR(F(I),X(I))
C PRINT VALUES OF X SO THAT APPROACH TO EQUILIBRIUM CAN BE SEEN
      PRINT 102,(X(I),I=2,M)
  17 CONTINUE
C SET VALUE OF XD, PRINT RESULTS AND RETURN
  21 XD=X(M)
      PRINT 101,XD,K
      RETURN
  101 FORMAT(/60X,'XD CONVERGED TO ',F10.4,' AFTER K=',I5,' CONVERGENCE
  1 STEPS')
  102 FORMAT(12F10.4)
  103 FORMAT(/40X,'SUBROUTINE FINDXD',8X,'XB',8X,'R',9X,'FNTU'/60X,
  13F10.4/)
  END

```

A.3.1 MAINLINE1.

This program calculates the transient response of the basic column described in chapter 2. The way the program works was outlined in section(3.3) and illustrated in fig. 3.2.

For each transient response to be computed, 3 data cards are needed to specify the column variables. The data input is as follows:

```
Card 1.      HV,HL,FV,FL,ZT,HC,HREB
              Format(7F10.3)

Card 2.      ICLASS,ITERT,IFLAG,IPUNCH,IPRINT,NTIME
              Format(5I2,I5)

Card 3.      XB,XD,R,FNTU,DZ,DT,FNTU2,XDFIN
              Format(8F10.3)
```

The meanings of these variables are:

HV	vapour holdup	default value =0.0
HL	liquid holdup	
FV	vapour flowrate after the upset	
FL	liquid flowrate after the upset	
ZT	total column height	
HC	condenser holdup	default value=0.0
HREB	reboiler holdup	default value =infinity
ICLASS	see table A.2.1	
ITERT	number of iterations at each time step	default value=2
IFLAG	not used	
IPUNCH	a value of 1 indicates that the values of x are to be punched	

on cards for storage or use in a plotting program

IPRINT the x values are printed every
 IPRINT time steps during the transient response

NTIME number of time steps for which response is to be computed

XB initial reboiler composition

XD initial distillate composition

R reflux ratio at initial steady state

FNTU number of transfer units at initial steady state

DZ height interval, usually 0.1 or 0.05.

DT time interval. The default value of $1/b_2$
 should be used whenever possible (see section(3.4)).

FNTU2 number of transfer units at final steady state

XDFIN distillate composition at final steady state

A sample format of the printed output is given on the next page, and a listing of MAINLINE1 follows.

A.3.1.1 Storage Requirements

The core storage required by MAINLINE1 and its associated subroutines on an IBM 360/44 computer with a 32 bit word length is listed in table A.3.1. In arriving at these figures, it was assumed that the transient response need not be stored for subsequent recovery on punched cards, and that the smallest height interval DZ needed in the mainline program was 0.05. Further savings in core storage could be made by eliminating those subroutines which are not needed, and by removing some of the printout statements.

TABLE A.3.1 STORAGE REQUIREMENTS.

	Bytes
MAINLINE1	6288 (decimal)
SSTATE	1544
FINDXD	2128
FINDTU	1284
FINDXB	2308
FINDR	1648
YSTAR	424
Total	15624

A.3.1.2 Speed Of The Computer Solution.

The time required to compile and bind MAINLINE1 and its subroutines was approximately 75 seconds for an IBM 360/44 computer and 5 seconds for a Burroughs B6700. The Burroughs computer took approximately 5 seconds CPU time to compute the initial steady state and transient response for 300 time intervals and 10 height intervals. The IBM computer required about 20 seconds for the same solution.

The time required to compute the transient response is proportional to the number of time intervals needed, and also proportional to the number of height intervals. Since it is recommended that the time interval is number of height intervals will require four times the amount of computation to obtain the transient response for the same time period.

```

C C *****
C C **                               *****
C C ** MAINLINE1 IS THE MAINLINE PROGRAM FOR THE BASIC COLUMN. *****
C C **                               *****
C C *****
C C DESCRIPTION OF ARRAYS
C C
C C X LIQUID COMPOSITION IN PACKING AT OLD TIME
C C V LIQUID COMPOSITION IN PACKING AT NEW TIME
C C Y VAPOUR COMPOSITION IN PACKING AT OLD TIME
C C U VAPOUR COMPOSITION IN PACKING AT NEW TIME
C C FA EQUILIBRIUM VAPOUR COMPOSITION IN PACKING AT OLD TIME
C C FB EQUILIBRIUM VAPOUR COMPOSITION IN PACKING AT NEW TIME
C C XFIXED AND YFIXED HOLD THE TERMS CONTAINING X,Y& FA WHICH DO NOT
C C CHANGE WITHIN THE ITERATION LOOP.
C C
C C
C C
C C
C C
C C
C C DIMENSION IXP(42,201) .FA(42)
C C DIMENSION X(162),Y(162),FB(162),V(42),U(42),XFIXED(42),YFIXED(42)
C C 1 IFLAG=0.
C C
C C READ IN DATA
C C
C C 4 READ 101,HV,HL,FV,FL,ZT,HC,HREB
C C
C C 3 READ 104,ICLASS,ITERT,IFLAG,IPUNCH,IJK,NTIME
300 READ 101,XB,XD,R,FNTU,DZ,DT
C C WRITE(6,1112)
C C
C C CALCULATE INITIAL STEADY STATE
C C
C C CALL SSTATE(ICLASS,XB,XD,R,FNTU,DZ,Y,X,FB,NR,IFLAG)
C C
C C IF IFLAG.EQ.1,AN IMPOSSIBLE CONDITION WAS SPECIFIED A NEW
C C SET OF DATA IS READ
C C IF(IFLAG.EQ.1)GO TO 1
C C NRM1=NR-1
C C IZPR=NR/10
C C IF(IZPR.EQ.0)IZPR=1
C C
C C PRINT INITIAL PROFILES FOR X,Y AND F
C C PRINT 116
51 PRINT 102,(X(I),I=2,NR,IZPR)
C C PRINT 102,(Y(I),I=2,NR,IZPR)
C C PRINT 102,(FB(I),I=2,NR,IZPR)
445 B2=FL/HL/DZ/ZT
C C
C C SET DEFAULT VALUES OF VARIABLES
C C
C C IF(ITERT.EQ.0)ITERT=2
C C IF(NTIME.EQ.0)NTIME=40
C C IF(DT.LE.0.0)DT=1./B2
C C
C C TFACT IS RATIO OF DIMENSIONLESS TIME INCREMENT DTHETA
C C AND ACTUAL TIME INCREMENT DT
C C
C C TFACT=FL*FNTU/HL/ZT
C C DTHETA=DT*TFACT
C C
C C PRINT HEADINGS AND PARAMETER LISTS INCL. INITIAL AND FINAL R.
C C PRINT 106
C C PRINT 107,XB,XD,R,FNTU,DZ,ZT,DT,TFACT,DTHETA
C C RINIT=R
C C XBINIT=XB
C C R=FL/FV
C C PRINT 109,HV,HL,HC,HREB,FV,FL,R

```

```

C
C   IN IXP THE VALUES OF X AT EACH TIME STEP ARE STORED TO BE RECOVERED ON
C   PUNCHED CARD LATER IF IPUNCH=1
C   DO 46 I=2,NR,IZPR
46   IXP(I,2)=X(I)*10000.+0.5
C
C   EVALUATE CONSTANTS
C   DTI=1./DT
C
C   CALCULATE CONDENSER CONSTANTS
C   IF(HC.EQ.0.)GO TO 70
C   CTC=FV*DT/HC/2.
C   CTCA=(1.-CTC)/(1.+CTC)
C   CTC=CTC/(1.+CTC)
C
C   CALCULATE COEFFICIENTS
70 IF(HV.EQ.0.0)GO TO 43
C   B1=FV/HV/DZ/ZT
C   C1=FV*FNTU/ZT/HV
C   C2=C1*HV/HL
C   DTJ=DTI
C   GO TO 44
C
C   THE NEXT FOUR ARE ALTERNATIVE COEFFICIENTS FOR USE WHEN
C   THERE IS NO VAPOUR HOLDUP
C
43 B1=FV/DZ/ZT
C   C1=FV*FNTU/ZT
C   C2=C1/HL
C   DTJ=0.
C
C   CALCULATE COEFFICIENTS
44 AA=-B1+C1/2.+DTJ
C   AB=B1+C1/2.+DTJ
C   AC=AB-C1
C   AD=AA-C1
C   AE=C1/2.
C   BA=C2/2.
C   BB=-B2-DTI
C   BC=B2-DTI
C   PRINT 1106
C   PRINT 108,B1,B2,C1,C2,DTI,DTJ,CTCA,CTC
C   PRINT 105,AA,AB,AC,AD,AE,BA,BB,BC
C   PRINT 1206
C
C   KOUNT=3
C   BEGIN TIME LOOP
C
C   DO 15 NTIM=1,NTIME
C   TIME=NTIM*DT
C   THETA=TIME*TFACT
C   U(2)=Y(2)
C
C   FB(I)=F(I,N+1), FA(I)=F(I,N)
C
C   DO 20 I=2,NR
20 FA(I)=FB(I)
C
C   XFIXED AND YFIXED CONTAIN THOSE TERMS CONTAINING THE VALUES OF X,Y AND F AT
C   THE PREVIOUS TIME AND THUS DO NOT CHANGE WITHIN THE ITERATION LOOP.
C
C   DO 27 I=2,NR
C   YFIXED(I)=AC*Y(I-1)+AD*Y(I)+AE*(FA(I)+FA(I-1))
27 XFIXED(I)=BA*(FA(I+1)+FA(I))-BA*(Y(I)+Y(I+1))+BC*X(I)+BB*X(I+1)
C
C   BEGIN ITERATION LOOP
C
C   DO 24 ITER=1,ITER
C
C   CALCULATE U(I) UP THE COLUMN.(U(I) IS THE NEW VALUE OF Y(I)).
C   DO 21 I=3,NR
21 U(I)=(YFIXED(I)-AA*U(I-1)+AE*(FB(I-1)+FB(I)))/AB
C
C   CALCULATE X(M) FROM THE CONDENSER BOUNDARY CONDITION
C
C   IF(HC)71,71,72
71 V(NR)=U(NR)
C   GO TO 73
72 V(NR)=X(NR)*CTCA+CTC*(U(NR)+Y(NR))
C
C   CALCULATE V(I) DOWN THE COLUMN.(V(I) IS THE NEW VALUE OF X(I)).

```



```

C
73 DO 22 I=2,NR11
    IK=NR-I+1
22 V(IK)=(XFIXED(IK)+BA*(FB(IK+1)+FB(IK)-U(IK)-U(IK+1))-BC*V(IK+1))/B B
    IB
C
C    CALCULATE NEW VALUES OF F
C
    DO 124 M=2,NR
    CALL YSTAR(FB(M),V(M))
124 IF(ABS(V(M)-0.5).GE.0.5)PRINT 103,NTIM,ITER,M
C
C    UPDATE REBOILER CONCENTRATION
C
    IF(HREB)24,24,75
75 DO 129 JJ=1,2
    XBN=XB+DT/HREB/2.*((FV-FL)*(X(NR)+V(NR))+FL*(X(2)+V(2))
    1 -FV*(U(2)+Y(2)))
129 CALL YSTAR(U(2),XBN)
24 CONTINUE
C
C    END OF ITERATION LOOP
C
C
C    SET X AND Y TO THE NEW VALUES STORED IN V AND U
C
74 DO 25 I=2,NR
    X(I)=V(I)
25 Y(I)=U(I)
    IF(HREB.NE.0.)XB=XBN
C
    DO 417 I=2,NR,IZPR
417 IXP(I,KOUNT)=X(I)*10000.+0.5
    PRINT 1102,NTIM,XB,(X(I),I=2,NR,IZPR)
C
    KOUNT=KOUNT+1
15 CONTINUE
C
C    END OF TIME LOOP
C
    NT2=NTIME+2
C
C    PUNCH LOOP
C
    IF(IPUNCH.NE.1)GO TO 4
    IF(IPUNCH.EQ.1)PUNCH 117,XD,X(NR),XBINIT,XB,RINIT,R,FNTU

    IF(IPUNCH.EQ.1)PUNCH 118,HV,HL,HC,HREB,DZ
    KOUNT=KOUNT-1
    DO 125 I=2,NR,2
    IXP(I,1)=IXP(I,KOUNT)
125 PUNCH 98,(IXP(I,II),II=1,KOUNT)
    GO TO 4
99 CONTINUE
98 FORMAT(20I4)
101 FORMAT(8F10.3)
102 FORMAT(/11F10.4)
1102 FORMAT(15,12F10.4)
103 FORMAT(40X,5I8)
104 FORMAT(5I2,6I5)
106 FORMAT(/40X,'***** PARAMETER LIST *****')
1106 FORMAT(/40X,'***** COEFFICIENT LIST *****')
1206 FORMAT(/60X,'START OF TIME INTEGRATION'/' TIME'/' STEPS      XB',
    18X,'X(I)',1//)
105 FORMAT(/6X,'AA',8X,'AB',8X,'AC',8X,'AD',8X,'AE',8X,'BA',8X,'BB',8X
    1,'BC',/10F10.4)
107 FORMAT(/6X,'XB',8X,'XD',5X,'INITIAL R',3X,'FNTU',8X,'DZ',8X,'ZT',8
    1X,'DT',8X,'TFACT',5X,'DTHETA'/9F10.4)
108 FORMAT(/6X,'B1',8X,'B2',8X,'C1',8X,'C2',7X,'DTI',7X,'DTJ',6X,'CTCA
    1',6X,'CTC'/8F10.4)
109 FORMAT(/6X,'HV',8X,'HL',8X,'HC',6X,'HREB',8X,'FV',8X,'FL',6X,'FINA
    1L R'/8F10.4)
1112 FORMAT(1H8/1H1//)
113 FORMAT(F10.3,3F10.4,20X,2F10.4,10X,F10.4)
115 FORMAT(50X,'FINAL STEADY STATE'/)
116 FORMAT(/20X,'INITIAL STEADY STATE PROFILES OF X,Y AND F RESPECTIVE
    1LY ARE')
117 FORMAT(10X,F6.4,2F11.4,F10.4,2X,F4.2,6X,F4.2,8X,F6.2)
118 FORMAT(F6.1,3F9.1,F9.3)
119 FORMAT(/110,' ITERATIONS PER TIME STEP')
    END

```

SUBROUTINE FINDXD

XB 0.2000 R 0.8000 FNTU 5.0000

0.2086	0.2177	0.2307	0.2492	0.2753	0.3113	0.3596	0.4217	0.4966	0.5806	0.6673
0.2096	0.2198	0.2344	0.2550	0.2837	0.3229	0.3746	0.4397	0.5164	0.6002	0.6851
0.2095	0.2195	0.2338	0.2540	0.2823	0.3210	0.3722	0.4367	0.5131	0.5969	0.6821

XD CONVERGED TO 0.6825 AFTER K= 4 CONVERGENCE STEPS

INITIAL STEADY STATE PROFILES OF X,Y AND F RESPECTIVELY ARE

0.2095	0.2195	0.2338	0.2541	0.2825	0.3213	0.3725	0.4371	0.5136	0.5974	0.6825
0.3041	0.3121	0.3236	0.3398	0.3625	0.3935	0.4345	0.4862	0.5473	0.6144	0.6825
0.3172	0.3310	0.3505	0.3778	0.4152	0.4648	0.5272	0.6003	0.6779	0.7520	0.8172

***** PARAMETER LIST *****

XB	XD	INITIAL R	FNTU	DZ	ZT	DT	TFACT	DTHETA
0.2000	0.6825	0.8000	5.0000	0.1000	5.0000	0.7143	0.7000	0.5000
HV	HL	HC	HREB	FV	FL	FINAL R		
0.0000	10.0000	10.0000	0.0000	10.0000	7.0000	0.7000		

2 ITERATIONS PER TIME STEP

SMOOTHING INTERVAL = 4

***** COEFFICIENT LIST *****

B1	B2	C1	C2	DTI	DTJ	CTCA	CTC
20.0000	1.4000	10.0000	1.0000	1.4000	0.0000	0.4737	0.2632
AA	AB	AC	AD	AE	BA	BB	BC
-15.0000	25.0000	15.0000	-25.0000	5.0000	0.5000	-2.8000	0.0000

START OF TIME INTEGRATION

TIME STEPS	XB	X(I).....										
4	0.2000	0.2071	0.2150	0.2264	0.2429	0.2661	0.2986	0.3408	0.3974	0.4743	0.5656	0.6634
8	0.2000	0.2055	0.2119	0.2213	0.2338	0.2523	0.2810	0.3212	0.3758	0.4483	0.5380	0.6389
12	0.2000	0.2041	0.2090	0.2170	0.2295	0.2449	0.2697	0.3059	0.3572	0.4269	0.5155	0.6182
16	0.2000	0.2036	0.2078	0.2143	0.2242	0.2391	0.2615	0.2948	0.3430	0.4102	0.4976	0.6013
20	0.2000	0.2031	0.2068	0.2125	0.2213	0.2348	0.2554	0.2865	0.3323	0.3973	0.4835	0.5879

TABLE A.4.1 OPERATING VARIABLES

RUN	X(0)	X(1.0)	V	ERR	R	ERR	DP	ERR	NTU
1	40.5	95.9	0.377	0.006	0.859	0.004	168.	2.	6.54
2	48.2	99.2	0.379	0.006	1.000	0.000	163.	2.	7.84
3	39.9	95.9	0.374	0.006	0.859	0.004	168.	2.	6.61
4	36.2	67.1	0.374	0.006	0.684	0.006	188.	2.	2.07
5	38.3	94.4	0.374	0.006	0.856	0.004	168.	2.	6.15
6	35.4	73.7	0.366	0.005	0.746	0.005	176.	2.	2.88
7	46.7	99.1	0.376	0.006	1.000	0.000	153.	5.	7.75
8	12.2	70.4	0.373	0.006	0.930	0.003	230.	5.	5.30
9	14.8	94.0	0.371	0.006	1.000	0.000	195.	5.	7.16
10	12.3	66.3	0.371	0.006	0.933	0.003	220.	5.	4.74
11	12.2	50.1	0.376	0.006	0.886	0.004	240.	10.	3.72
12	14.2	93.3	0.370	0.006	1.000	0.000	195.	5.	7.05
13	11.9	48.3	0.373	0.006	0.885	0.004	285.	10.	3.63
14	11.7	63.7	0.375	0.006	0.931	0.003	260.	10.	4.68
15	13.0	91.9	0.369	0.006	1.000	0.000	190.	5.	6.86
16	16.3	66.0	0.238	0.004	0.961	0.002	64.	2.	3.70
17	15.5	59.2	0.241	0.004	0.934	0.005	67.	2.	3.43
18	14.6	45.9	0.237	0.004	0.857	0.006	71.	2.	2.83
19	14.9	53.5	0.242	0.004	0.913	0.005	70.	2.	3.17
20	17.5	72.6	0.240	0.004	1.000	0.000	59.	2.	3.89
21	17.6	80.0	0.289	0.004	0.962	0.004	97.	2.	4.85
22	19.5	89.3	0.290	0.004	1.000	0.000	90.	2.	5.61
23	15.9	71.1	0.288	0.004	0.931	0.005	105.	2.	4.48
24	16.0	56.0	0.293	0.004	0.877	0.005	119.	2.	3.43
25	16.1	64.4	0.290	0.004	0.910	0.005	111.	2.	3.97
26	18.3	87.9	0.289	0.004	1.000	0.000	97.	2.	5.50
27	24.2	93.7	0.294	0.004	1.000	0.000	89.	2.	6.14
28	19.6	60.2	0.292	0.004	0.856	0.005	111.	2.	3.27
29	23.7	93.0	0.294	0.004	1.000	0.000	89.	2.	6.00
30	19.8	60.8	0.290	0.004	0.866	0.005	112.	2.	3.23
31	20.0	74.7	0.290	0.004	0.924	0.004	101.	2.	4.23
32	22.9	93.5	0.294	0.004	1.000	0.000	92.	2.	6.19
33	26.4	95.7	0.323	0.005	1.000	0.000	108.	2.	6.61
34	21.1	82.8	0.321	0.005	0.922	0.004	124.	2.	5.11
35	25.3	96.3	0.324	0.005	1.000	0.000	114.	2.	6.95
36	20.6	74.9	0.323	0.005	0.904	0.004	128.	2.	4.34
37	20.9	74.5	0.323	0.005	0.904	0.004	127.	2.	4.24
38	24.1	95.2	0.323	0.005	1.000	0.000	115.	2.	6.62
39	25.0	97.5	0.364	0.006	1.000	0.000	155.	2.	7.61
40	25.3	97.1	0.366	0.006	1.000	0.000	155.	2.	7.35
41	25.3	97.6	0.361	0.005	1.000	0.000	156.	2.	7.65
42	28.6	96.7	0.348	0.005	1.000	0.000	133.	5.	6.88
43	21.7	70.2	0.343	0.005	0.862	0.003	165.	2.	3.96
44	27.4	97.3	0.350	0.005	1.000	0.000	137.	5.	7.30
45	21.3	74.8	0.345	0.005	0.890	0.003	140.	5.	4.33
46	25.9	97.3	0.355	0.005	1.000	0.000	155.	5.	7.35
47	18.9	94.1	0.365	0.005	1.000	0.000	146.	5.	6.74
48	15.1	60.3	0.352	0.005	0.872	0.004	180.	2.	4.25
49	17.6	93.9	0.362	0.005	1.000	0.000	166.	2.	6.81
50	14.2	42.8	0.340	0.005	0.791	0.008	148.	8.	3.01

TABLE A.4.1 CONTINUED

RUN	X(0)	X(1.0)	V	ERR	R	ERR	DP	ERR	NTU
51	16.1	91.5	0.358	0.005	1.000	0.000	168.	2.	6.39
52	26.7	96.0	0.360	0.005	1.000	0.000	155.	2.	6.70
53	18.4	69.9	0.337	0.005	0.890	0.007	166.	4.	4.31
54	20.6	94.4	0.347	0.005	1.000	0.000	156.	2.	6.66
55	11.3	81.7	0.339	0.005	1.000	0.000	154.	2.	5.54
56	9.2	43.7	0.318	0.005	0.897	0.002	178.	2.	3.92
57	9.0	27.7	0.311	0.005	0.788	0.008	180.	5.	2.60
58	8.3	32.1	0.326	0.005	0.838	0.007	190.	2.	3.42
59	7.5	35.2	0.320	0.005	0.878	0.003	190.	2.	3.89
60	7.0	81.4	0.337	0.005	1.000	0.000	171.	2.	6.29
61	14.9	89.3	0.346	0.005	1.000	0.000	158.	2.	6.11
62	13.6	91.0	0.355	0.005	1.000	0.000	167.	2.	6.59
63	11.7	84.9	0.349	0.005	0.977	0.001	180.	5.	6.22
64	11.4	64.4	0.337	0.005	0.932	0.002	188.	2.	4.83
65	11.2	64.6	0.335	0.005	0.929	0.002	178.	2.	4.98
66	11.3	66.1	0.341	0.005	0.930	0.002	188.	2.	5.11
67	11.2	43.2	0.333	0.005	0.840	0.005	198.	4.	3.83
68	10.7	63.8	0.340	0.005	0.937	0.002	188.	2.	4.89
69	11.1	80.8	0.347	0.005	0.975	0.001	178.	2.	5.45
70	18.2	92.4	0.332	0.005	1.000	0.000	135.	2.	6.36
71	16.2	96.2	0.367	0.006	1.000	0.000	180.	2.	7.75
72	15.3	95.7	0.370	0.006	1.000	0.000	180.	2.	7.67
73	9.8	87.8	0.355	0.005	1.000	0.000	186.	2.	6.57
74	6.9	83.0	0.347	0.005	1.000	0.000	187.	2.	6.49
75	6.7	81.6	0.352	0.005	1.000	0.000	181.	2.	6.39
76	18.7	99.3	0.397	0.006	1.000	0.000	214.	2.	10.22
77	22.3	95.8	0.336	0.005	1.000	0.000	137.	2.	6.97
78	23.1	94.7	0.305	0.005	1.000	0.000	101.	2.	6.54
79	21.8	93.5	0.304	0.005	1.000	0.000	103.	2.	6.29
80	21.0	93.8	0.301	0.005	1.000	0.000	129.	2.	6.44
81	17.3	97.7	0.391	0.006	1.000	0.000	202.	2.	8.43
82	20.0	93.6	0.346	0.005	1.000	0.000	137.	2.	6.49
83	27.4	98.2	0.343	0.005	1.000	0.000	115.	5.	7.92
84	27.6	97.8	0.343	0.005	1.000	0.000	115.	5.	7.58
85	27.0	96.9	0.328	0.005	1.000	0.000	130.	2.	7.07
86	27.2	96.6	0.331	0.005	1.000	0.000	136.	2.	6.95
87	26.6	96.6	0.334	0.005	1.000	0.000	136.	5.	6.98
88	27.0	96.8	0.334	0.005	1.000	0.000	137.	5.	7.03
89	26.4	96.4	0.328	0.005	1.000	0.000	141.	5.	6.90
90	10.6	91.9	0.360	0.005	1.000	0.000	103.	2.	7.22
91	37.3	98.7	0.299	0.004	1.000	0.000	190.	8.	7.72
92	16.5	80.7	0.280	0.004	1.000	0.000	104.	2.	4.75

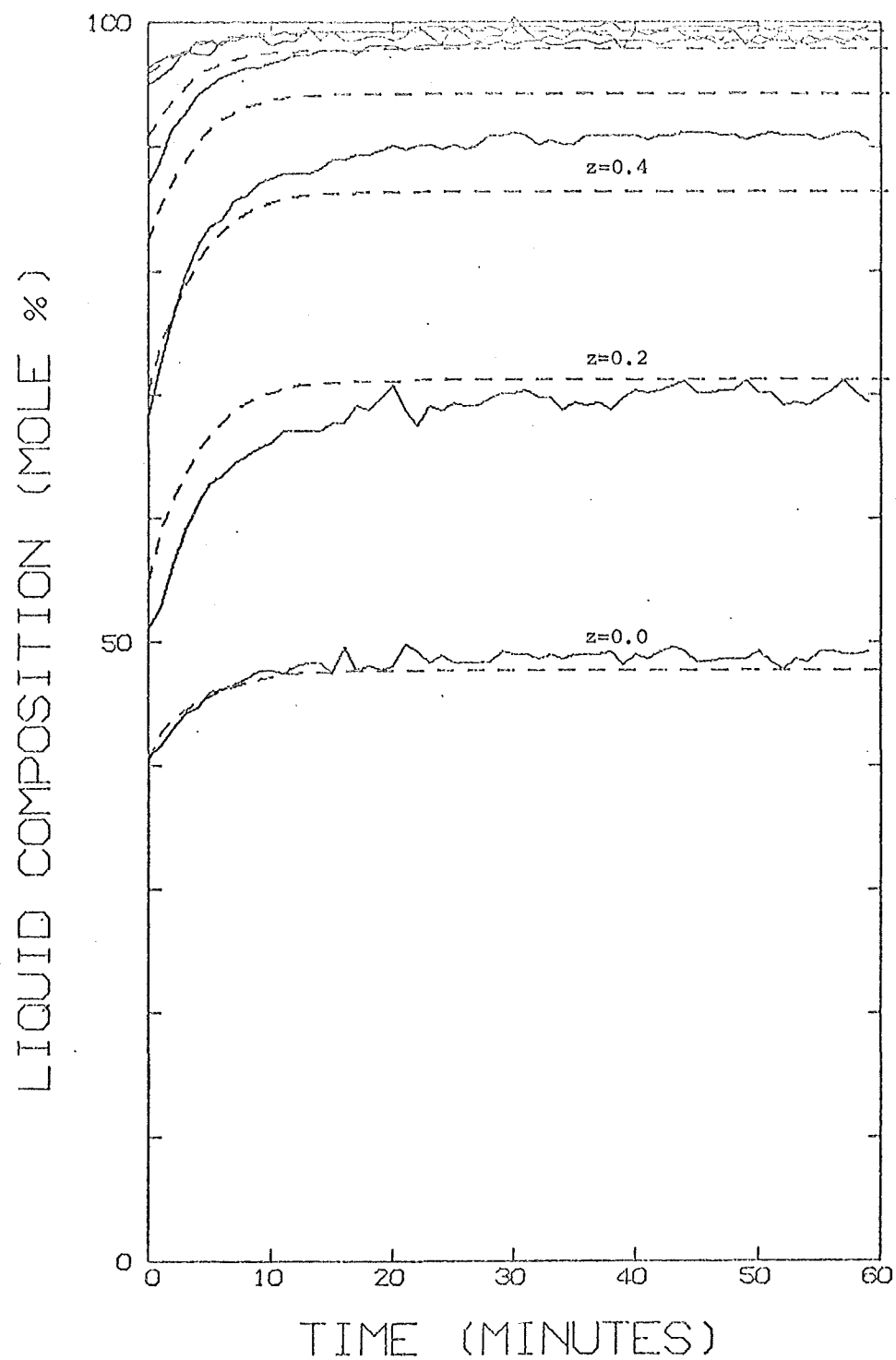


FIG A.5.1 TRANSIENT NUMBER 1.

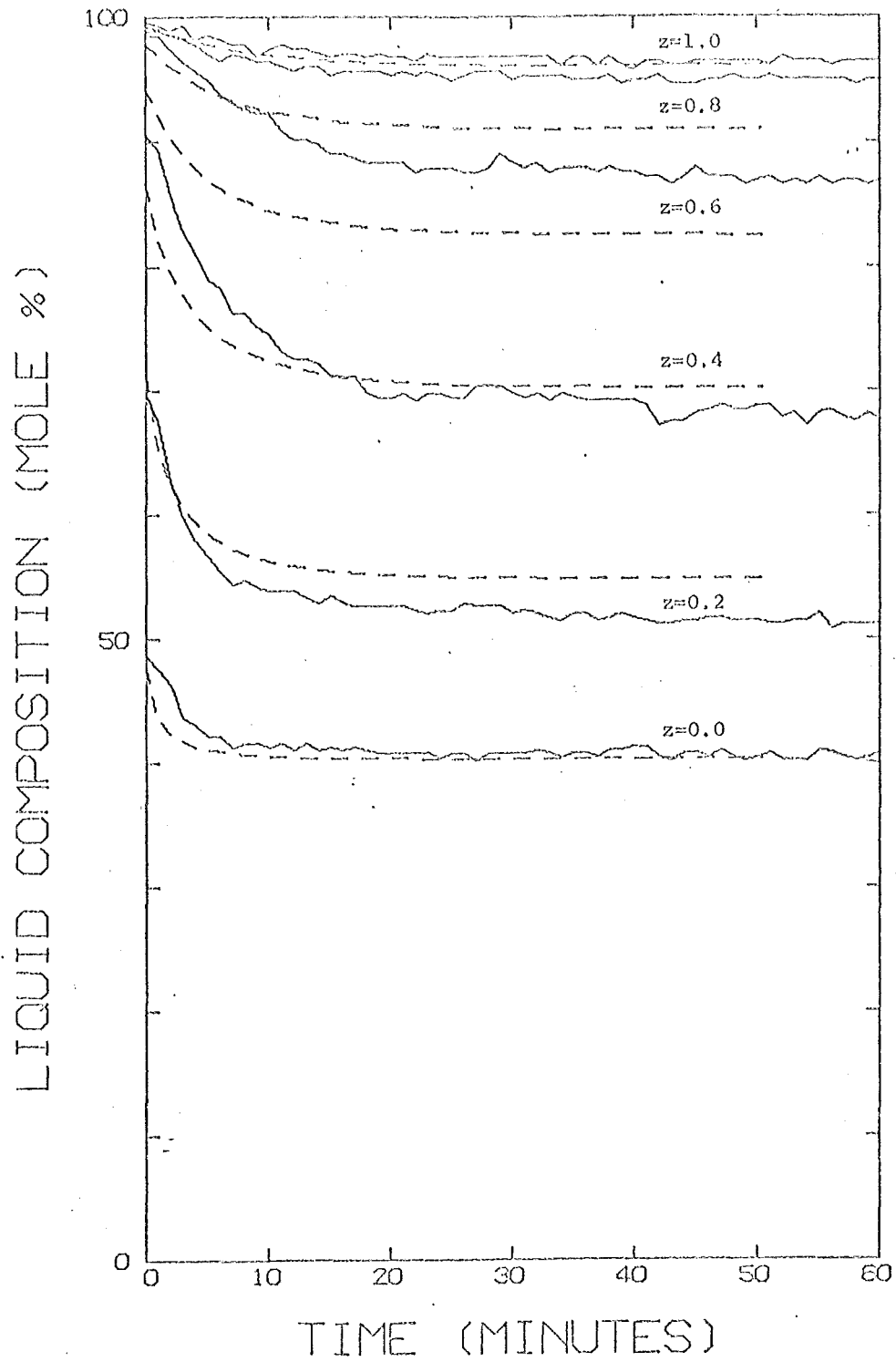


FIG A.5.2 TRANSIENT NUMBER 2.

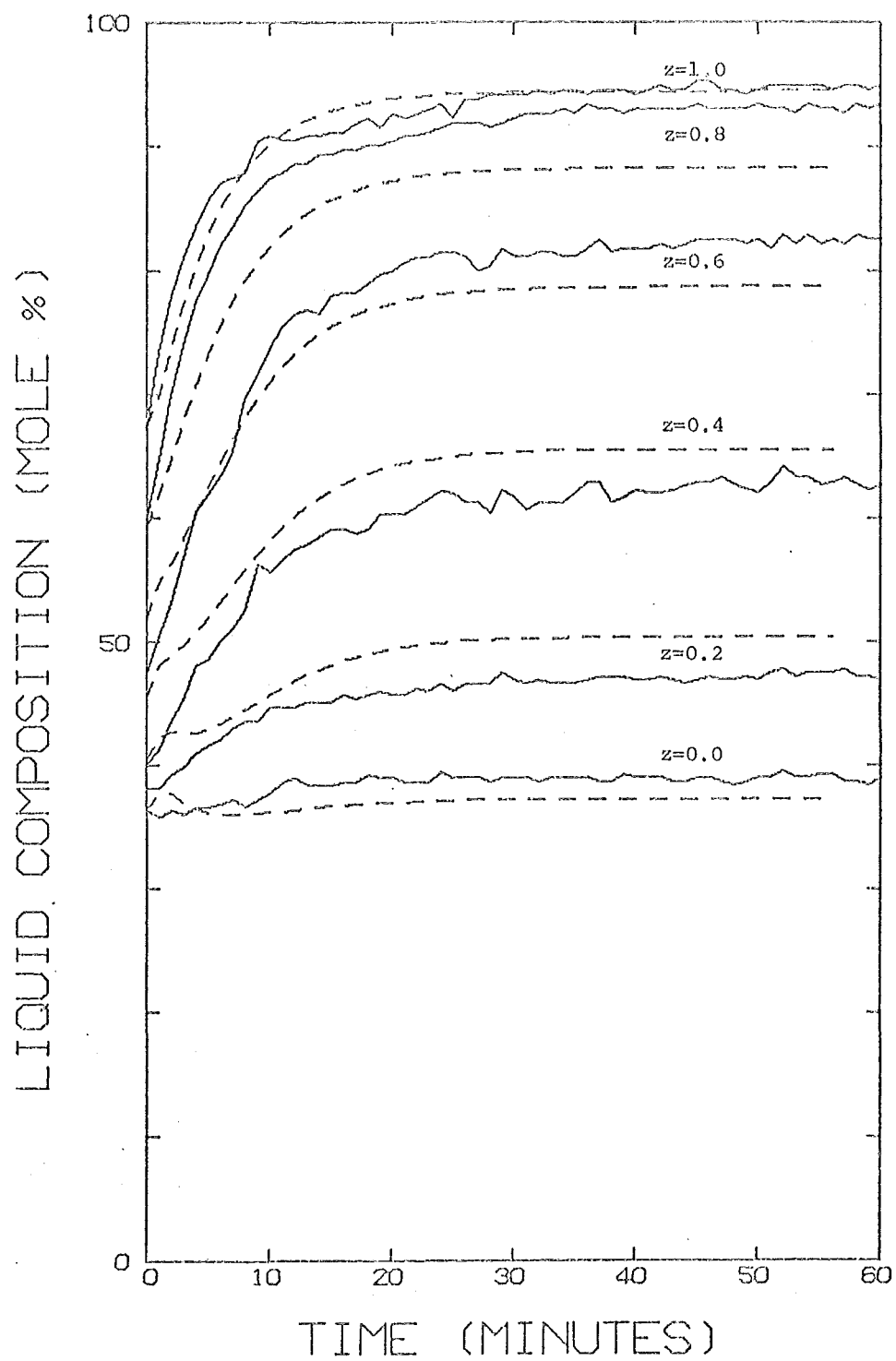


FIG A.5.3 TRANSIENT NUMBER 4.

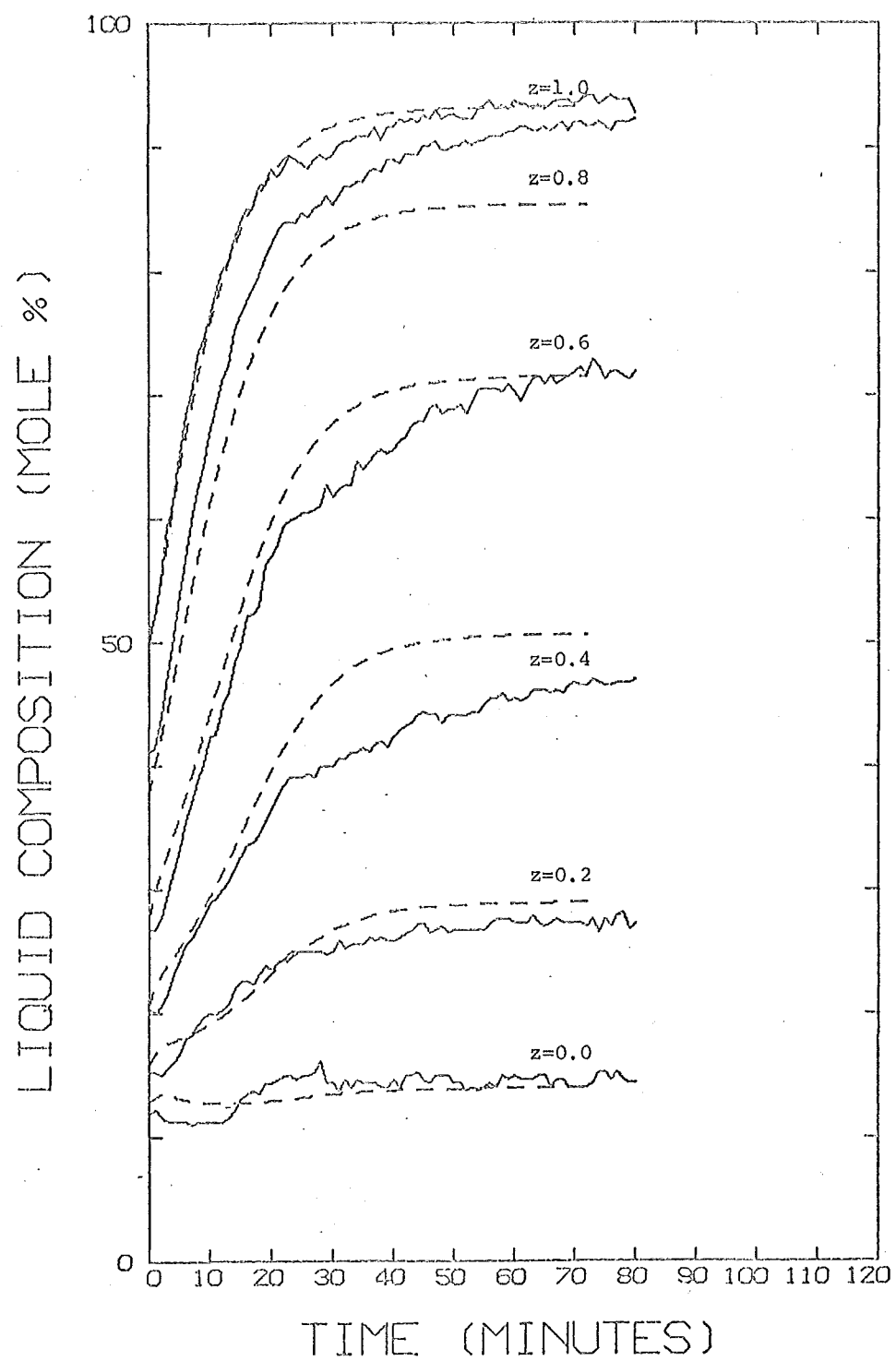


FIG A.5.4 TRANSIENT NUMBER 10.

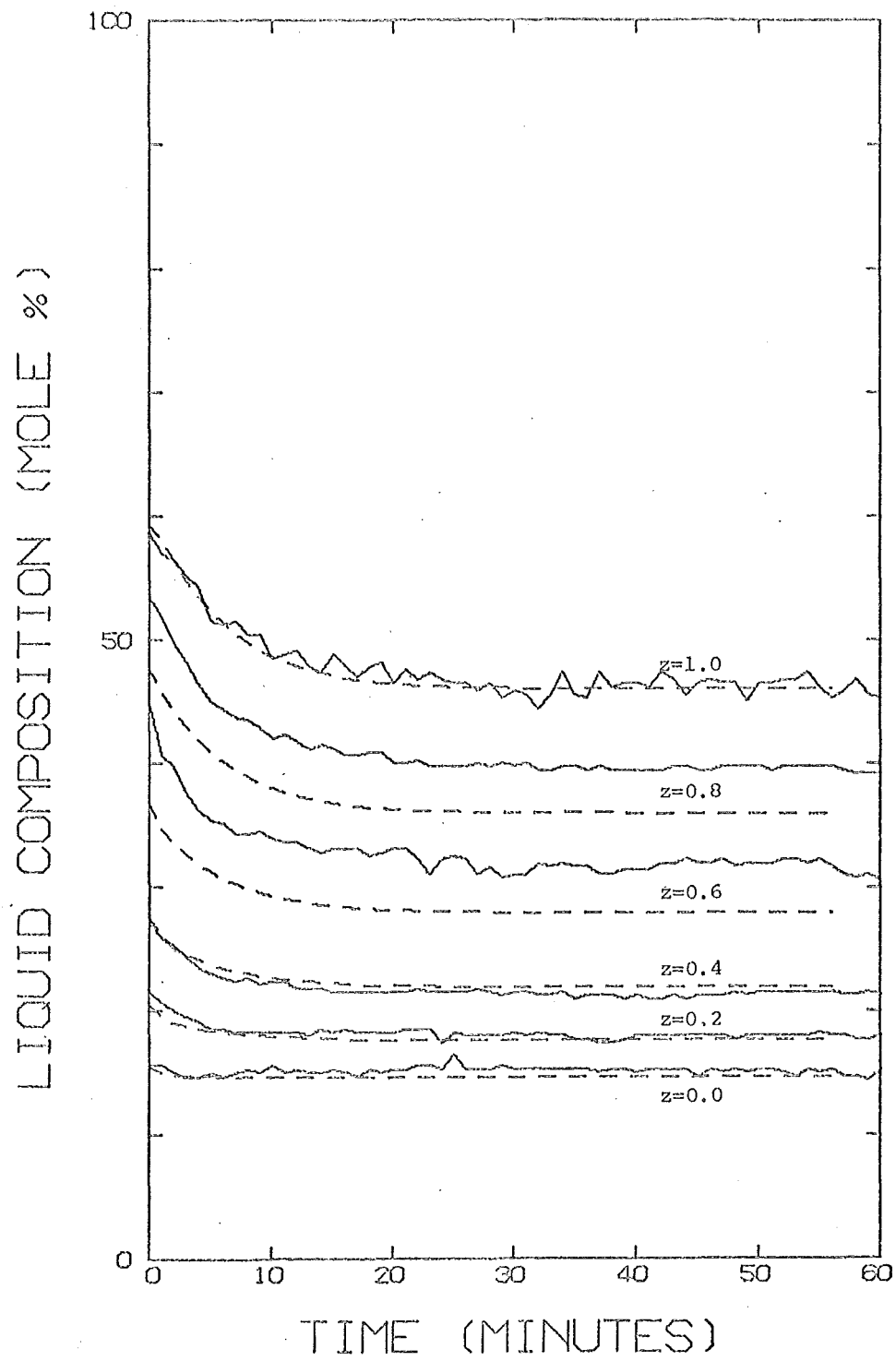


FIG A.5.5 TRANSIENT NUMBER 15.

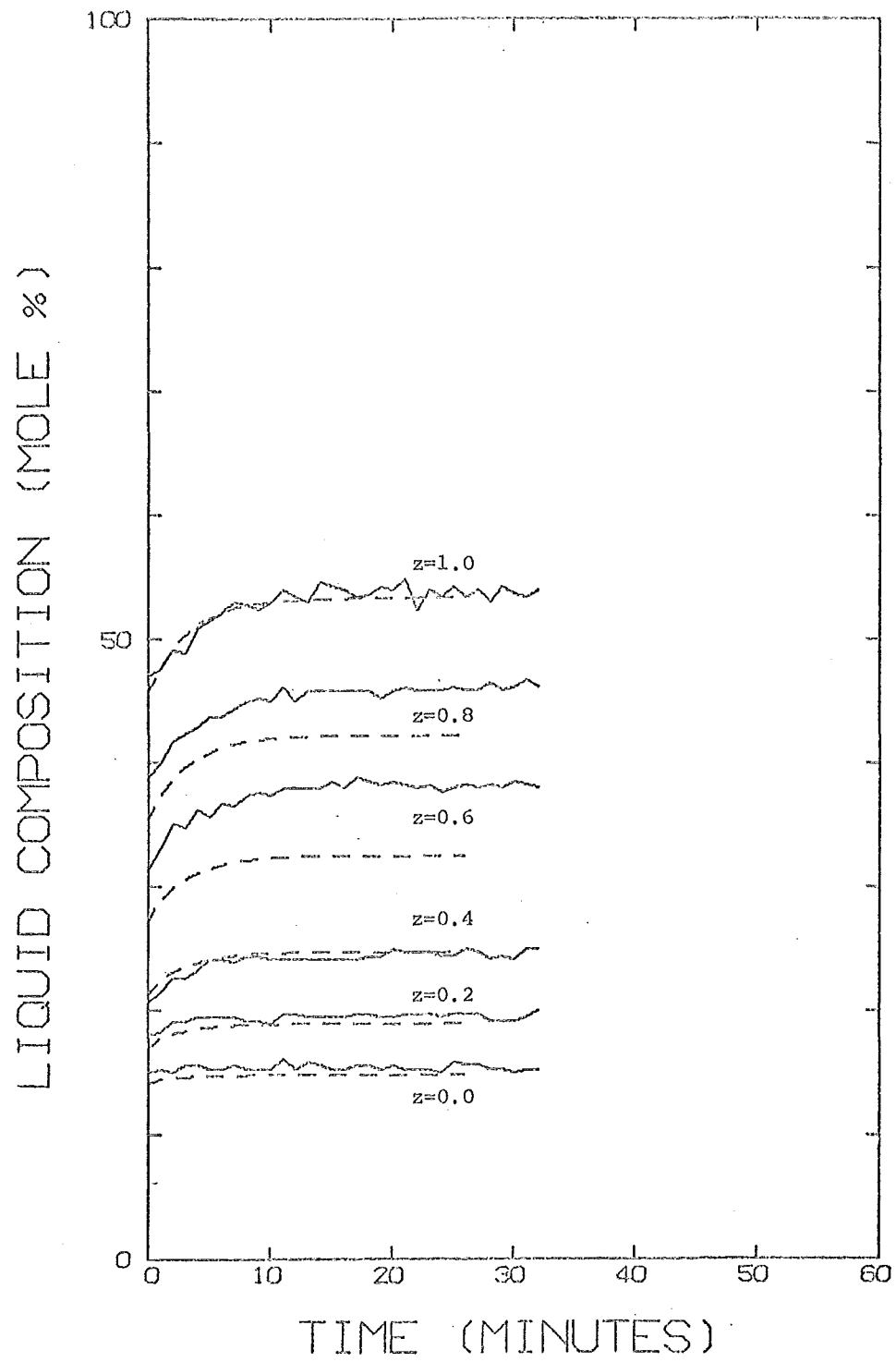


FIG A.5.6 TRANSIENT NUMBER 16.

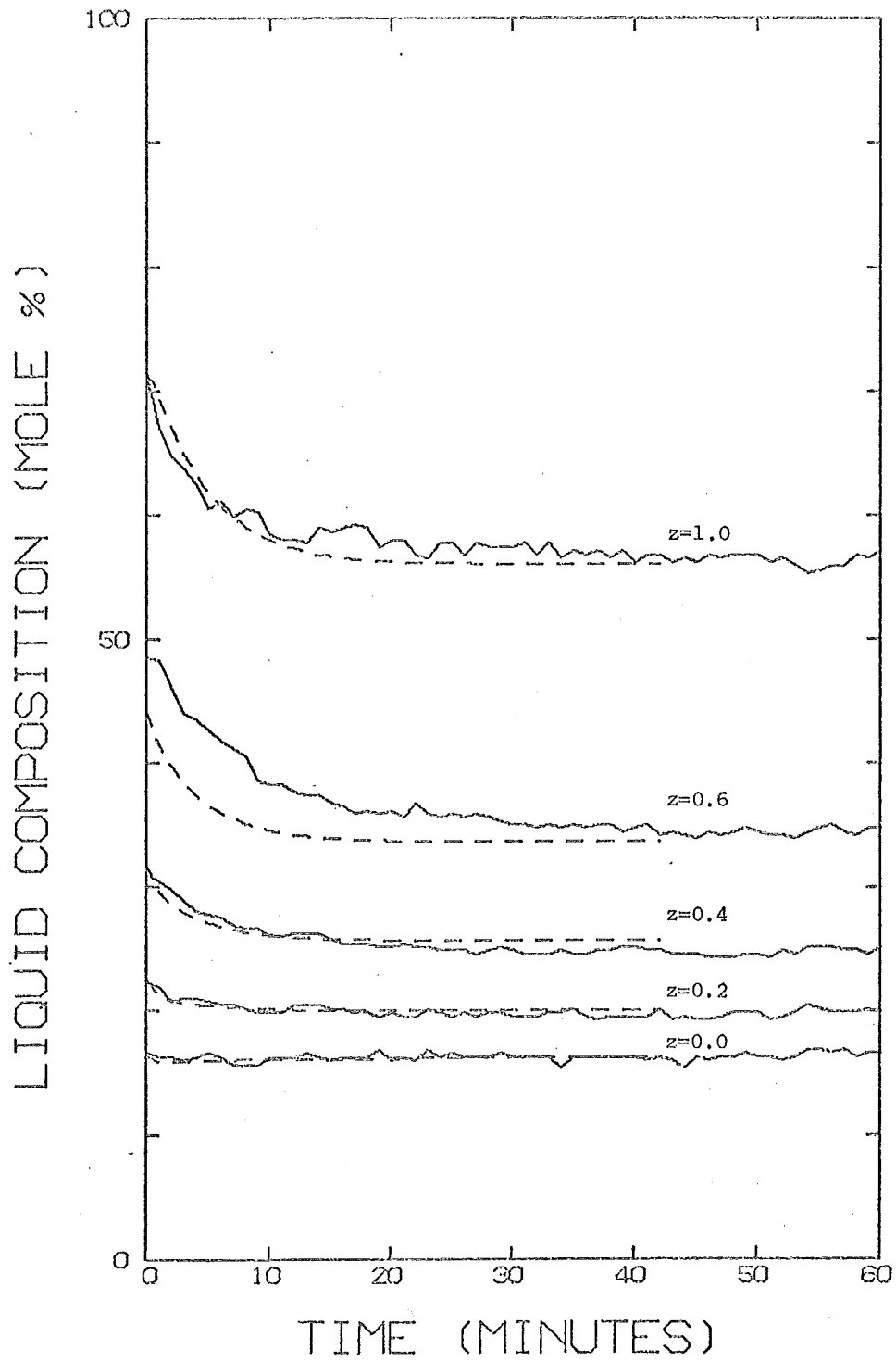


FIG A.5.7 TRANSIENT NUMBER 19.

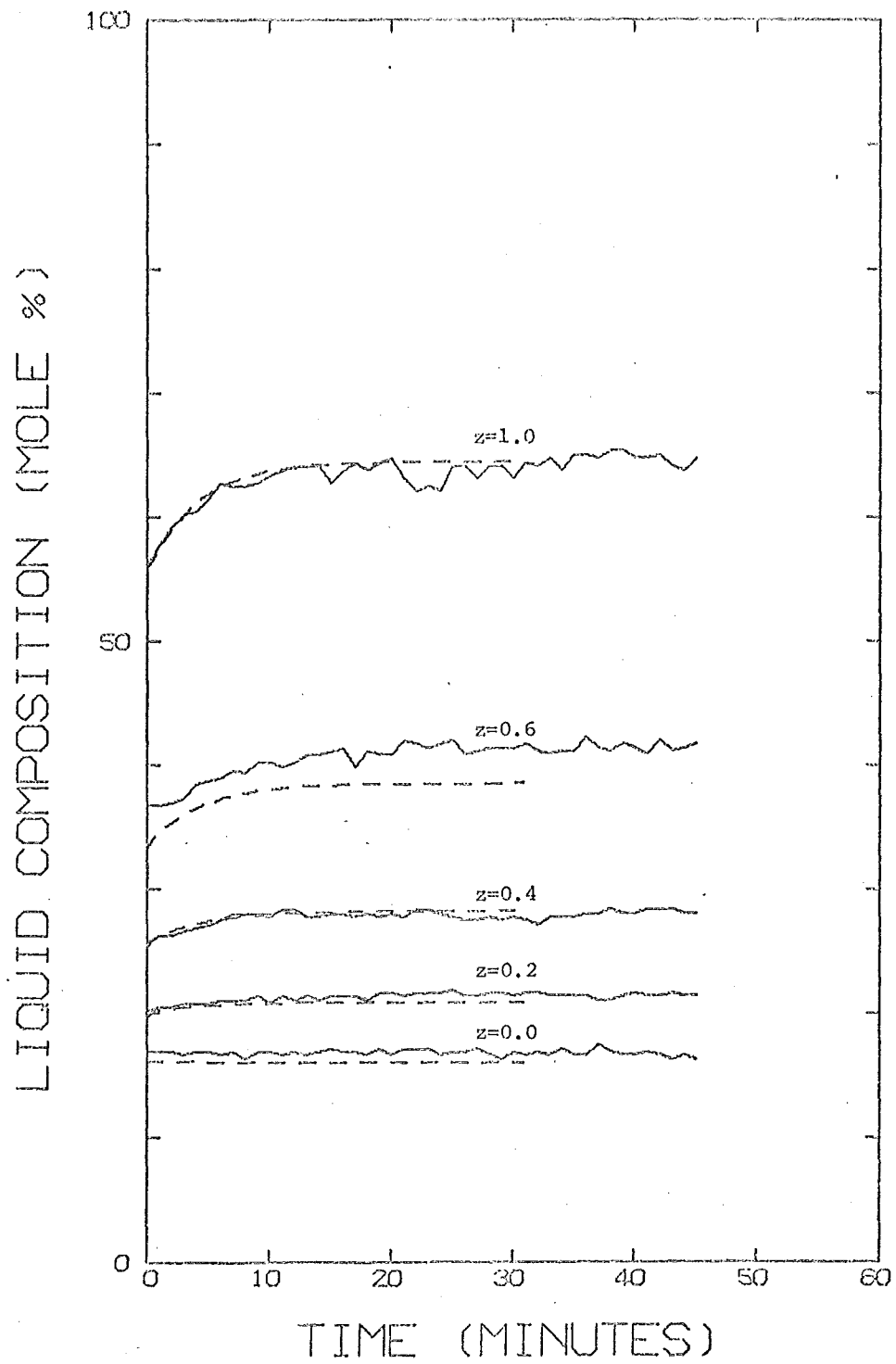


FIG A.5.8 TRANSIENT NUMBER 20.

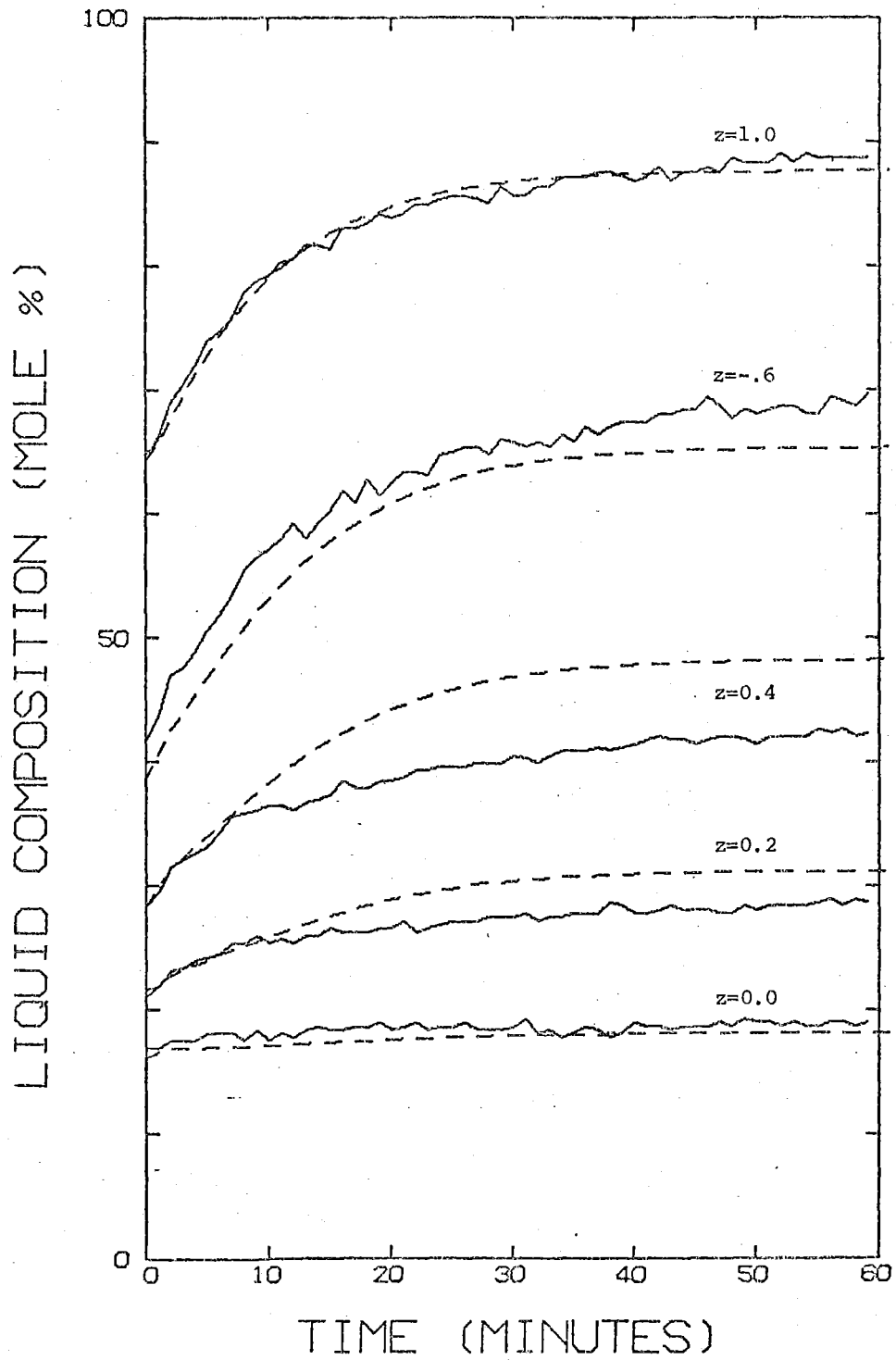


FIG A.5.9 TRANSIENT NUMBER 21.

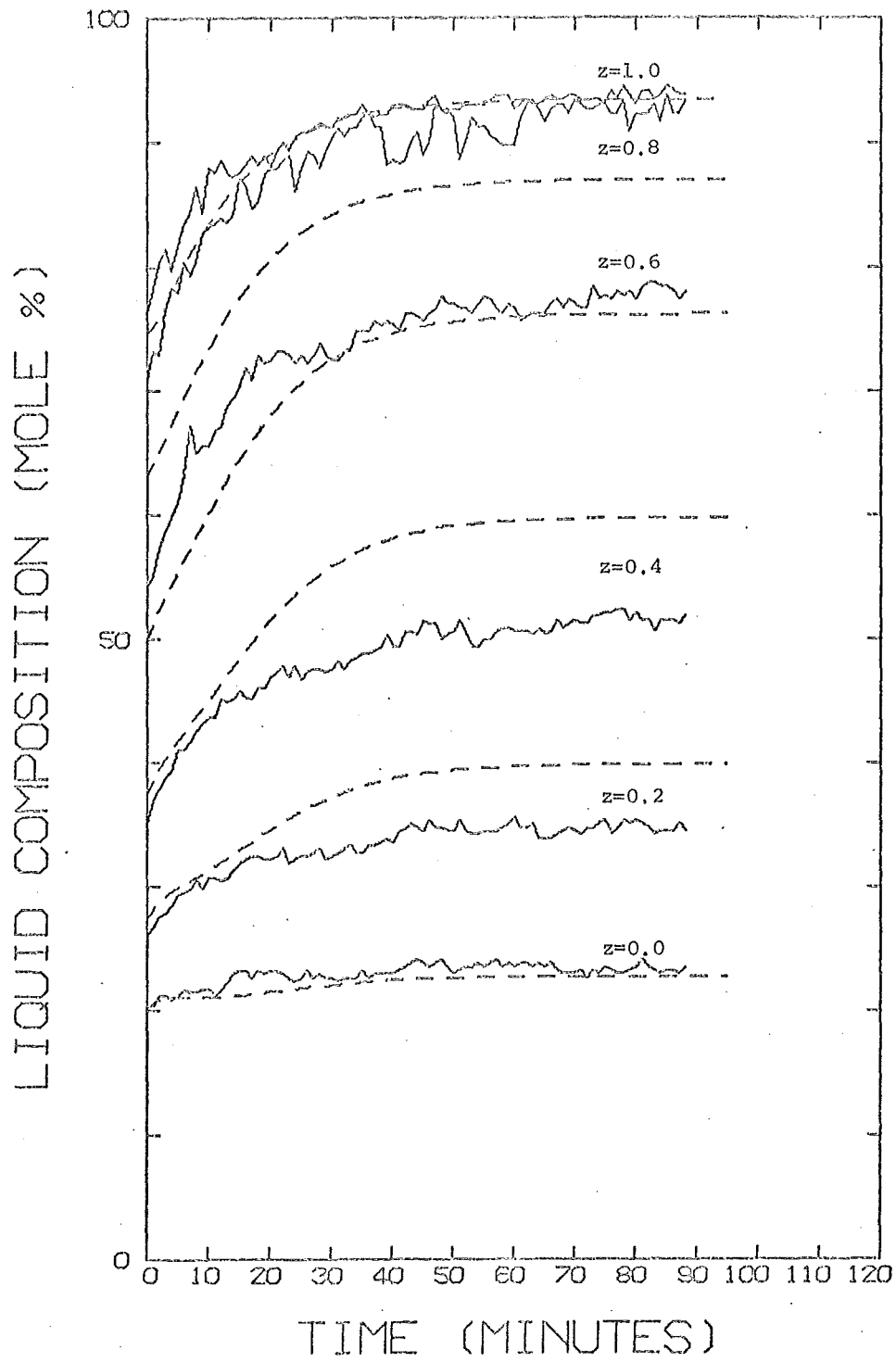


FIG A.5.10 TRANSIENT NUMBER 26